University of California
Los Angeles

Pattern Formation via Eigenstructure Assignment

A dissertation submitted in partial satisfaction
of the requirements for the degree
Doctor of Philosophy in Mechanical Engineering

by

Andy Wu

2016

Abstract of the Dissertation

Pattern Formation via Eigenstructure Assignment

by

Andy Wu

Doctor of Philosophy in Mechanical Engineering

University of California, Los Angeles, 2016

Professor Tetsuya Iwasaki, Chair

Complex dynamical systems often exhibit formation of a pattern in observed variables in the steady state. These patterns can range from the synchronization of multiple agents to the coordinated oscillation of the observed variables. The research in this dissertation formulates a general pattern formation problem as the design of a feedback controller such that selected outputs of a linear plant exponentially converge to $Re^{\Lambda t}\eta_o$ for some vector η_o, with prescribed matrices R and Λ. We show that the problem reduces equivalently to an eigenstructure assignment problem, and provide a necessary and sufficient condition for existence of a feasible controller as well as a parameterization of all such controllers. An important special case is when the system consists of multiple subsystems (or "agents") subjected to local interactions to reach consensus or an arbitrary pattern specified by their relative positioning in the state space. This general theory is further specialized to give a complete solution to a heterogeneous multi-agent synchronization problem. Three numerical examples are provided to demonstrate the efficacy of the proposed design method: the first emphasizes the importance of the desired pattern in reducing the complexity of the controller, the second illustrates the significance of adaptive pattern formation through sensory feedback, and the third suggests an extension for achieving stable limit cycles by additional nonlinearities. The theory for controller design to achieve stable limit cycles is further explored with the consideration of the nonlinear central pattern generator (CPG)-based controller. Through a linear approximation of the CPG-based controller using a describing function, it is shown that the limit cycle design reduces to an eigenstructure assignment problem. Two examples

are provided which demonstrate the application of this theory in limit cycle design: one in which a single limit cycle is designed using the eigenstructure assignment method for a three link mechanical arm and a second in which a single CPG-based controller is designed to achieve different limit cycles for two different plants in order to replicate the gait change of a leech moving in different fluid environments.

The dissertation of Andy Wu is approved.

Lieven Vandenberghe

Tsu-Chin Tsao

James S. Gibson

Tetsuya Iwasaki, Committee Chair

University of California, Los Angeles

2016

To Saba, who has always been by my side during this entire journey...

...specifically, my right side.

Table of Contents

List of Figures

List of Tables

Acknowledgments

First and foremost, I would like to thank my advisor, Professor teD Iwasaki, whose guidance, intelligence, and patient demeanor have been invaluable in completing my research. Thank you for taking a chance on me and believing in my potential, I hope I was able to exceed your expectations. Additionally, I would like to thank Professor Gibson, Professor Tsao, and Professor Vandenberghe for agreeing to be on my committee and providing helpful input regarding the direction of my research. I am also extremely appreciative for the financial support provided by the National Science Foundation under grant number 1068997. This grant was instrumental in furthering this research in addition to keeping me fed, clothed, and sheltered throughout my tenure at UCLA. I must also thank Angie, Abel, Lance, and the rest of the MAE administrative staff for being extremely understanding and helpful despite being overworked. Without their help, I doubt I could ever hope to navigate all the logistics of graduate school.

Finally, I have to thank all the people who have given me support outside of academics. I am eternally grateful to my family for their unconditional support and for the sacrifices that they have made to put me in a position to succeed. To Paul, for his mentorship and insightful conversations which have allowed me to contemplate situations beyond that of my immediate circumstances. To all the close friends that I have made during my studies including, but not limited to, Saba, Chin, Mike, Nolan, and Luke. Whether it was playing ball, foosing, climbing, or having a barbecue, you guys were always there to make difficult times bearable, and good times great. I could not have imagined a better setting for this chapter of my life; I am truly fortunate to have found the community that I have and the people I am with.

Vita

2011	B.S. (Mechanical Engineering), University of California, Berkeley.
2013	M.S. (Mechanical Engineering), University of California, Los Angeles.
2012-1016	Graduate Student Researcher, Mechanical and Aerospace Engineering Department, University of California, Los Angeles.

Publications

Wu, Andy and Iwasaki, Tetsuya. "Feedback control for oscillations with CPG architecture," *Proceedings of the 53rd Annual Conference on Decision and Control (CDC)*. IEEE, 2014.

Wu, Andy and Iwasaki, Tetsuya. "Eigenstructure assignment with application to consensus of linear heterogeneous agents," *Proceedings of the 54th Annual Conference on Decision and Control (CDC)*. IEEE, 2015.

Wu, Andy and Iwasaki, Tetsuya. "Pattern Formation via Eigenstructure Assignment General Theory and Multi-agent Application," *IEEE Transactions on Automatic Control, (Under Review)*

CHAPTER 1

Introduction

In linear systems, controllers are commonly designed in order to achieve a specified asymptotic behavior. Eigenstructure assignment is a classical design methodology used to specify (a subset of) closed-loop eigenvalues and associated eigenvectors to achieve a desired behavior for a linear system. It was originally motivated by the exploitation of the extra freedom offered by multiple control inputs beyond assigning the full set of closed-loop eigenvalues by static state feedback [2–5]. The extra eigenvector specification allows for multi-mode decoupling/shaping, and was used extensively for flight control [6–10] and later for fault detection [11–15].

As a theoretical basis, exact characterizations of assignable eigenvectors using the freedom beyond the pole placement were given in [16, 17] for the state feedback case. Later works, [18–20], saw the use of static output feedback controllers and provided insights into assignable eigenstructures. However, the use of static gains in the absence of full state information considerably restricts the freedom in assigning eigenstructures. This motivated approximate eigenstructure assignment through projection [21–23]. More recently, [24] suggested the use of *dynamic* feedback with *partial* pole placement to leave more freedom for eigenvector assignment. However, the focus of the paper was not solely on the eigenstructure assignment and the issue was not addressed in depth. To date, a complete theory for eigenstructure assignment has yet to be established.

Pattern formation problems have recently gained much attention in multiple contexts [1,25–28], and their connections to eigenstructure assignment have been gradually recognized. Various dynamical properties for pattern formation, including consensus, synchronization, and coordinated oscillations, turned out to be related to eigenstructure assignment as we will

briefly review in the following two paragraphs. Individual problems have been formulated and approached independently, but complete solutions are not yet available. A general theory of eigenstructure assignment, if developed, would shed new light on pattern formation problems.

The design of nonlinear oscillators for coordinated oscillations was considered in [28], using the biological structure of central pattern generators (CPGs). The problem was formulated as the search for a matrix that specifies the interconnections between agents (i.e. neurons) so that a stable limit cycle is achieved with a prescribed oscillation profile. It was shown that the problem reduces approximately to an eigenstructure assignment through multivariable harmonic balance, with eigenvalue and eigenvector specifying the frequency and relative amplitudes/phases, respectively. The idea was extended for feedback control design to generate coordinated oscillations for a linear plant [29], however, the resulting eigenstructure assignment problem was formulated as a static output feedback stabilization problem which is difficult to solve in general and their solution was found through the use of heuristic algorithms. Because is no theory to determine the feasiblility and parameterization of controllers to assign a specified eigenstructure, a systematic method for designing controllers to achieve limit cycles in a nonlinear closed-loop could not be established. A complete theory on eigenstructure assignment would allow for a systematic method for designing controllers for limit cycles and bypass the need to rely on heuristic algoritms.

Another pattern formation problem of recent popularity in the controls community is the consensus of multiple agents. Earlier researches [25, 30–33] have noted the importance of the communication or graph structure in reaching consensus between agents. A fundamental observation is that the inter-agent coupling is designed so that the target state of consensus is achieved in the eigenspace of the corresponding graph Laplacian associated with the zero eigenvalue. Building on those developments, a linear homogeneous consensus problem was solved in [34], and later extended to the case of heterogeneous agents [1]. This reference showed an internal model principle in terms of a regulator equation, clearly indicating a strong connection to eigenstructure assignment [35]. However, the structure of the controller given by [1] is potentially restrictive as the control input to each agent is independent of sensory feedback from any other agent. This drawback has been overcome for some classes

of heterogeneous agents, including integrators [36], minimum-phase agents [37], and right-invertible agents [38], but a general theory without restrictions on agent dynamics has yet to be established.

This dissertation formulates a general pattern formation problem of designing a linear static or dynamic output feedback controller for a linear time-invariant plant to achieve the following specifications for the autonomous closed-loop system: Given a matrix R and matrix with non-negative eigenvalues Λ and starting with an arbitrary initial state, selected plant outputs exponentially converge to a trajectory $Re^{\Lambda t}\eta_o$ for some vector η_o dependent on the initial state. The spatial shape (relative positioning of output variables) is specified by R, and its time evolution (constancy, growth, or oscillation) is specified by Λ. Thus $Re^{\Lambda t}\eta_o$ can be viewed as a spatio-temporal pattern exhibited by the dynamical system. In the literature, pattern formations have often been considered for networks of multiple agents (e.g. vehicle formations [25–27], lattice and interconnected systems [39, 40]), but here we broaden the scope to include general unstructured and structured systems. Due to the linearity and autonomy of the system, the size of the pattern varies depending on the initial conditions through η_o. The dependence is inevitable within the linear framework, but we discuss possible extensions through additional nonlinear frameworks.

In Chapter 2, the linear pattern formation problem is shown to be equivalent to an eigenstructure assignment problem in which a subset of eigenvectors and eigenvalues are assigned to the closed-loop system, while unassigned eigenvalues are placed in the open left-half plane; examples of different types of linear pattern formations and their specifications are provided. We provide nececessary and sufficient condition for solvability of the eigenstructure assignment problem in terms of a regulator equation, and a parameterization of all feasible controllers which embeds an internal model of the desired dynamics explicitly or implicitly is given. Moreover, we prove separation principles, reducing the output feedback natural eigenstructure assignment to a double observer design plus full control, state feedback eigenstructure assignment.

In Chapter 3, the general eigenstructure theory is extended to the case in which structured controllers are designed for multi-agent systems. Using the results from Chapter 2, we

propose a systematic method for structured controller synthesis in which heterogeneous agents have a subset of their dynamics homogenized to achieve common asymptotic behavior. The proposed method is used to design a structured controller that has no restrictions on individual agent dynamics, for multi-agent synchronization. The performance of this controller is juxtaposed to the one proposed by [1], emphasizing the importance of sensory feedback to the controller for adaptive synchronization. Furthermore, we provide conditions for which the dynamics for the heterogeneous multi-agent pattern formation controller can be simplified and substantiate this with an example of synchronization using a static controller. Lastly, we touch on the design of structured controllers to achieve limit cycles for a set of agents through the addition of a nonlinear damping term in the control input to a root agent; an example illustrates the possibility of the proposed method.

In Chapter 4, the problem of designing nonlinear controller with a central pattern generator (CPG) architecture to achieve closed-loop limit cycles is considered. The nonlinear controller is linearized via a describing function and the resulting problem is reduced to an eigenstructure assignment problem using an output feedback controller. An example is provided to show the reliability of the eigenstructure method for limit cycle design for a three link mechanical arm actuated at each joint. This problem is further extended to the design of multiple limit cycles with a single CPG-based controller. The multiple limit cycle problem essentially reduces to a simultaneous stabilization problem for which we provide formulations that can be practically solved using heuristic algorithms. A numerical simulation is provided showing a single controller that achieves different specified limit cycles when placed in a closed-loop with two different plants. Moreover, we demonstrate an effect where changing the plant results in switching between the two limit cycles similar to the manner in which animals change gaits in different environments.

Finally, in Chapter 5, we summarize the contributions of this research, potential applications to the community, and future avenues for which this research can be expanded.

Notation: Let $\mathbb{R}$, $\mathbb{C}_-$, and $\mathbb{I}_n$ denote the sets of real numbers, complex numbers with negative real parts, and integers $\{1, \ldots, n\}$, respectively. For a matrix M, the notations $M^\intercal$, $M^\dagger$, and $\mathrm{eig}(M)$ denote the transpose, the Moore-Penrose inverse, and the set of eigen-

values respectively. The symbol $\mathrm{diag}(A_1, \ldots, A_n)$ denotes the block-diagonal matrix with $A_1, \ldots, A_n$ on the diagonal, and $\mathrm{col}(B_1, \ldots, B_n)$ denotes the matrix obtained by stacking $B_1, \ldots, B_n$ in a column. For a state-space system $\dot{x} = Ax + Bu$, $y = Cx + Du$, the mapping from u to y is denoted by $y = \mathring{P}u$ with $P := \left[\begin{smallmatrix} D & C \\ B & A \end{smallmatrix}\right]$. The same notation $y = \mathring{P}u$ is used for the static case where $y = Du$ and $P := D$. For signals x and y, the notation $x(t) \to y(t)$ means that $\|x(t) - y(t)\| \to 0$ as $t \to \infty$.

CHAPTER 2

Pattern Formation as Eigenstructure Assignment

We first consider the general setting where the pattern $Re^{\Lambda t}\eta_o$ is to be formed through feedback interactions of dynamical elements, which may be completely unstructured. To this end, let a linear time-invariant plant be given by a state-space realization

$$\dot{x} = Ax + Bu, \quad y = Cx, \quad z = Hx, \tag{2.1}$$

where $x(t) \in \mathbb{R}^n$ is the state, $u(t) \in \mathbb{R}^m$ is the control input, $y(t) \in \mathbb{R}^p$ is the measured output, and $z(t) \in \mathbb{R}^h$ is the performance output. We assume that (A, B) is stabilizable, and (H, A) and (C, A) are detectable. Consider a static controller or a dynamic controller with state x_c,

$$u = Ky \quad \text{or} \quad \begin{aligned} \dot{x}_c &= A_c x_c + B_c y, \\ u &= C_c x_c + D_c y, \end{aligned} \tag{2.2}$$

and let the closed-loop system be denoted by

$$\dot{\mathfrak{x}} = \mathcal{A}\mathfrak{x}, \quad z = \mathcal{H}\mathfrak{x}, \tag{2.3}$$

where $\mathfrak{x} = x$ or $\mathrm{col}(x, x_c)$ is the state vector.

Problem 1. Let a system with desired dynamics

$$\dot{\eta} = \Lambda\eta, \quad \zeta = R\eta, \tag{2.4}$$

be given, where $\eta(t) \in \mathbb{R}^r$, $\zeta(t) \in \mathbb{R}^h$, (R, Λ) is observable, and all the eigenvalues of Λ have nonnegative real-parts. Given the plant (2.1), find a necessary and sufficient condition for the existence of a controller (2.2) such that the closed-loop system (2.3) satisfies the following properties:

(a) For each $\mathfrak{x}(0)$, there exists $\eta(0)$ such that $z(t) \to \zeta(t)$.

(b) For each $\eta(0)$, there exists $\mathfrak{x}(0)$ such that $z(t) \to \zeta(t)$.

(c) $(\mathcal{H}, \mathcal{A})$ is detectable.

Parametrize the set of all such controllers.

Properties (a) and (b) ensure that the closed-loop behavior of $z(t)$ matches the desired dynamics $\zeta(t)$ in the steady state, regardless of the initial conditions. It is reasonable to require Property (c) for the control design since otherwise there is an unstable mode that makes an internal variable diverge while the output specifications (a) and (b) are satisfied.

Problem 1 can be viewed as a pattern formation problem. In particular, the signal $z(t)$ is required to converge to the pattern specified by $\zeta(t) = Re^{\Lambda t}\eta(0)$ for some $\eta(0)$. A pattern is defined as relative behaviors of the entries of $\zeta(t)$. There are two primary types of patterns captured by the linear framework depending on the eigenvalues of Λ; oscillation (complex) and constant (real). The relative amplitudes (and phases) of the entries of $\zeta(t)$ are specified by R, and the absolute amplitudes can be constant or growing over time, as specified by the real part of the eigenvalues and their multiplicity. The actual values at particular time instants depend on the initial state $\eta(0)$. Below, we demonstrate how the specifications on R and Λ can be chosen to achieve different patterns with each of the patterns generated using the design method that will be presented later in the dissertation.

An oscillation pattern

$$\zeta_k(t) = \alpha_k \sin(\omega t + \beta_k), \quad k \in \mathbb{I}_h, \tag{2.5}$$

can be specified by

$$\Lambda = \begin{bmatrix} 0 & \omega \\ -\omega & 0 \end{bmatrix}, \quad R_k = \begin{bmatrix} a_k \cos(b_k) & a_k \sin(b_k) \end{bmatrix} \tag{2.6}$$

where $\alpha_k = \gamma_a a_k$ and $\beta_k = b_k + \gamma_b$ with (γ_a, γ_b) dependent on the initial condition, and R_k is the k^{th} row of R. Note that a_k and b_k, respectively, determine the relative amplitude and phase between the outputs, ζ_k. The absolute amplitudes and phases depend on the initial

states because the closed-loop system is linear. For example, consider an oscillation pattern defined by

$$\omega = 3, \quad a_k = k, \quad b_k = (\pi/2)(k-1), \quad k \in \mathbb{I}_3.$$

For this pattern, we can anticipate that starting from different initial conditions will result in different steady-state amplitudes. In the figure on the left, the outputs start with an initial

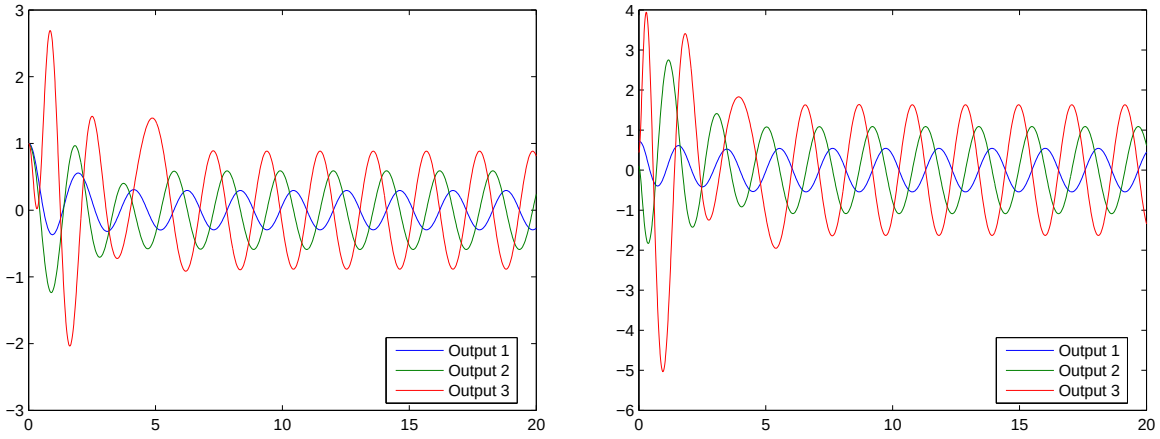

Figure 2.1: Linear oscillation patterns with initial conditions starting at 1 (L) and random initial conditions(R).

condition of 1. By contrast, the figure on the right starts with random initial conditions. The relative amplitudes and phase relationships are kept, but the absolute amplitudes scale depending on the initial condition and the phases are offset by a constant phase. We will later show in an example that the amplitude can be locked with the addition of a nonlinearity.

The pattern $\zeta_k = \alpha_k e^{\lambda t}$ is given by the specification

$$\Lambda = \lambda \geq 0, \quad R_k = a_k, \quad k \in \mathbb{I}_h,$$

where $\alpha_k = \gamma_a a_k$ with γ_a dependent on the initial condition. This is a trajectory that either exponentially diverges ($\lambda > 0$) or converges to a constant value ($\lambda = 0$). As with the previous oscillation case, a_k can only specify the steady-state values of an output relative to other outputs. For example, consider a pattern defined by

$$\lambda = 0, \quad a_k = k, \quad k \in \mathbb{I}_3.$$

In this case, the steady-state pattern obtained by the outputs will be constants as shown in the following figure. Both figures in Fig. 2.2 start with zero initial conditions except for a

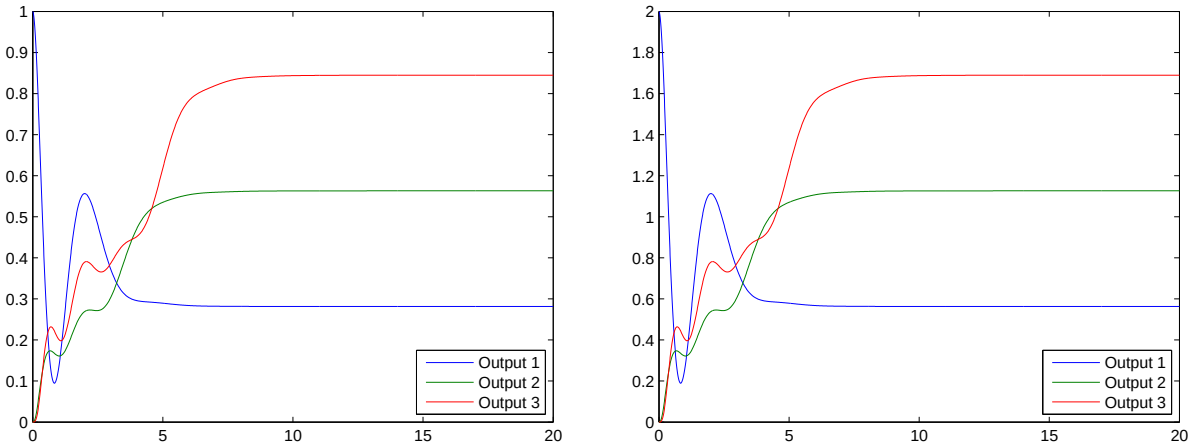

Figure 2.2: Zero initial state except for initial condition of 1 (L) and 2 (R) for output 1.

displacement of 1 and 2, respectively, for the state corresponding to output 1. Thus, we see that the three outputs reach steady-state constants that have the same relative magnitude, but with absolute value dependent on the initial condition. By essentially scaling the initial condition by two, the steady-state value for each output doubled.

It is also possible to combine the basic specifications to obtain different steady-state behaviors. For example, assigning two zero eigenvalues as a double integrator with specifications

$$\Lambda = \begin{bmatrix} 0 & 1 \\ 0 & 0 \end{bmatrix}, \quad R = \begin{bmatrix} 1 & 0 \\ 0 & 1 \end{bmatrix}, \tag{2.7}$$

achieves $\zeta_1 = \gamma_v t + \gamma_p$ and $\zeta_2 = \gamma_v$ for some scalars $\text{col}(\gamma_p, \gamma_v) := \eta(0)$, specifying the (initial) position and velocity. Other variations include cases where some outputs converge to constants with prescribed relative magnitudes, while other outputs converge to oscillations with prescribed frequency and relative phases and amplitudes.

Consider, for example, the case in which R_k and Λ are defined by (2.7) for $k \in \mathbb{I}_3$. In this situation, we are setting R_k to be the same for every pair of outputs. We can interpret

this to mean that each output corresponding to position will reach the same value and each output corresponding to velocity to reach the same value. Fig. 2.3 shows the position and velocity for one set of random initial conditions. For comparison, Fig. 2.4 shows the position

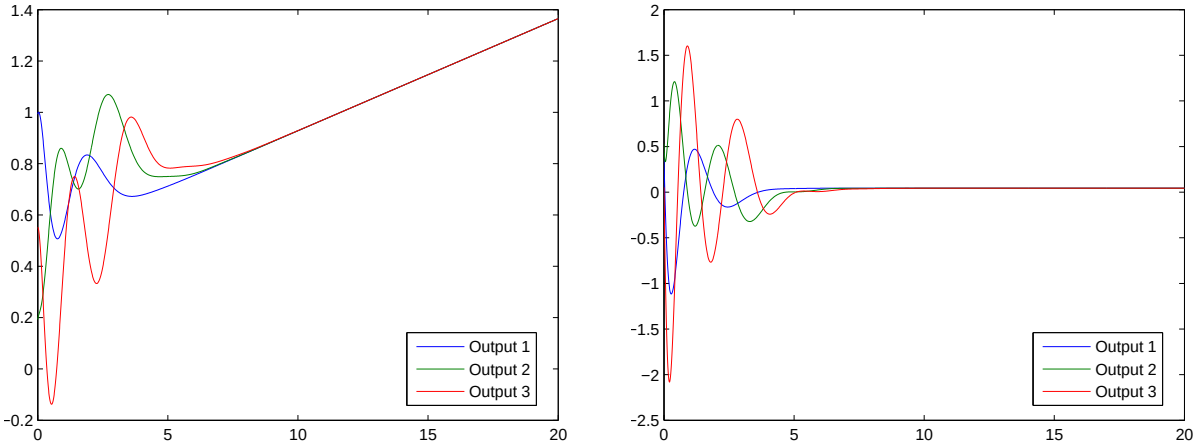

Figure 2.3: Position (L) and Velocity (R) for one set of random initial conditions.

and velocity for a different set of random initial conditions. One should note that because

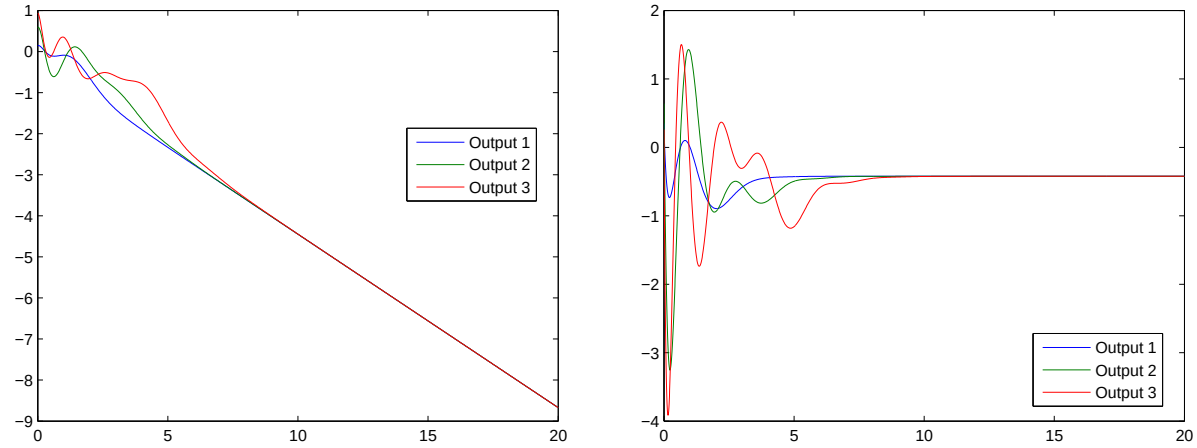

Figure 2.4: Position (L) and Velocity (R) for a different set of random initial conditions.

we set R_k to be the same for every output, the sets of outputs synchronize regardless of their initial conditions. This property is of interest because it will be integral to the design of structured controllers to achieve synchronization in multi-agent systems. This will be

revisted in Chapter 3.

Problem 1 is a less restrictive version of the concept of system intersection proposed by [41] in that it requires only steady-state convergence. Regardless, Problem 1 results in similar conditions that can be characterized by the closed-loop eigenvalues and eigenvectors as follows.

Lemma 1 *Consider Problem 1. For a given controller, the closed-loop system (2.3) satisfies the design specifications (a)–(c) if and only if the following statements hold.*

(i) There exists a full column-rank matrix $\mathcal{V}$ such that

$$\mathcal{A}\mathcal{V} = \mathcal{V}\Lambda, \quad \mathcal{H}\mathcal{V} = R. \tag{2.8}$$

(ii) $eig(\mathcal{A}) \setminus eig(\Lambda) \subset \mathbb{C}_-$.

Proof. See Appendix B. ∎

Condition (i) requires that the spectrum of the closed-loop matrix $\mathcal{A}$ contains the eigenvalues of Λ, and the associated eigenvectors $\mathcal{V}$ give the prescribed output eigenstructure R. Thus, the desired trajectory $\zeta(t)$ generated by (2.4) can be reproduced by the closed-loop system. Condition (ii) constrains the closed-loop eigenvalues not associated with Λ to the open left-half plane. This ensures that the output $z(t)$ coincides with $\zeta(t)$ in the steady state since all the other modes decay to zero. Problem 1 is now formulated as an eigenstructure assignment where the controller parameters are sought to satisfy conditions (i) and (ii).

Definition 1 *A controller is said to solve Problem 1 with eigenmatrix $\mathcal{V}$ if the closed-loop system satisfies conditions (i) and (ii) in Lemma 1.*

When the controller is dynamic with n_c dimensional state space, the eigenmatrix can be partitioned as $\mathcal{V} = \text{col}(X, \Xi)$, where $X \in \mathbb{R}^{n\times r}$ and $\Xi \in \mathbb{R}^{n_c\times r}$ specify the eigenstructures for the plant and controller states, respectively. For brevity, we may use the same notation for the case of static controller ($n_c = 0$), with the understanding that Ξ is an empty $(0 \times r)$ matrix and any terms containing Ξ are considered absent.

2.1 Controller Equivalence

We aim to parametrize the set of all controllers solving Problem 1. However, some controllers may be considered equivalent for the purpose of achieving the design specifications. It turns out that removal of such redundancy simplifies the controller parametrization. The purpose of this section is to formally define the notion of equivalence and identify a subset of feasible controllers such that all feasible controllers can be covered by those equivalent to members of this subset.

In many linear control designs, specifications are given in terms of the closed-loop transfer function with internal stability. In this case, controllers are equivalent if they are stabilizable and detectable realizations of the same transfer function. However, this notion of equivalence does not apply to feasible controllers for Problem 1. For example, a solution to Problem 1 may be given as an open-loop controller with uncontrollable and unstable modes that comprise an internal model for the desired dynamics; this controller transfer function is identically zero (this will be discussed later). The key is to preserve unstable uncontrollable modes and define equivalence within the state space framework as follows.

Definition 2 *Two controllers are said to be equivalent if they are related by a combination of state coordinate transformations and addition/removal of stable unobservable or uncontrollable modes that are decoupled from unstable modes.*

The crucial property of controller equivalence is that the state variables being added or removed do not contribute to $u(t)$ in the steady state regardless of $y(t)$. With this property, a controller equivalent to a feasible controller also solves Problem 1. Moreover, they share the same plant eigenmatrix.

Lemma 2 *Suppose a dynamic controller $\mathring{\mathcal{K}}$ with state $x_c \in \mathbb{R}^{n_c}$ solves Problem 1 with $\mathcal{V} := col(X, \Xi)$. Let $T \in \mathbb{R}^{n_c \times n_c}$ be an arbitrary nonsingular matrix. Define the controller $\mathring{\mathcal{K}}_o$ by the coordinate transformation of $\mathring{\mathcal{K}}$ so that $x_o := Tx_c$ is the state vector of $\mathring{\mathcal{K}}_o$. Then $\mathring{\mathcal{K}}_o$ solves Problem 1 with $\mathcal{V}_o := col(X, T\Xi)$.*

Proof. Let $\mathcal{K} := \left[\begin{smallmatrix} D_c & C_c \\ B_c & A_c \end{smallmatrix}\right]$ solve Problem 1 and $\mathcal{A} = \mathsf{A} + \mathsf{B}\mathcal{K}\mathsf{C}$ be the closed-loop system with state vector $\mathrm{col}(x, x_c)$. Define $T_c = \mathrm{diag}(I, T)$. Applying the coordinate transformation, T_c, to the closed-loop system, we obtain $\mathcal{A}_o = T_c(\mathsf{A} + \mathsf{B}\mathcal{K}\mathsf{C})T_c^{-1}$. The eigenvalues of the closed-loop system are unchanged under a coordinate transformation so condition (ii) is satisfied. Additionally, because of the structures of A, B, and C, $\mathcal{A}_o$ can also be rewritten as $\mathcal{A}_o = \mathsf{A} + \mathsf{B}\mathcal{K}_o\mathsf{C}$, with $\mathcal{K}_o := \left[\begin{smallmatrix} D_c & C_cT^{-1} \\ TB_c & TA_cT^{-1} \end{smallmatrix}\right]$. Condition (i) of Lemma 1 is thereby satisfied for $\mathcal{K}_o$ and $\mathcal{V}_o$. Thus, $\mathring{\mathcal{K}}_o$ solves Problem 1 with $\mathcal{V}_o := \mathrm{col}(X, T\Xi)$. ∎

Lemma 2 implies that given a controller that solves Problem 1, then there exists an infinite number of controllers that also solve Problem 1 as long as they are related by a coordinate transformation. This property will be useful in showing the next property of controllers that solve Problem 1.

Lemma 3 *Let $\mathring{\mathcal{K}}_a$ be a controller that solves Problem 1 with eigenmatrix $\mathcal{V}_a := col(X, \Xi_a)$. Let $\mathring{\mathcal{K}}_b$ be a controller obtained by adding and/or removing arbitrary stable modes that are unobservable or uncontrollable. Then $\mathring{\mathcal{K}}_b$ solves Problem 1 with eigenmatrix $\mathcal{V}_b := col(X, \Xi_b)$ for some Ξ_b.*

Proof. Let us first consider the case where $\mathring{\mathcal{K}}_b$ is obtained by removing stable unobservable/uncontrollable modes. Suppose $\mathring{\mathcal{K}}_a$ has stable modes that are uncontrollable or unobservable. Without loss of generality due to Lemma 2, let $\mathring{\mathcal{K}}_a$ be given in a Kalman canonical form:

$$\begin{bmatrix} u \\ \dot{x}_1 \\ \dot{x}_2 \\ \dot{x}_3 \end{bmatrix} = \begin{bmatrix} D_1 & C_1 & C_2 & 0 \\ B_1 & A_1 & * & 0 \\ 0 & 0 & A_2 & 0 \\ B_3 & * & * & A_3 \end{bmatrix} \begin{bmatrix} y \\ x_1 \\ x_2 \\ x_3 \end{bmatrix} \tag{2.9}$$

where A_2 and A_3 contain some of the stable modes that are uncontrollable and unobservable, respectively, and A_1 contains all the other modes. Let $\mathring{\mathcal{K}}_b$ be the controller obtained by

removing the states x_2 and x_3 from $\mathring{\mathcal{K}}_a$. Condition (i) of Lemma 1 gives $HX = R$ and

$$\begin{bmatrix} A + BD_1C & BC_1 & BC_2 & 0 \\ B_1C & A_1 & * & 0 \\ 0 & 0 & A_2 & 0 \\ B_3C & * & * & A_3 \end{bmatrix} \begin{bmatrix} X \\ \Xi_1 \\ \Xi_2 \\ \Xi_3 \end{bmatrix} = \begin{bmatrix} X \\ \Xi_1 \\ \Xi_2 \\ \Xi_3 \end{bmatrix} \Lambda, \tag{2.10}$$

where $\Xi_a = \mathrm{col}(\Xi_1, \Xi_2, \Xi_3)$. We can immediately see that $\Xi_2 = 0$ because A_2 shares no common eigenvalues with Λ. It then follows from the first two row blocks of (2.10) that $\mathring{\mathcal{K}}_b$ satisfies condition (i) with $\mathcal{V} := \mathrm{col}(X, \Xi_1)$. To show that (ii) is satisfied, let $\mathcal{A}_a$ and $\mathcal{A}_b$ be the closed-loop $\mathcal{A}$ matrices for controllers $\mathring{\mathcal{K}}_a$ and $\mathring{\mathcal{K}}_b$, respectively. Then $\mathcal{A}_a$ is the coefficient matrix in the left hand side of (2.10), and $\mathcal{A}_b$ is the 2×2 block matrix in the upper left corner of $\mathcal{A}_a$. Due to the structure of $\mathcal{A}_a$, we have

$$\mathrm{eig}(\mathcal{A}_a) = \mathrm{eig}(\mathcal{A}_b) \cup \mathrm{eig}(A_2) \cup \mathrm{eig}(A_3).$$

Since A_2 and A_3 are Hurwitz, satisfaction of (ii) by $\mathcal{A}_a$ implies satisfaction of (ii) by $\mathcal{A}_b$.

Next we consider the case where $\mathring{\mathcal{K}}_b$ is obtained by adding stable unobservable/uncontrollable modes to $\mathring{\mathcal{K}}_a$. Let (A_1, B_1, C_1, D_1) be the state space matrices of $\mathring{\mathcal{K}}_a$. Define $\mathring{\mathcal{K}}_b$ by (2.9) where A_2, A_3, C_2, and B_3 are arbitrary matrices with A_2 and A_3 being Hurwitz. We then see that $\mathring{\mathcal{K}}_b$ satisfies condition (i), or $HX = R$ and (2.10) with $\Xi_b := \mathrm{col}(\Xi_1, \Xi_2, \Xi_3)$, where $\Xi_1 := \Xi_a$, $\Xi_2 = 0$, and Ξ_3 is the unique solution to the Sylvester equation given by the last row block of (2.10). The existence of Ξ_3 is always guaranteed because A_3 and Λ do not share any common eigenvalues. Thus we have shown that there always exists Ξ_b satisfying (i) when $\mathring{\mathcal{K}}_b$ is a controller obtained by adding stable unobservable or uncontrollable modes to $\mathring{\mathcal{K}}_a$. Finally, satisfaction of (ii) by $\mathring{\mathcal{K}}_b$ can be shown in a similar manner to the previous paragraph. ∎

Lemma 3 shows us that the addition or removal of stable unobservable or uncontrollable modes that are decoupled from unstable modes from a controller that solves Problem 1 results in another controller that also solves Problem 1. Combining Lemmas 2 and 3, we can conclude that given any controller equivalent to one that solves Problem 1 must also

solve Problem 1. This property will be very useful in parameterization the set of all feasible controllers that solve Problem 1.

The following result shows that the controller eigenmatrix Ξ can be normalized for the purpose of solving Problem 1.

Lemma 4 *Suppose $\mathring{\mathcal{K}}_a$ solves Problem 1 with $\mathcal{V}_a := col(X, \Xi_a)$. Then there is a controller $\mathring{\mathcal{K}}_b$ equivalent to $\mathring{\mathcal{K}}_a$, that solves Problem 1 with eigenmatrix $\mathcal{V}_b := col(X, \Xi_b)$ where $\Xi_b := col(I, 0)$.*

Proof. Consider the case where $\mathring{\mathcal{K}}_a$ in the statement is dynamic; the static case can be shown similarly. Let x_a be the state vector of $\mathring{\mathcal{K}}_a$, and define $\mathring{\mathcal{K}}_c$ with state vector $x_c := \mathrm{col}(x_a, x_o)$ by adding stable unobservable modes

$$\dot{x}_o = Ax_o + Bu + G(Cx_o - y)$$

to $\mathring{\mathcal{K}}_a$, where G is a matrix such that $A + GC$ is Hurwitz. It can then be verified that the closed-loop system (2.3) satisfies (2.8) with eigenmatrix $\mathcal{V}_c := \mathrm{col}(X, \Xi_c)$ where $\Xi_c := \mathrm{col}(\Xi_a, X)$.

Now, since $\mathcal{V}_a$ is a full column-rank matrix, Ξ_c also has full column rank. Hence, there is a nonsingular matrix T that transforms Ξ_c into the form $T\Xi_c = \Xi_b := \mathrm{col}(I, 0)$. Then, defining $\mathring{\mathcal{K}}_b$ with state vector $x_b := Tx_c$ by the coordinate transformation T on the controller $\mathring{\mathcal{K}}_c$, one can verify that $\mathring{\mathcal{K}}_b$ solves Problem 1 with $\mathcal{V}_b := \mathrm{col}(X, \Xi_b)$. ∎

By Lemma 4, $\mathcal{V}$ in (2.8) can be assumed to have the structure $\mathcal{V} = \mathrm{col}(X, \Xi_o)$ with $X \in \mathbb{R}^{n\times r}$ and $\Xi_o := \mathrm{col}(I_r, 0)$ without loss of generality when searching for the controllers that solve Problem 1. We will thus restrict our attention to the subset of feasible controllers having this structure for the eigenmatrix.

2.2 Separation Principle and State Feedback

Separation principles hold for various control problems including stabilization and H_2 optimal control, where the output feedback design reduces to independent designs of an

observer and a state feedback gain. This section shows that a separation principle also holds for the output feedback eigenstructure assignment, where the problem is broken down into a standard observer design and a state feedback eigenstructure assignment. We will also show how the state feedback problem can be solved, and discuss a subtlety unique to our problem. To this end, let us first state the following.

Theorem 1 (Separation Principle) *There exists an output feedback controller $u = \mathring{\mathcal{K}} y$ that solves Problem 1 if and only if there exists a state feedback controller $u = \mathring{\mathcal{K}}_s x$ that solves Problem 1 with $C = I$. In particular, an output feedback controller that solves Problem 1 is given by*

$$u = \mathring{\mathcal{K}}_s \hat{x}, \quad \dot{\hat{x}} = A\hat{x} + Bu + G(C\hat{x} - y), \tag{2.11}$$

where G is a matrix such that $A + GC$ is Hurwitz, and $\mathring{\mathcal{K}}_s$ is a state feedback controller that solves Problem 1 with $C = I$.

Proof. Suppose there exists an output feedback controller $u = \mathring{K}_o y$ that solves Problem 1. The closed-loop system is given by (2.3) with $\mathcal{A} = \mathsf{A} + \mathsf{B}K_o\mathsf{C}$, where $\mathsf{A} = \mathrm{diag}(A, 0)$, $\mathsf{B} = \mathrm{diag}(B, I)$, and $\mathsf{C} = \mathrm{diag}(C, I)$, with identity and zero matrices of dimension equal to the controller order. We then see that the state feedback controller $u = \mathring{K}_s x$ with $K_s := K_o\mathsf{C}$ solves Problem 1. Thus, if there exists an output feedback controller that solves Problem 1, then there exists a state feedback controller that solves Problem 1 with $C = I$.

To show the converse, suppose there exists a state feedback controller $u = \mathring{\mathcal{K}}_s x$ that solves Problem 1 with $C = I$, i.e., conditions (i) and (ii) of Lemma 1 are satisfied for $\mathcal{A} = \mathcal{A}_s := \mathsf{A} + \mathsf{B}\mathcal{K}_s$ and some matrix $\mathcal{V} = \mathcal{V}_s := \mathrm{col}(X, \Xi_s)$. With this $\mathring{\mathcal{K}}_s x$, consider the controller in (2.11) and the closed-loop system

$$\begin{bmatrix} \dot{\mathfrak{x}}_s \\ \dot{e} \end{bmatrix} = \begin{bmatrix} \mathcal{A}_s & * \\ 0 & A + GC \end{bmatrix} \begin{bmatrix} \mathfrak{x}_s \\ e \end{bmatrix}. \tag{2.12}$$

where $e := \hat{x} - x$, $\mathfrak{x}_s := \mathrm{col}(x, x_s)$, and x_s is the state vector associated with the dynamics of $\mathring{\mathcal{K}}_s$. Because $\mathcal{A} := \mathcal{A}_s$ satisfies conditions (i) and (ii) of Lemma 1 and $A + GC$ is Hurwitz,

the closed-loop eigenvalues are the eigenvalues of Λ with the rest having negative real-parts. Thus, condition (ii) is satisfied. Furthermore, the eigenvectors of (2.12) associated with Λ are given by $\mathrm{col}(\mathcal{V}_s, 0)$, implying that condition (i) is satisfied with eigenvector $\mathcal{V} := \mathrm{col}(\mathcal{V}_s, X)$ for the closed-loop system with the original state coordinates $\mathfrak{x} := \mathrm{col}(\mathfrak{x}_s, \hat{x})$. ∎

Since the observer design is trivial, Problem 1 is essentially reduced to a state feedback eigenstructure assignment. The following is the solution to the *static* state feedback case.

Theorem 2 (Static State Feedback) *Consider Problem 1 with $C = I$. The following statements are equivalent.*

(i) There exists a static state feedback controller $u = Kx$ that solves Problem 1.

(ii) There exist matrices F and full column-rank X satisfying

$$AX + BF = X\Lambda, \quad HX = R. \tag{2.13}$$

In this case, all such controllers are parametrized by

$$u = Kx, \quad K := FX^\dagger + ZY^\dagger, \tag{2.14}$$

where Z is an arbitrary matrix such that

$$eig(Y^\dagger AY + Y^\dagger BZ) \subset \mathbb{C}_-, \tag{2.15}$$

and Y is the orthogonal complement of X.

Proof. Suppose (i) holds. Then the conditions in Lemma 1 are satisfied for $\mathcal{A} := A + BK$, $\mathcal{H} := H$, and $\mathcal{V} = X$ with some full column-rank matrix X. Defining $F = KX$, the conditions in (2.13) are satisfied. Thus, we have (i) $\Rightarrow$ (ii). To see the converse, define a state feedback controller by (2.14) and note that Z satisfying (2.15) always exists because stabilizability of (A, B) implies stabilizability of $(Y^\dagger AY, Y^\dagger B)$. Applying a similarity transformation to $A + BK$, we have

$$\begin{bmatrix} X^\dagger \\ Y^\dagger \end{bmatrix} (A + BK) \begin{bmatrix} X & Y \end{bmatrix} = \begin{bmatrix} \Lambda & * \\ 0 & Y^\dagger(AY + BZ) \end{bmatrix}, \tag{2.16}$$

where $*$ denotes irrelevant entries. Because $Y^\dagger(AY + BZ)$ is Hurwitz, we see that (2.14) is a static controller that solves Problem 1 and therefore, (ii) $\Rightarrow$ (i). It remains to show that all feasible state feedback gains are given by (2.14) for some F and Z satisfying (2.13) and (2.15). Let $u = Kx$ be a controller solving Problem 1 with eigenmatrix X. Define $F := KX$ and $Z := KY$ so that (2.14) holds. Then, F satisfies (2.13), which further implies that (2.16) holds, and thus Z satisfies (2.15). ∎

Condition (2.13) is similar to the regulator equation that gives solvability of the output regulation problem [42], and has arisen in the context of eigenstructure assignment [35] and output synchronization [1], topics associated with Problem 1.

Solvability of Problem 1 under static feedback requires existence of F and full column-rank X satisfying (2.13), but the full rank requirement is restrictive in general. Consider, for example the case in which

$$A = \begin{bmatrix} -1 & 0 \\ 0 & -1 \end{bmatrix}, \quad B = \begin{bmatrix} 0 \\ 1 \end{bmatrix}, \quad H = \begin{bmatrix} 2 & 1 \\ 0 & 3 \end{bmatrix}, \quad \Lambda = \begin{bmatrix} 0 & 1 \\ 0 & 0 \end{bmatrix}, \quad R = \begin{bmatrix} 1 & 2 \\ 3 & 6 \end{bmatrix}.$$

The target trajectory is given by

$$\zeta(t) = Re^{\Lambda t}\eta(0) = (a + b\,t) \begin{bmatrix} 1 \\ 3 \end{bmatrix}, \quad \begin{array}{l} a := \eta_1(0) + 2\eta_2(0), \\ b := \eta_2(0). \end{array}$$

In this case, there is a unique solution (X, F) satisfying (2.13):

$$X = \begin{bmatrix} 0 & 0 \\ 1 & 2 \end{bmatrix}, \quad F = \begin{bmatrix} 1 & 3 \end{bmatrix}.$$

The matrix X does not have full column rank, implying that there is no *static* state feedback controller to achieve the output pattern formation. However, the existence of solution (X, F) to (2.13) turns out to imply that the problem can be solved by a *dynamic* state feedback controller. This is shown as a special case of the general result presented in the next section.

2.3 General Solution

This section provides a general and complete solution to Problem 1 with no assumptions on the controller structure (e.g. observer-based). The following result gives a necessary and sufficient condition for solvability of Problem 1, and a parametrization of all feasible controllers.

Theorem 3 (General Dynamic Output Feedback) *The following statements are equivalent.*

(i) There exists a controller that solves Problem 1.

(ii) There exist matrices F and X such that (2.13) holds.

In this case, all such controllers are captured as those equivalent to the class of controllers parametrized by

$$\begin{bmatrix} u \\ \dot{\xi} \end{bmatrix} = \begin{bmatrix} F \\ \Lambda \end{bmatrix} \xi + \mathring{Q}(y - CX\xi). \tag{2.17}$$

where matrices F and X satisfy (2.13), and $\mathring{Q}$ stabilizes the augmented plant $(A, \mathfrak{B}, C)$ where $\mathfrak{B} := \begin{bmatrix} B & -X \end{bmatrix}$.

Proof. See Appendix C. ∎

The controller in (2.17) is illustrated in Fig. 2.5. We see that the internal model of the targeted eigenstructure is embedded in the controller. The mechanisms underlying the pattern formation is most evident when the plant is stable. In this situation, choosing $\mathring{Q}$ to be zero makes the transfer function from y to u zero and reduces (2.17) to the open-loop control

$$u = F\xi, \quad \dot{\xi} = \Lambda\xi,$$

and the control input u to the plant is nonzero when $\xi(0) \neq 0$ because of the internal model. With this controller, the closed-loop system satisfies the eigenstructure condition

$$\begin{bmatrix} A & BF \\ 0 & \Lambda \end{bmatrix} \begin{bmatrix} X \\ I \end{bmatrix} = \begin{bmatrix} X \\ I \end{bmatrix} \Lambda, \quad HX = R,$$

and the reference signal $F\xi$ drives the stable plant as

$$\begin{aligned} & \dot{x} = Ax + BF\xi \\ \Rightarrow \quad & \dot{x} = Ax + (X\Lambda - AX)\xi \\ \Rightarrow \quad & \dot{x} - X\dot{\xi} = A(x - X\xi) \\ \Rightarrow \quad & \|x(t) - X\xi(t)\| \to 0 \\ \Rightarrow \quad & z(t) = Hx(t) \to HXe^{\Lambda t}\xi(0) = Re^{\Lambda t}\xi(0). \end{aligned}$$

Thus the rate of convergence $z(t) \to \zeta(t)$ is determined by A. In the general case with nonzero $\mathring{Q}$, we have similar equations:

$$\begin{aligned} & \dot{x} - X\dot{\xi} = (A + \mathfrak{B}\mathring{Q}C)(x - X\xi), \\ & \dot{\xi} = \Lambda\xi + \mathring{Q}_2 C(x - X\xi), \end{aligned} \tag{2.18}$$

where $\mathring{Q} = \mathrm{col}(\mathring{Q}_1, \mathring{Q}_2)$, and the rate of convergence is dictated by the dynamics of $A + \mathfrak{B}\mathring{Q}C$ instead of A.

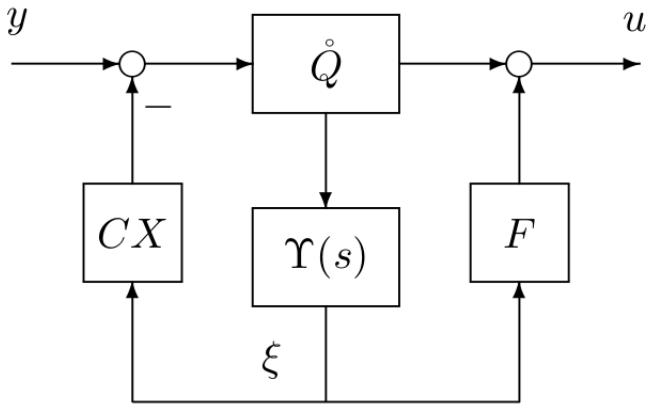

Figure 2.5: Block diagram of controller in (2.17.) where $\Upsilon(s) := (sI - \Lambda)^{-1}$

Given the parameterization in (2.17), the maximum controller order necessary to solve Problem 1 is determined as sum of the dimension of $\xi(t) \in \mathbb{R}^r$, and the order of the system $\mathring{Q}$ that stabilizes the augmented plant. Under state feedback, $\mathring{Q}$ can be a static gain, and the controller order is r. Under output feedback, there always exists a stabilizing controller of order less than or equal to the plant order, n, so Problem 1 can be solved with a controller of order less than or equal to $n + r$.

In these cases, the internal model explicitly appears in the controller (2.17), accounting for part of the controller state space of dimension r. However, when X is full column-rank, the internal model can be made implicit by embedding it as part of the plant or observer state space, thereby reducing the controller order. In particular, Problem 1 can be solved with a static gain under state feedback (Theorem 2) or an observer-based controller of the plant order under output feedback (Theorem 1). These results are special cases of Theorem 3.

The state feedback result in Theorem 2 is obtained by setting $\mathring{Q}$ to be a static gain of the form $\mathrm{col}(K, J)$ in Theorem 3. Let K be chosen as in (2.14), and J be any matrix that makes $\Lambda - JX$ Hurwitz. This choice of $\mathring{Q}$ stabilizes the augmented plant with $C = I$, and reduces the controller in (2.17) to

$$u = Kx, \quad \dot{\xi} = \Lambda\xi + J(x - X\xi).$$

The dynamics of ξ are made stable by J, and are unobservable from u. Therefore, ξ can be removed to yield the static control $u = Kx$. Note that the internal model (Λ, X) is no longer explicit but is embedded in the plant state space as in (2.16).

The observer-based controller (combination of Theorems 1 and 2) can also be parameterized by (2.17) with a specific choice of $\mathring{Q}$. In particular, $q = \mathring{Q}w$ is a dynamic system of the form

$$\begin{aligned}
\dot{x}_q &= Y^\dagger(A + BK + GC)Yx_q - Y^\dagger Gw \\
q &= \begin{bmatrix} KY \\ X^\dagger(A + BK + GC)Y \end{bmatrix} x_q - \begin{bmatrix} 0 \\ X^\dagger G \end{bmatrix} w
\end{aligned}$$

where observer gain G and state feedback gain K are specified as in Theorems 1 and 2. It can be shown that this $\mathring{Q}$ of order $n - r$ stabilizes the augmented plant. Under a change of coordinates defined by $\hat{x} = X\xi + Yx_q$ on the state $\mathrm{col}(\xi, x_q)$ of (2.17), we can obtain the controller in (2.11) with $\mathring{\mathcal{K}}_s := K$.

2.4 Further Separation for Natural Eigenstructure Assignment

Consider the case where the target eigenstructure (R, Λ) is already embedded in the plant as part of its natural dynamics:

$$AX = X\Lambda, \quad HX = R, \tag{2.19}$$

with some full column-rank X. The goal is to stabilize the remaining dynamics without affecting the natural eigenstructure. Since solvability (2.13) is confirmed with $F = 0$, Theorem 3 can be used to solve Problem 1. However, property (2.19) turns out to permit an additional separation principle. We start with the simplest case of full control ($B = I$), state feedback ($C = I$).

Lemma 5 (Full Control, State Feedback) *Consider Problem 1 with $B = C = I$. Suppose there exists a full column-rank matrix X satisfying (2.19). Then, the controller $u = -Lx$ solves Problem 1 if L is chosen such that $LX = 0$ and $A - L$ has eigenvalues eig(Λ) with the rest having negative real parts.*

Proof. Noting that the closed-loop system satisfies

$$(A - L)X = X\Lambda,$$

the result follows directly from Lemma 1. ∎

The following result shows a separation principle for the state feedback case where Problem 1 is reduced to a standard state feedback stabilization and an eigenstructure assignment with full control, state feedback.

Lemma 6 *Consider Problem 1 with state feedback ($C = I$) and suppose there exists a full column-rank matrix X satisfying (2.19). Let K be a state feedback gain to stabilize $A + BK$, and introduce the pre-compensator*

$$u = Kx_s, \quad \dot{x}_s = Ax_s + Bu + v, \tag{2.20}$$

such that the augmented plant is described by

$$\dot{\varepsilon} = A\varepsilon + v, \quad \varepsilon := x - x_s,$$

where v is the new control input. Then, the controller (2.20) with $v = -L\varepsilon$ solves Problem 1 if L is a static gain satisfying the conditions in Lemma 5.

Proof. The closed-loop system can be written as

$$\begin{bmatrix} \dot{x} \\ \dot{x}_s \end{bmatrix} = \begin{bmatrix} A & BK \\ L & A + BK - L \end{bmatrix} \begin{bmatrix} x \\ x_s \end{bmatrix}.$$

By Lemma 5, we have $LX = 0$ and the above system satisfies condition (i) of Lemma 1 with eigenmatrix $\mathcal{V} := \mathrm{col}(X, 0)$.

Defining $e_s = x - x_s$, the system can be rewritten as

$$\begin{bmatrix} \dot{e}_s \\ \dot{x}_s \end{bmatrix} = \begin{bmatrix} A - L & 0 \\ L & A + BK \end{bmatrix} \begin{bmatrix} e_s \\ x_s \end{bmatrix}.$$

By definition, $A + BK$ is Hurwitz and the eigenvalues of $A - L$ not shared by Λ are also stable. Thus, condition (ii) of Lemma 1 is satisfied and the controller solves Problem 1. ∎

The controller in Lemma 6 is a dynamic state feedback controller with an observer-based structure:

$$u = Kx_s, \quad \dot{x}_s = Ax_s + Bu + L(x - x_s). \tag{2.21}$$

While a state observer within a state feedback controller is unusual, this control architecture is beneficial for the eigenstructure assignment. In fact, the x_s dynamics do not constitute an observer in a strict sense; x_s does not converge to x since the eigenvalues of Λ are embedded in the error dynamics $\dot{e}_s = (A - L)e_s$. Using the core idea from Lemma 6, let us state the general separation result for the output feedback case.

Theorem 4 (Separation with Double Observers) *Consider Problem 1 and suppose there exists a full column-rank matrix X satisfying (2.19). Then, a feasible controller is given by*

$$\begin{aligned} u = Kx_s, \quad & \dot{x}_s = Ax_s + Bu + L(x_o - x_s), \\ & \dot{x}_o = Ax_o + Bu + G(Cx_o - y), \end{aligned} \tag{2.22}$$

where K and G stabilize $A + BK$ and $A + GC$, and $u = -Lx$ solves Problem 1 with $B = C = I$.

Proof. The result follows directly from an application of Theorem 1 and Lemma 6. ∎

Theorem 4 shows that the output feedback problem can be separated into three independent designs; state feedback stabilization with K, standard observer with G, and state feedback, full control eigenstructure assignment with L. The resulting controller has a double observer structure, and is not of minimal order due to the dynamics associated with x_s. Although the natural eigenstructure assignment can be solved without the x_s dynamics by choosing the static gain K from Theorem 2, the use of an additional observer shifts the search for a controller that solves Problem 1 for the general plant (A, B, C) to a search for a controller that solves Problem 1 for the plant with $B = C = I$. The controller gain, L is not restricted by the plant input/output structure, permitting flexibility in the controller structure. The benefit of this property becomes apparent when it is applied to multi-agent problems for which a communication topology is a common constraint. The basic idea is to use block-diagonal K and G to stabilize the agents by local minor feedback, and then add inter-agent coupling through L to achieve coordination between agents. We will explore this idea in the next section.

CHAPTER 3

Structured Eigenstructure Assignment for Multi-agent Systems

The multi-agent pattern formation problem falls under a special case of our eigenstructure assignment framework for which a structured controller is designed for a structured plant. We consider the design of feedback controllers for linear heterogeneous agents with the objective that selected outputs of the k^{th} agent exponentially converge to $R_k e^{\Lambda t}\eta_o$ for some η_o, where information is exchanged between selected agents. Synchronization occurs in a special case where the same R_k is used for all agents. Our approach utilizes our general eigenstructure theory and separation principles to design local controllers that assign the desired dynamics to "homogenize" the modified agents, sharing the same spirit as in [38]. We then apply a standard result for synchronization of homogeneous agents [34] to achieve the desired formation between agents. Unlike the previous results, our controller solves the pattern formation problem with no restrictions on the agent dynamics, exploiting sensory feedback from neighboring agents.

In this chapter, we will consider a special class of the eigenstructure assignment problem; the design of a structured controller for pattern formation between heterogeneous linear agents. In particular, the control objective is to make selected outputs of every agent converge to desired trajectories described by (2.4). We assume that agents must respect communication constraints; the control input to a specific agent may depend only on information from itself and neighboring agents. A general controller that requires no assumptions on plant dynamics is provided to solve the heterogeneous multi-agent pattern formation problem and various special cases for controller order reduction are discussed. Three examples are provided to demonstrate how the eigenstructure theory can be utilized for structured

controller design. In the first example, we consider a multi-agent system where the desired steady-state behavior is described by a single eigenvalue/eigenvector pair; this will illustrate how the controller complexity can be greatly simplified when the plant and assigned eigenstructure satisfies certain properties. In the second example, we juxtapose the performance of our general pattern formation controller with the one proposed by [1], specifically noting the difference in synchronization behavior between the two controllers when subjected to a disturbance. Finally, in the third example, we touch on the possiblity of extending the linear pattern formation problem by considering the addition of a nonlinearity to the control input of a single agent in order to lock the amplitude of a multi-agent design for coordinated oscillations.

3.1 General Multi-Agent Pattern Formation Theory

Let us first consider the set of N introspective agents, where the dynamics of the k^{th} agent are given by

$$\dot{x}_k = A_k x_k + B_k u_k, \quad y_k = C_k x_k, \quad z_k = H_k x_k, \tag{3.1}$$

for $k \in \mathbb{I}_N$, where (A_k, B_k) is stabilizable, (H_k, A_k) and (C_k, A_k) are detectable, and n_k is the dimension of state x_k. The system can be described by (2.1) with x and A defined by

$$x := \mathrm{col}(x_1, \ldots, x_N), \quad A = \mathrm{diag}(A_1, \ldots, A_N), \tag{3.2}$$

and other signals and matrices are defined similarly.[1] Let a matrix with non-negative eigenvalues $\Lambda \in \mathbb{R}^{r \times r}$, matrices $R_k \in \mathbb{R}^{h_k \times r}$, and sets of integers $\mathbb{N}_k \subseteq \mathbb{I}_N$ for $k \in \mathbb{I}_N$ be given, where $\mathbb{N}_k$ specifies the neighbors of agent k, from which information may be communicated, and by definition $k \notin \mathbb{N}_k$. We will design a distributed controller of the form

$$\begin{bmatrix} u_k \\ \varepsilon_k \end{bmatrix} = \mathring{\mathcal{K}}_k \begin{bmatrix} y_k \\ v_k \end{bmatrix}, \quad v = -L\varepsilon, \tag{3.3}$$

[1] For the remainder of this chapter, we will use this notation. That is, when constants and signals are defined by capital and lower case letters with subscripts $k \in \mathbb{I}_N$ (e.g., A_k and x_k), the same symbols without the subscripts (e.g., A and x) denote the corresponding block-diagonal matrix and the column vector defined similarly to (3.2). This notation is used whenever a symbol appears with and without the subscript k, except for R, X and F that are defined by stacking R_k, X_k and F_k, respectively, in a column.

where L provides the inter-agent coupling, such that the outputs of the agents satisfy $z_k(t) \to R_k e^{\Lambda t}\eta_o$ for some $\eta_o \in \mathbb{R}^r$ depending on the initial state. More precisely, we will solve Problem 1 with the block-diagonal plant (3.1) to find the structured controller (3.3) that assigns the eigenstructure (Λ, R) with $R := \mathrm{col}(R_1, \ldots, R_N)$. This is a general pattern formation problem on the outputs z_k; when $R_k = R_o$ for all $k \in \mathbb{I}_N$, we obtain a consensus problem.

We define $\mathbb{L} \subset \mathbb{R}^{N\times N}$ as the set of Laplacian matrices $\mathcal{L}$ for directed graphs, containing a spanning tree, with positive weights. That is, $\mathcal{L} \in \mathbb{L}$ if and only if $\mathcal{L}$ satisfies the following properties: (a) the row sum is equal to zero, (b) all the off-diagonal entries are nonpositive, and (c) at least one of the cofactors is nonzero. It is well known that such $\mathcal{L} \in \mathbb{L}$ has a simple eigenvalue at the origin, and the rest of the eigenvalues are in the open right-half plane [30]. For a given $\Lambda \in \mathbb{R}^{r\times r}$, we denote by $\mathbb{L}_\Lambda$ the set of $\mathcal{L} \in \mathbb{L}$ such that the smallest real-part of the nonzero eigenvalues of $\mathcal{L}$ is greater than the largest real part of the eigenvalues of Λ. For the control design, we assume that the directed graph specified by $\mathbb{N}_k$ contains a spanning tree, and consider the Laplacian $\mathcal{L} \in \mathbb{L}$ satisfying

$$\begin{array}{l} \mathcal{L}_{k\ell} \leq 0 \text{ for } \ell \in \mathbb{N}_k, \\ \mathcal{L}_{k\ell} = 0 \text{ for } \ell \notin \mathbb{N}_k \cup \{k\}, \end{array} \qquad \mathcal{L}_{kk} = -\sum_{\ell\in\mathbb{N}_k} \mathcal{L}_{k\ell}. \tag{3.4}$$

where the digraph topology is specified by $\mathbb{N}_k$ for $k \in \mathbb{I}_N$.

The following result is instrumental for later developments.

Lemma 7 *Let $\Lambda \in \mathbb{R}^{r\times r}$ and $\mathcal{L} \in \mathbb{L}_\Lambda$ be given. Then*

$$\begin{array}{l} (\boldsymbol{\Lambda} - L)\mathfrak{J} = \mathfrak{J}\Lambda, \\ \boldsymbol{\Lambda} := I_N \otimes \Lambda, \quad L := \mathcal{L} \otimes I_r, \quad \mathfrak{J} := col(I_r, \ldots, I_r) \end{array} \tag{3.5}$$

holds, and the eigenvalues of $\boldsymbol{\Lambda} - L$ other than those of Λ have negative real parts. Consequently, we have

$$\dot{\varepsilon} = (\boldsymbol{\Lambda} - L)\varepsilon \quad \Rightarrow \quad \varepsilon(t) \to \mathfrak{J}e^{\Lambda t}c \tag{3.6}$$

for some constant vector c dependent on $\varepsilon(0)$.

Proof.

The following lemmas are useful.

Lemma 8 *[43] For square matrices A and B of dimensions n and m, the eigenvalues of $A \otimes B$ are given by $\lambda_i \mu_j$ with $i \in \mathbb{I}_n$ and $j \in \mathbb{I}_m$, where λ_i and μ_i are the eigenvalues of A and B, respectively.*

Lemma 9 *[30] The Laplacian, $\mathcal{L}$, of a directed graph with a directed spanning tree and adjacency matrix with non-negative weights has a simple eigenvalue at the origin with the rest in the open right-half plane.*

Lemma 10 *[44] If matrices $A, B \in \mathbb{C}^{n \times n}$ commute, then they can be simultaneously triangularized. That is, there exists a $U \in \mathbb{C}^{n \times n}$ such that both $U^{-1}AU$ and $U^{-1}BU$ are upper triangular matrices.*

We now prove Lemma 7. Equation (3.5) is verified by noting that $\Lambda \mathcal{J} = \mathcal{J} \Lambda$ and $L\mathcal{J} = 0$. By Lemma 8, the eigenvalues of L are those of $\mathcal{L}$ with each having a multiplicity of r. Furthermore, Lemma 9 implies that L has r eigenvalues at the origin with the others having strictly positive real part. Additionally, the eigenvalues of $\mathbf{\Lambda}$ are those of Λ, each repeated N times. By Lemma 10 we can define a U such that $U^{-1}\mathbf{\Lambda}U$ and $U^{-1}LU$ are both upper triangular since $\mathbf{\Lambda}$ and L commute. This implies that the eigenvalues of $\mathbf{\Lambda} - L$ are the difference of the eigenvalues of $\mathbf{\Lambda}$ and L, i.e., $\lambda_i - \mu_j$ with λ_i for $i \in \mathbb{I}_r$ from Λ and μ_j for $j \in \mathbb{I}_N$ from $\mathcal{L}$. Thus, r eigenvalues of $\mathbf{\Lambda} - L$ coincide with those of Λ, and the remaining have strictly negative real parts due to $\mathcal{L} \in \mathbb{L}_\Lambda$. Finally, (3.6) follows from a standard linear system theory. ∎

This result is directly useful for solving the pattern formation problem for multi-agents with homogeneous dynamics.

Lemma 11 (Homogeneous Multi-agents) *Consider Problem 1 for the multi-agent plant given by (3.1). Suppose $A_k = \Lambda$ and $C_k = H_k = R_k = I$ for all $k \in \mathbb{I}_N$. Then the controller*

(2.21) solves Problem 1 if

$$K := diag(K_1, \ldots, K_N), \quad L := \mathcal{L} \otimes I,$$

where $\mathcal{L} \in \mathbb{L}_\Lambda$ *and* $\Lambda + B_k K_k$ *is Hurwitz.*

Proof. Define a controller by (2.21). The closed-loop system can be written as

$$\begin{bmatrix} \dot{x} \\ \dot{x}_s \end{bmatrix} = \begin{bmatrix} \boldsymbol{\Lambda} & BK \\ L & \boldsymbol{\Lambda} + BK - L \end{bmatrix} \begin{bmatrix} x \\ x_s \end{bmatrix},$$

where $\boldsymbol{\Lambda} = I_N \otimes \Lambda$. Due to the structure of L, we note that $L\mathcal{I} = 0$ where $\mathcal{I} = \mathrm{col}(I_r, \ldots, I_r)$ and moreover,

$$\begin{bmatrix} \boldsymbol{\Lambda} & BK \\ L & \boldsymbol{\Lambda} + BK - L \end{bmatrix} \begin{bmatrix} \mathcal{I} \\ 0 \end{bmatrix} = \begin{bmatrix} \mathcal{I} \\ 0 \end{bmatrix} \Lambda,$$

which implies that (i) is satisfied for $\mathcal{V} = \mathrm{col}(\mathcal{I}, 0)$. Under a coordinate transformation, $e_s = x - x_s$, the system can be rewritten as

$$\begin{bmatrix} \dot{e}_s \\ \dot{x}_s \end{bmatrix} = \begin{bmatrix} \boldsymbol{\Lambda} - L & 0 \\ L & \boldsymbol{\Lambda} + BK \end{bmatrix} \begin{bmatrix} e_s \\ x_s \end{bmatrix}.$$

It is clear that the eigenvalues of this system are the union of the eigenvalues of $\boldsymbol{\Lambda} - L$ and the eigenvalues of $\boldsymbol{\Lambda} + BK$. By definition, $\boldsymbol{\Lambda} + BK$ is Hurwitz and from Lemma 7, $\boldsymbol{\Lambda} - L$ shares eigenvalues with Λ, and the rest in the open left-half plane. Thus we can conclude that the controller (2.21)solves Problem 1 when the conditions in (11) are satisfied.

■

The essential part of the result has appeared in [34]. Our contribution is to explicitly show the underlying principles for the control law within the framework of natural eigenstructure assignment. More importantly, this result is essential for the heterogeneous multi-agent pattern formation problem because the general heterogeneous problem can be reduced to a homogeneous one through local feedback as we show below.

Theorem 5 *Consider Problem 1 for the multi-agent plant given by (3.1) with signals and matrices defined as in (3.2). The following statements are equivalent.*

(i) Problem 1 is solvable by a controller (2.2).

(ii) There exist F_k and X_k such that

$$A_k X_k + B_k F_k = X_k \Lambda, \quad H_k X_k = R_k, \quad k \in \mathbb{I}_N. \tag{3.7}$$

Suppose these conditions hold, let $\mathcal{L} \in \mathbb{L}_\Lambda$ be given, and for each $k \in \mathbb{I}_N$, let G_k, Φ_k, K_k, and J_k be chosen to make the following three matrices Hurwitz:

$$A_k + G_k C_k, \;\; \Lambda + \Gamma_k \Phi_k, \;\; \Omega_k := A_k + B_k K_k - X_k J_k, \tag{3.8}$$

where Γ_k is defined using the unique solution M_k to the Sylvester equation:

$$\Lambda M_k - M_k \Omega_k = J_k, \quad \Gamma_k = \begin{bmatrix} M_k B_k & I - M_k X_k \end{bmatrix}.$$

Then the distributed controller given by

$$\dot{\hat{x}}_k = A_k \hat{x}_k + B_k u_k + G_k (C_k \hat{x}_k - y_k) \tag{3.9}$$

$$\dot{\hat{\eta}}_k = \Lambda \hat{\eta}_k + \Gamma_k w_k + v_k, \quad w_k = \Phi_k \hat{\eta}_k, \quad \varepsilon_k = \hat{\eta}_k - \eta_k, \tag{3.10}$$

$$\begin{bmatrix} \eta_k \\ u_k \\ \dot{\xi}_k \end{bmatrix} = \begin{bmatrix} I \\ F_k \\ \Lambda \end{bmatrix} \xi_k + \begin{bmatrix} M_k \\ K_k \\ J_k \end{bmatrix} (\hat{x}_k - X_k \xi_k) + \begin{bmatrix} 0 & 0 \\ I & 0 \\ 0 & I \end{bmatrix} w_k, \tag{3.11}$$

$$v = -L\varepsilon, \quad L = \mathcal{L} \otimes I_r, \tag{3.12}$$

solves Problem 1, where $k \in \mathbb{I}_N$.

Proof.

The equivalence (i) $\Leftrightarrow$ (ii) follows directly from Theorem 3. It remains to show that if the conditions in (3.7) hold, the controller presented in (3.9)- (3.12) yields the closed-loop system satisfying the conditions in Lemma 1 and solves Problem 1. In view of Theorem 1, it suffices to show that the state feedback controller $u = \mathring{\mathcal{K}} x$ with $\mathring{\mathcal{K}}$ specified by (3.10)-(3.12) with $\hat{x}_k$ replaced by x_k solves Problem 1.

The closed-loop system in (2.3) is given by

$$\begin{bmatrix} \dot{x} \\ \dot{\xi} \\ \dot{\hat{\eta}} \end{bmatrix} = \begin{bmatrix} A+BK & B(\mathcal{F}-K\mathcal{X}) & B\mathcal{O} \\ J & \Lambda - J\mathcal{X} & \mathcal{P} \\ LM & L(I-M\mathcal{X}) & \Lambda+\Gamma\Phi-L \end{bmatrix} \begin{bmatrix} x \\ \xi \\ \hat{\eta} \end{bmatrix}$$

where $\mathcal{F}$, $\mathcal{X}$, $\mathcal{O}$, and $\mathcal{P}$ are block diagonal matrices with F_k, X_k, $\mathcal{O}_k$, and $\mathcal{P}_k$ on the diagonal, respectively, and $\mathcal{O}_k$ and $\mathcal{P}_k$ are defined by $\Phi_k = \mathrm{col}(\mathcal{O}_k, \mathcal{P}_k)$. It can readily be verified through direct calculations that the system satisfies condition (i) of Lemma 1 with $\mathcal{V} = \mathrm{col}(X, \mathcal{I}, 0)$, where we note that $L\mathcal{I} = 0$, $\Lambda J = J\Lambda$, $\mathcal{F}\mathcal{I} = F$, and $\mathcal{X}\mathcal{I} = X$.

Using a coordinate transformation $(x, \xi, \hat{\eta}) \leftrightarrow (\eta, e, \varepsilon)$, the closed-loop system can be rewritten as

$$\begin{bmatrix} \dot{\eta} \\ \dot{e} \\ \dot{\varepsilon} \end{bmatrix} = \begin{bmatrix} \Lambda+\Gamma\Phi & 0 & \Gamma\Phi \\ \mathcal{B}\Phi & \Omega & \mathcal{B}\Phi \\ 0 & 0 & \Lambda - L \end{bmatrix} \begin{bmatrix} \eta \\ e \\ \varepsilon \end{bmatrix}, \quad \begin{aligned} \eta &:= \xi + Me, \\ e &:= x - \mathcal{X}\xi, \\ \varepsilon &:= \hat{\eta} - \eta. \end{aligned}$$

where $\mathcal{B}$ is the block diagonal matrix with $\mathcal{B}_k := [\ B_k\ \ -X_k\ ]$ on the diagonal. We then see that condition (ii) of Lemma 1 is satisfied due to the Hurwitz requirement for (3.8) and Lemma 7. ∎

The pattern formation mechanism underlying the controller in Theorem 5 is best illustrated in Figs. 3.1, 3.2, and 3.3 and works in two distinct steps; the first is a local controller design (Figs. 3.1 and 3.2) to assign the eigenstructure of the desired dynamics to each agent and homogenize the group, and the second is the inter-agent coupling to reach the desired formation through information exchange between neighboring agents (Fig. 3.3). To better see this, consider the case in which full-state feedback is available ($C_k = I$) and the observer in (3.9) is replaced by $\hat{x}_k = x_k$. We first apply Theorem 3 to assign the eigenstructure (Λ, X_k) to each agent with $Q_k := \mathrm{col}(K_k, J_k)$ and introduce an auxiliary input w_k. This local controller is given by (3.11) with each agent under minor feedback described by

$$\begin{bmatrix} \dot{x}_k \\ \dot{\xi}_k \end{bmatrix} = \begin{bmatrix} A_k + B_k K_k & B_k(F_k - K_k X_k) \\ J_k & \Lambda - J_k X_k \end{bmatrix} \begin{bmatrix} x_k \\ \xi_k \end{bmatrix} + \mathsf{B}_k w_k.$$

where $\mathtt{B}_k := \mathrm{diag}(B_k, I)$. By applying a coordinate transformation (see Lemma 12 in the appendix) defined by

$$\begin{bmatrix} \eta_k \\ \theta_k \end{bmatrix} = \begin{bmatrix} M_k & I - M_k X_k \\ I & -X_k \end{bmatrix} \begin{bmatrix} x_k \\ \xi_k \end{bmatrix},$$

dynamics for desired formation and the rest are decoupled as

$$\begin{bmatrix} \dot{\eta}_k \\ \dot{\theta}_k \end{bmatrix} = \begin{bmatrix} \Lambda & 0 \\ 0 & \Omega_k \end{bmatrix} \begin{bmatrix} \eta_k \\ \theta_k \end{bmatrix} + \begin{bmatrix} \Gamma_k \\ \mathcal{B}_k \end{bmatrix} w_k,$$

where $\mathcal{B}_k := [\ B_k\ \ -X_k\ ]$. Leaving the stable dynamics θ_k unobservable, the agent with the local controller is given by $\mathring{S}_k$ in Fig. 3.1. The modified agents now share homoge-

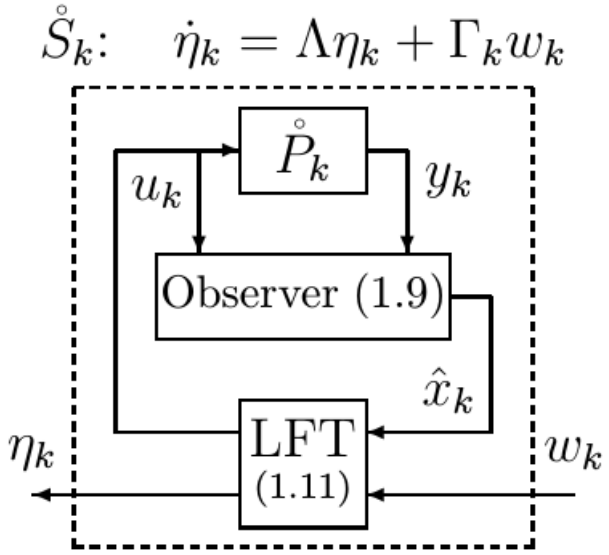

Figure 3.1: Local feedback for quasi-homogeneous state feedback agents

neous dynamics Λ. Using the idea in Lemma 6 to achieve separation, we introduce the pre-compensator in (3.10) and obtain the augmented agents $\mathring{S}_o$ as in Fig. 3.2. At this point, the agents $\mathring{S}_o$ are set up so that $z_k(t) \to R_k e^{\Lambda t}\varepsilon_o$ holds if $\varepsilon_k(t) \to -e^{\Lambda t}\varepsilon_o$ for some ε_o. We now see that the original problem with heterogeneous agents reduced to a problem with full control, state feedback, homogeneous agents $\mathring{S}_o$. By Lemma 7, this problem can be solved by a constant Laplacian gain control L, giving inter-agent coupling (Fig. 3.3).

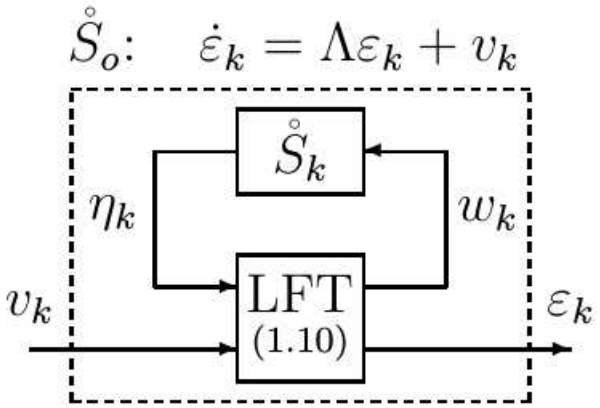

Figure 3.2: Local feedback for homogeneous full control, state feedback agents

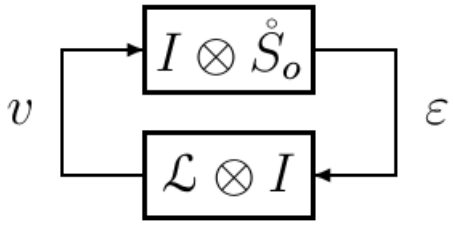

Figure 3.3: Inter-agent coupling for coordination

3.2 Special Cases

Using the idea of equivalence, some of the dynamics of the controller in Theorem 5 can be removed if certain conditions are satisfied, as we will briefly cover in the following three corollaries.

Corollary 1 *If C_k=I, then the observer dynamics in (3.9) can be replaced by $\hat{x}_k := x_k$.*

Proof. Let the controller in Theorem 5 be described by (3.9) and $u_k = \mathring{K}_k\hat{x}_k$, where $\mathring{K}_k$ contains (3.10) and (3.11). Suppose $C_k = I$ and define $e_k = \hat{x}_k - x_k$. Then

$$\dot{e}_k = (A_k + G_k)e_k, \quad u_k = \mathring{K}_k(e_k + x_k).$$

By Lemma 3, since the dynamics for e_k are stable and uncontrollable, we can remove them from the controller. Thus, the controller becomes $u_k = \mathring{K}_k x_k$. ∎

Corollary 2 *If Γ_k is full row-rank, then (3.10) can be replaced by*

$$w_k = -\Gamma_k^\dagger v_k, \quad \varepsilon_k = -\eta_k, \tag{3.13}$$

where $v_k = -L_k\varepsilon$ and L_k is the row block of L associated with agent k.

Proof. See Appendix D. ∎

Corollary 3 *If X_k is full column-rank, then (3.11) can be replaced by*

$$\eta_k = M_k\hat{x}_k, \quad u_k = K_k\hat{x}_k + \begin{bmatrix} I & 0 \end{bmatrix} w_k.$$

where K_k is defined by (2.14) with subscript k added.

Proof. Suppose X_k is full column rank, and define K_k as described. Then there exists J_k that makes Ω_k Hurwitz. In particular, it can be shown through a transformation like (2.16) that Ω_k is Hurwitz if and only if $\Lambda - J_kX_k$ is Hurwitz. Moreover, $A_k + B_kK_k$ contains the desired eigenstructure (X_k, Λ) and the rest of the eigenvalues are in the open left-half plane. Therefore $A_k + B_kK_k$ can be block-diagonalized into $\mathrm{diag}(\Lambda, H_k)$ for some Hurwitz matrix H_k via a similarity transformation of the form $\begin{bmatrix} X_k & * \end{bmatrix}$. Let M_k be the matrix formed by the first r rows of the inverse of this transformation matrix. Then it can be verified that M_k is the unique solution to the Sylvester equation in Theorem 5, and yields $\eta_k = M_k\hat{x}_k$ in (3.11) due to $M_kX_k = I$. Since u_k does not directly depend on ξ_k due to $F_k = K_kX_k$, we see that ξ_k has stable, unobservable dynamics which can be removed from the controller. ∎

Moreover, if every agent satisfies the conditions in the previous three corollaries, then the heterogeneous multi-agent pattern formation problem can be solved with a structured static feedback.

Corollary 4 *In Theorem 5, suppose X_k is full column-rank and Γ_k has full row-rank for all $k \in \mathbb{I}_N$. Then Problem 1 can be solved by a static gain under state feedback, or by an observer-based controller under output feedback:*

$$\dot{\hat{x}}_k = A_k\hat{x}_k + B_ku_k + G_k(C_k\hat{x}_k - y_k), \quad k \in \mathbb{I}_N \tag{3.14}$$

$$u = \mathcal{K}\hat{x}, \quad \mathcal{K} := K - (MB)^\dagger LM, \quad L = \mathcal{L} \otimes I_r \tag{3.15}$$

where $\mathcal{L}$, G_k, X_k, F_k, and Ω_k are specified in Theorem 5, Y_k is the orthogonal complement of X_k, Z_k is chosen such that $Y_k^\dagger \mho_k$ is Hurwitz, and

$$M_k := X_k^\dagger + T_k Y_k^\dagger, \quad \mho_k := A_k Y_k + B_k Z_k,$$
$$\Lambda T_k - T_k \Omega_k = X_k^\dagger \mho_k, \quad K_k := F_k X_k^\dagger + Z_k Y_k^\dagger.$$

Proof. We will show that if the conditions in (3.7) hold, then the controller presented in (3.14) and (3.15) satisfies the conditions of Lemma 1 and solves Problem 1. In view of Theorem 1, it suffices to show that the state feedback controller $u = \mathcal{K}x$ with $\mathcal{K}$ specified by (3.15) solves Problem 1.

Suppose there exist F_k, and X_k satisfying (3.7). Define a controller $u = \mathcal{K}x$ by (3.15) and the subsequent definitions in Corollary 4. The closed-loop system of the N agents with the controller satisfies

$$(A + B\mathcal{K})X = AX + BKX = AX + BF = X\Lambda,$$

where we note that $LMX = L\mathcal{I} = 0$ for $\mathcal{I} := \mathrm{col}(I, \ldots, I)$, and $X :=\mathrm{col}(X_1, \ldots, X_N)$ and $F :=\mathrm{col}(F_1, \ldots, F_N)$. Thus, condition (i) of Lemma 1 holds for $\mathcal{V} = X$. To confirm that all other eigenvalues are in the open left half plane, define X, Y, M, Π, and $\tilde{\Omega}$ to be the block diagonal matrices with X_k, Y_k, M_k, Π_k, and $Y^\dagger \mho$ on the diagonal, where $\Pi_k := Y_k - X_k T_k$. Then applying a similarity transformation, we obtain

$$\begin{bmatrix} M \\ \mathsf{Y}^\dagger \end{bmatrix} (A + B\mathcal{K}) \begin{bmatrix} \mathsf{X} & \Pi \end{bmatrix} = \begin{bmatrix} \Lambda - L & 0 \\ 0 & \tilde{\Omega} \end{bmatrix}$$

where we note that MB has full row rank since Γ_k has full row rank, and

$$\begin{bmatrix} \mathsf{X}^\dagger \\ \mathsf{Y}^\dagger \end{bmatrix} \begin{bmatrix} \mathsf{X} & \mathsf{Y} \end{bmatrix} = I \quad \Rightarrow \quad \begin{bmatrix} M \\ \mathsf{Y}^\dagger \end{bmatrix} \begin{bmatrix} \mathsf{X} & \Pi \end{bmatrix} = I.$$

By Lemma 7, we can conclude that with a Laplacian, $\mathcal{L} \in \mathbb{L}_\Lambda$, the matrix $\Lambda - L$ has eigenvalues in the open left half plane except for one set of eigenvalues at at Λ. Because $Y_k^\dagger \mho_k$ is Hurwitz, then $\tilde{\Omega}$ is implicitly Hurwitz and we now see that condition (ii) of Lemma

1 is satisfied. Therefore, we conclude that the controller provided by in Corollary 4 solves Problem 1. ∎

Condition (3.7) for solvability of the multi-agent pattern formation problem has been obtained in a slightly different setting outside of the eigenstructure assignment framework [1]. The condition was interpreted as the internal model of a virtual exosystem embedded in the dynamics of each agent through local feedback. Our contributions beyond [1] include the general controller formula fully supported by analytical understanding of the controller architecture as described earlier. In fact, the main result (Theorem 5) of [1] can be seen as a special case of the controller from Theorem 5.

To reproduce their controller, we set $J_k = 0$, which results in $M_k = 0$ and $\eta_k = \xi_k$. Let Φ_k have the form $\mathrm{col}(0, \mathcal{P}_k)$. Then the dynamics of $\hat{\eta}$ and ξ reduce to

$$\begin{bmatrix} \dot{\varepsilon} \\ \dot{\hat{\eta}} \end{bmatrix} = \begin{bmatrix} \boldsymbol{\Lambda} - L & 0 \\ -L & \boldsymbol{\Lambda} + \mathcal{P} \end{bmatrix} \begin{bmatrix} \varepsilon \\ \hat{\eta} \end{bmatrix}, \quad \boldsymbol{\Lambda} := I \otimes \Lambda. \tag{3.16}$$

The dynamics of $\hat{\eta}$ can be removed from the controller because

$$\varepsilon_k(t) \to e^{\Lambda t} c, \quad L\varepsilon(t) \to 0, \quad \hat{\eta}(t) \to 0,$$

as seen from Lemma 7 and stability of $\Lambda + \mathcal{P}_k$, and the resulting controller is given by the observer (3.9) and

$$\dot{\varepsilon} = (\boldsymbol{\Lambda} - L)\varepsilon, \quad u_k = F_k \varepsilon_k + K_k(\hat{x}_k - X_k \varepsilon_k), \tag{3.17}$$

where ε_k is redefined as $-\varepsilon_k$, giving the controller in [1].

In this controller, the reference trajectory ε is generated by copies of local internal models $\dot{\varepsilon}_k = \Lambda \varepsilon_k$, interacting with each other through the Laplacian coupling L to achieve coordination $\varepsilon_k(t) \to \varepsilon_\ell(t)$ for all $k, \ell \in \mathbb{I}_N$. The observer-based local feedback makes x_k track $X_k \varepsilon_k$ by a mechanism similar to (2.18) so that $z(t) \to Re^{\Lambda t} c$. Unlike the general controller from Theorem 5, the reference generator receives no feedback which prevents the reference command from being adjusted in real time, possibly leading to undesirable results.

3.3 Design Examples

To illustrate the utility of the proposed theory, we apply the result of Theorem 5 and Corollary 4 to the multi-agent system and consider three design objectives. The first is the design of a distributed controller to reach consensus between multiple heterogeneous agents to a trajectory described by a single eigenvalue. The second is the consensus of all agents towards a constant velocity and linearly growing displacement. The response of the controller in Theorem 5 is compared with the controller (3.17) proposed by [1] when the plant is subjected to a disturbance. The third is on coordinated displacement oscillations with prescribed frequency, amplitudes, and relative phases. A stable limit cycle is obtained by adding a nonlinearity to the distributed controller at a root of the directed graph. In all examples, the graph is designed with nearest neighbor coupling and uniform connectivity weights, $\mathcal{L}_{i,i+1} = \mathcal{L}_{i+1,i} = -\mu$ for $i \in \mathbb{I}_{N-1}$, with $\mu = 0.25$ in the first example, $\mu = 5$ in the second, and $\mu = 10$ in the third.

For the design examples in this section, we consider a system of N linear heterogeneous agents, each of which consists of point masses connected in series by linear springs, constrained to move along a straight, frictionless line. For $k \in \mathbb{I}_N$, we define the k^{th} agent to be $k+1$ masses connected by k springs, actuated by a horizontal force, u_k^1, on the first mass and another horizontal force, u_k^2, on the last mass (Fig. 3.4). With uniform mass m and stiffness σ, the equations of motion for agent k is given by

$$\begin{aligned} m\ddot{\varkappa}_k^1 &= -\sigma(\varkappa_k^1 - \varkappa_k^2) + u_k^1, \\ m\ddot{\varkappa}_k^i &= \sigma(\varkappa_k^{i-1} - 2\varkappa_k^i + \varkappa_k^{i+1}), \quad i \in \mathbb{I}_k \setminus \{1\}, \\ m\ddot{\varkappa}_k^{k+1} &= -\sigma(\varkappa_k^{k+1} - \varkappa_k^k) + u_k^2 \end{aligned}$$

where $\varkappa_k^i$ is the displacement of the i^{th} mass in the k^{th} agent. This spring-mass system can be visualized in Fig. 3.4. Let the system be described by the first equation in (3.1) with state vector $x_k := \text{col}(\varkappa_k, \dot{\varkappa}_k) \in \mathbb{R}^{2(k+1)}$, and consider the state feedback case $C_k = I$ with $(\sigma, m) = (1, 1)$ for the first example, and $(\sigma, m) = (2, 1)$ for the remaining examples. Additionally, for the second and third example, we consider the same spring-mass system, but set $u_k^2 = 0$ for the controller design.

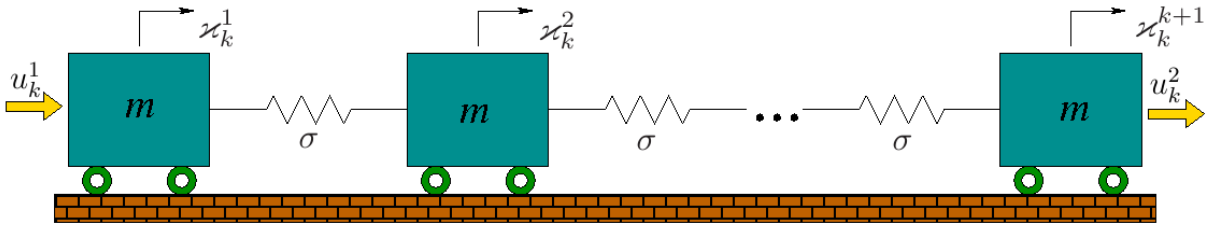

Figure 3.4: The k^{th} agent.

3.3.1 Example 1: Controller Design for Assigning Scalar Λ

We first consider a design example in which the eigenstructure assigned is a single eigenvalue/eigenvector pair. This type of example is of interest specifically because such an assignment implicitly satisfies the conditions for Corollary 4. What this further implies is that any heterogeneous multi-agent system that has a desired trajectory that is described by a single eigenvalue can always be solved with a structured static gain under state-feedback or a structured observer-based controller under output feedback.

The goal of the controller design is to achieve consensus in the sense that all agents converge to the same position as specified by the first and last masses. We set $\Lambda = 0$, $R_k = \text{col}(1, 2)$ and define H_k such that z_k is equal to $\text{col}(\varkappa_k^1, \varkappa_k^{k+1})$ for agent k. The specification on R_k ensures that the first mass of every agent converges to the same position and the last mass converges to the displacement twice that of the first mass. We allow nearest neighbor coupling, i.e. agent k can only communicate with agents $k+1$ and $k-1$ when $k \in \mathbb{I}_N \backslash \{1, N\}$, and agents 1 and N communicate with agents 2 and $N-1$, respectively. Correspondingly, the Laplacian matrix has a tri-diagonal structure.

From a physical standpoint, (3.7) characterizes the unique equilibrium state $x_k(t) \equiv X_k$, representing the positions and velocities of the k^{th} mass-spring system, and the corresponding constant force input $\text{col}(u_k^1(t), u_k^2(t)) \equiv F_k$ such that $z_k(t) \equiv R_k$, i.e., the displacement of the last mass is twice that of the first mass. We see that in the steady-state the masses are equidistant between $\mathfrak{x}_1$ and $\mathfrak{x}_{k+1}$ and the velocities are zero, while the forces (two entries in F_k) are in opposite directions with magnitude σ/k.

A distributed controller is obtained through Corollary 4, where uniform connectivity

weight 0.25 for the directed graph was selected to set the Laplacian matrix. This value gives weak inter-agent coupling when compared with the coupling of the local controllers with each agent. Figure 3.5 gives a numerical simulation of the the positions of the first and last mass of every agent in the closed-loop system, starting at zero initial states with the exception of the masses of agent 1 which were given equal, nonzero velocities. We see that the outputs z_k all converge to $\mathrm{col}(\eta, 2\eta)$ with $\eta = 0.166$ as desired.

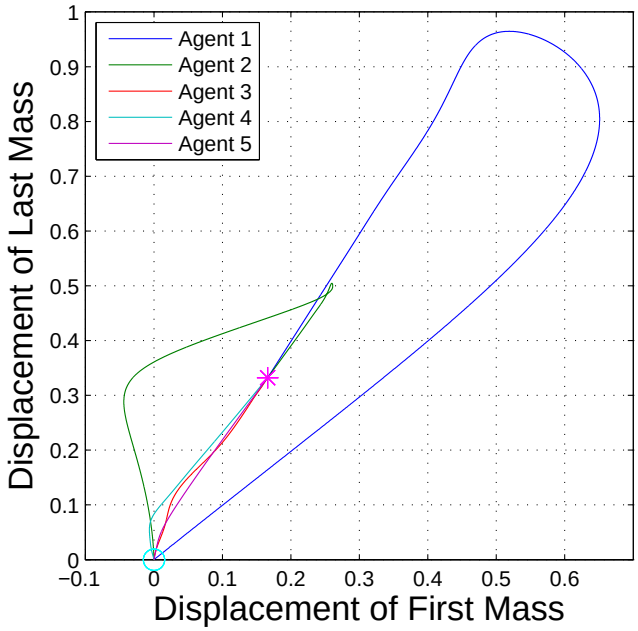

Figure 3.5: Trajectories of first and last masses on the z_k-plane for 5 heterogeneous agents, all starting from $z_k = 0$ and converging to $z_k = \mathrm{col}(0.166, 0.332)$.

One interesting behavior to note is that the agents first approach the line $z_k = R_k\eta$ with $\eta \in \mathbb{R}$ before moving along the line to reach consensus. This is because the inter-agent coupling was chosen to be much weaker than the intra-agent coupling between each agent and the local controller. The strong intra-agent coupling through K_k in (3.15) places the eigenvalues of $A_k + B_k K_k$ in the left half plane far from the origin, except for the one at $\lambda = 0$. These nonzero eigenvalues provide the fast convergence of z_k to $R_k\eta_k$ for some $\eta_k \in \mathbb{R}$. The additional inter-agent coupling through L in (3.15) moves $N-1$ out of the N eigenvalues at $\lambda = 0$ placed by K_k, slightly to the left to achieve consensus (i.e., a common value for η_k for all $k \in \mathbb{I}_N$). These eigenvalues give slow convergence under the weak inter-agent coupling.

3.3.2 Example 2: Control for Consensus

In our second example, we consider a consensus problem, where the design goal is to make the first masses of all the agents move together at a constant speed, i.e., $z_k(t) \to \text{col}(\gamma_v t + \gamma_p, \gamma_v)$ for some constants γ_p and γ_v, where $z_k := \text{col}(\varkappa_k^1, \dot{\varkappa}_k^1)$. The corresponding desired dynamics are described by (2.4) with Λ in (2.7) and

$$R_k = I_2, \quad H_k = \begin{bmatrix} 1 & 0_{1\times k} & 0 & 0_{1\times k} \\ 0 & 0_{1\times k} & 1 & 0_{1\times k} \end{bmatrix}, \quad k \in \mathbb{I}_4.$$

where $0_{1\times k}$ is the $1 \times k$ zero vector.

We design two consensus controllers, one by Theorem 5 and another by (3.17) from [1]. To ensure parity between the controllers, we used the same X_k and F_k (minimum norm solution to (3.7)) in both controllers as well as the same Laplacian matrix $\mathcal{L}$. The only remaining freedom was in the choice of static gains Φ_k and $\text{col}(K_k, J_k)$ for our controller and K_k (with $J_k = 0$) for the controller (3.17) in [1], to stabilize the matrices in (3.8). For each gain, the problem is in the form of state feedback stabilization to choose control gain $\mathfrak{K}$ to make $\mathfrak{A} + \mathfrak{B}\mathfrak{K}$ Hurwitz. We used the optimal LQR gain, $\mathfrak{K}_o$, that minimizes the cost function $\int_0^\infty (\|x(t)\|^2 + \|u(t)\|^2/10^3)\ dt$ for the modified plant $\dot{x} = (\mathfrak{A} + I)x + \mathfrak{B}u$. The identity was added to $\mathfrak{A}$ to ensure that the eigenvalues of $\mathfrak{A} + \mathfrak{B}\mathfrak{K}$ have real-part less than -1 to increase the rate of convergence.

We tested the two controllers by simulations of the closed-loop systems, starting with randomly generated initial conditions. The numerical experiments were conducted for 10,000 random initial conditions with values uniformly distributed between -1 and 1. We compared the two with respect to settling time, t_s, and the maximum input, $u_{\max}$, which are defined by

$$t_s := \min\ t_o \ \text{ s.t. } \max_{k\in\mathbb{I}_4} |\dot{\varkappa}_k^1(t) - \gamma_v| \le 0.05 \ \ \forall\ t \ge t_o,$$

$$u_{\max} := \max_{k\in\mathbb{I}_4,\ t\ge 0} |u_k^1(t)|,$$

where γ_v is the steady state velocity. The results of the 10,000 simulations for each case are shown in Fig. 3.6 with additional information on averages given in Table 3.1.

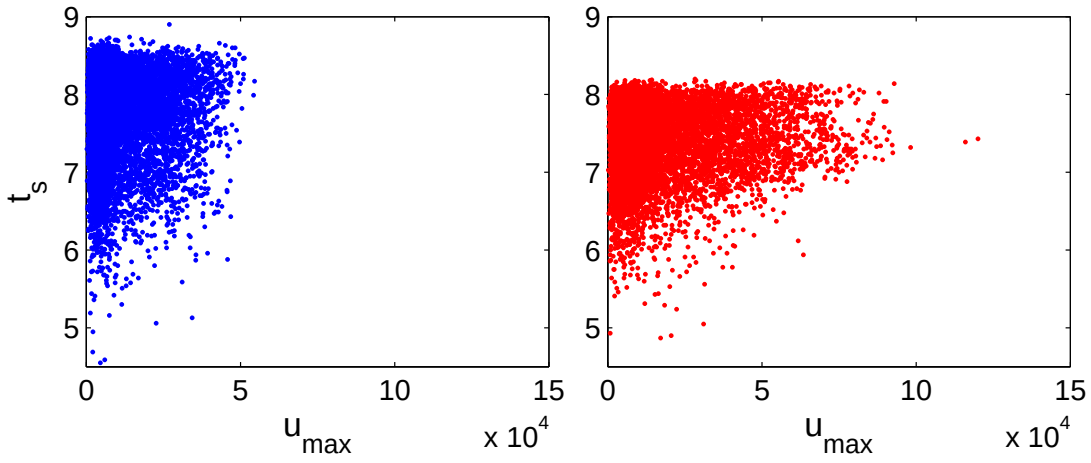

Figure 3.6: Settling time versus max input for Theorem 5 (Blue) and [1] (Red).

Table 3.1: Comparison of average settling time, $\bar{t}_s$, and max input, $\bar{u}_{\max}$.

Controller	$\bar{t}_s$	$\bar{u}_{\max}$
Wieland *et al.* 2011 [1]	7.08	11116
Theorem 5	7.65	3̇656

We see that the settling times for both controllers are comparable, with a slight advantage (roughly 8% on average) to the controller by [1]. The primary difference is the amount of control effort required to reach consensus. The controller from Theorem 5 outperforms the controller from [1] by a factor of 3. We attribute this difference to the use of feedback in the controller from Theorem 5. Because the reference generator from [1] receives no feedback, the target consensus trajectory is determined only by the initial conditions of the controller. In contrast, the controller from Theorem 5 reaches the target consensus trajectory through distributed communications based on the sensory feedback from the plant.

The advantage of feedback in our controller is best exemplified when there is a disturbance that pushes the states exactly onto a consensus trajectory. Because the agents are not subjected to friction, the control input is nonzero only when the agents are not in consensus. If the agents have reached consensus, then the masses remain in consensus when subjected to equal forcing. Without feedback, the reference generator of [1] is unaware of this and the controller attempts to return to the same reference trajectory determined by initial

conditions, requiring nontrivial control inputs. On the other hand, when there is feedback as in Theorem 5, the controller recognizes that the agents are still in consensus after the disturbance, requiring little effort to remain in consensus.

To illustrate this case, we chose the initial conditions so that the states for both closed-loop systems initially converge to similar consensus trajectories; the velocities of the agents converge to $\gamma_v = -0.0235$ and -0.0257 for the controllers in Theorem 5 and [1], respectively (Fig. 3.7). After reaching consensus, an impulse disturbance of 0.05 Newtons was applied at $t = 9$ s to every mass of each agent in the same direction; essentially an addition of equal velocity to every mass. Since this is a consensus trajectory satisfying (2.4), the controller in Theorem 5 does (almost) nothing as seen in Fig. 3.8. In contrast, the controller from [1] does not notice the disturbance due to the lack of feedback, and insists on the original trajectory at $\gamma_v = -0.0257$. This results in the large transient, especially in the control input which spikes to over 1800 in amplitude.

This example illustrates the importance of having feedback in a consensus controller so that the controller allows the agents to adapt their reference trajectories in real-time.

3.3.3 Example 3: Control for Coordinated Oscillations

In the second example, we design a controller using Theorem 5 so that the first mass of every agent oscillates with a specified frequency, amplitude, and relative phase between agents. We use the specification in (2.6) with

$$\omega = 5, \quad a_k = 5 - k, \quad b_k = (\pi/3)(k-1),$$
$$H_k = \begin{bmatrix} 1 & 0_{1\times(2k+1)} \end{bmatrix}, \quad k \in \mathbb{I}_4.$$

This choice of Λ and R leads to oscillations of the form (2.5) with $\alpha_k = \gamma_a a_k$ and $\beta_k = b_k + \gamma_b$ where (γ_a, γ_b) are constants determined by the initial condition. Since the closed-loop system is linear, it is impossible to regulate absolute amplitudes and phases. To remedy this, we added a local nonlinear feedback to the control of the first agent's first mass:

$$u_1^1 = \tilde{u}_1 + c(\alpha_1^2 - \tilde{\alpha}_1^2)\dot{\varkappa}_1^1, \quad \tilde{\alpha}_1^2 = (\varkappa_1^1)^2 - (\dot{\varkappa}_1^1/\omega)^2,$$

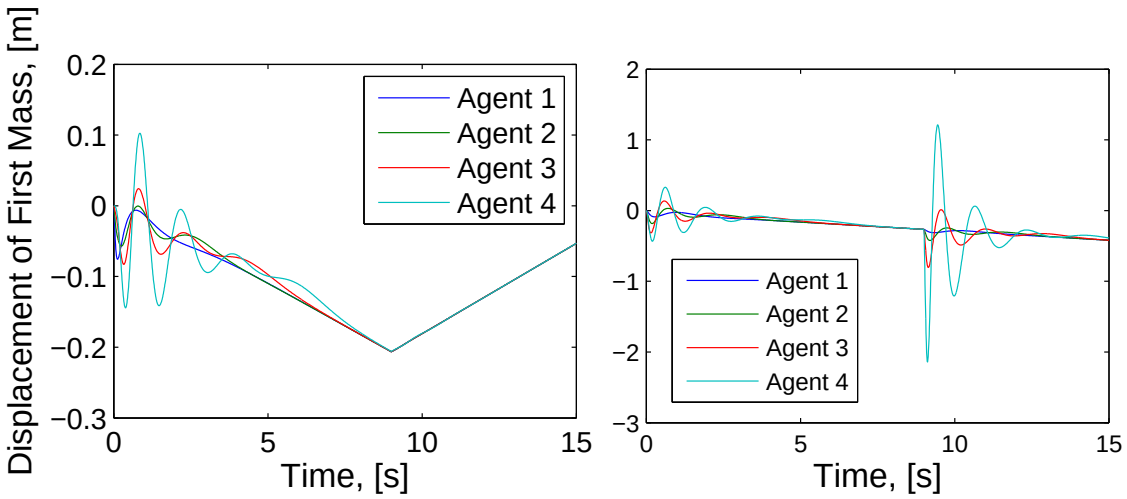

Figure 3.7: Position comparison of controller in Theorem 5 (left) and controller proposed by [1] (right) subjected to a disturbance at $t = 9$ s.

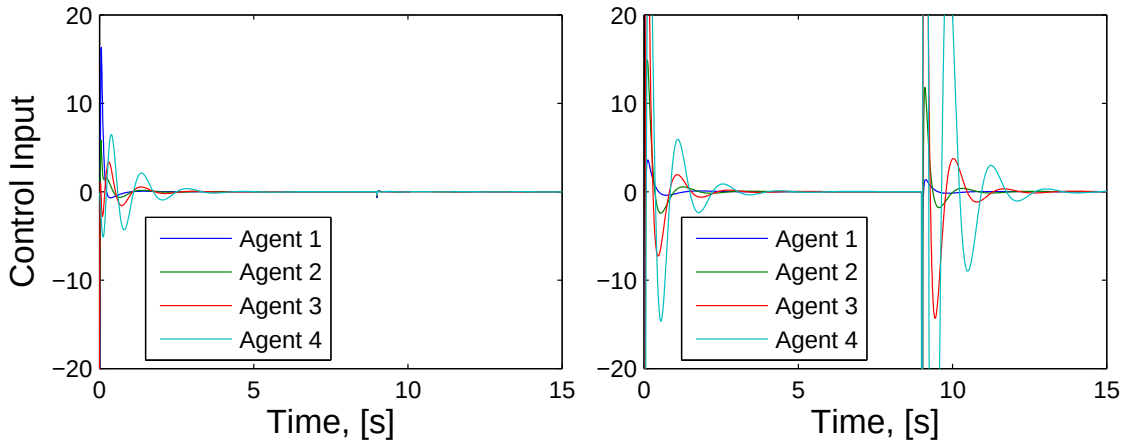

Figure 3.8: Control input comparison of controller in Theorem 5 (left) and controller proposed by [1] (right) subjected to a disturbance at $t = 9$ s.

where c and α_1 are positive constants, and $\tilde{u}_1$ is the force input generated by the original linear controller from Theorem 5. $\tilde{\alpha}_1$ is the amplitude of oscillation of the first agent at a given time which results from our specification that $\varkappa_1^1$ is sinusoidal. This nonlinearity does not affect the structure of the controller because it requires only information already available to the first agent. The additional feedback stabilize the amplitude of $\varkappa_1^1$ to α_1 with nonlinear damping that is positive when $\tilde{\alpha}_1 < \alpha_1$ and negative when $\tilde{\alpha}_1 > \alpha_1$; this amplitude regulation propagates to the other agents through proper inter-agent coupling so

that $\alpha_k = (a_k/a_1)\alpha_1$. In general, this nonlinearity must be applied on an agent which is a root of a spanning tree of the graph, otherwise, there will be an agent that does not receive information about the desired amplitude.

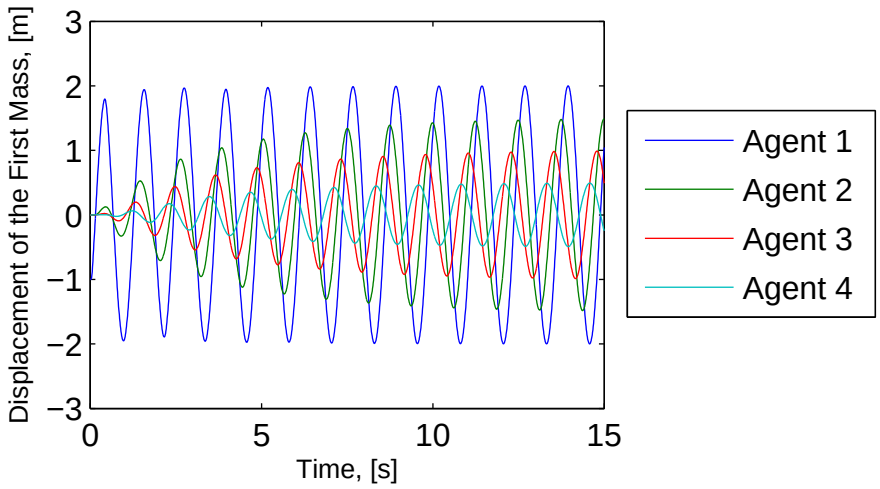

Figure 3.9: Limit cycle entrainment with the addition of a nonlinearity.

The closed-loop simulation result with $c = 20$ is shown in Fig. 3.9. In setting $\alpha_1 = 2$, the amplitudes of oscillation for $z_k(t)$ are locked to $\alpha_k = 2.5 - 0.5k$. We start at zero initial state with the exception of a displacement of -1 on the first agent's first mass. Figure 3.9 shows that the agents converge to the limit cycle of specified amplitudes and relative phases. While we provide no rigorous proof to guarantee that the agents will converge to a limit cycle, this example shows the potential for eigenstructure theory to encompass pattern formations beyond the linear domain. It would be possible to expand these linear results to nonlinear theories for pattern formation.

CHAPTER 4

Controllers with CPG Architecture

The problem of designing feedback controllers to achieve specified coordinated oscillations has not received as much attention as its utility would suggest. The ability to systematically design a controller to achieve coordinated oscillations would be particularly attractive in the field of robotics where repetitive motions are common and the ability to entrain to a specified profile autonomously would be a desirable property. Previous work in this field has primarily centered on the tracking of oscillatory inputs [45–47], but reference tracking may be too strong as a requirement in certain applications because the trajectory of the system will attempt to converge to the reference value specified at each time rather than remain on a specified oscillation orbit (a closed curve in the state space). If the timing is not important for the design, it would be more preferable to design feedback controllers to achieve coordinated oscillations as the projection of a stable limit cycle of the closed-loop system.

A limit cycle is a self-sustaining oscillation that arises from nonlinear dynamics and it can be structurally stable, i.e., the trajectory starting from an initial point in the neighborhood of the periodic orbit approaches the orbit. Limit cycles are well-studied and there are established methods to analyze and predict their existence [48–53]. Presently, there have not been many general theories for the design of feedback controllers to achieve stable limit cycles with prescribed amplitudes, phases, and frequencies. Classical dynamical system theories have been used to design coupled oscillators to achieve specified phases [54, 55] and PD controllers have been used in conjunction with coupled nonlinear oscillators to induce limit cycle behavior in robots [56, 57]. However, a general theory has yet to be developed to enable design of feedback controllers for dynamical systems to achieve stable limit cycles

with prescribed oscillation profiles. The central pattern generator (CPG) provides a solution to this design problem in the context of biological control systems, and has a potential to provide a basis for such general theory for engineering applications.

The CPG is a collection of interconnected neurons responsible for the repetitive movements of animal locomotion [58–63]. By itself, the CPG is a nonlinear oscillator and, when isolated from the body dynamics, the CPG will exhibit coordinated oscillation patterns similar to that of the observed body movements [64–67]. When placed in a closed-loop with animal body dynamics, the CPG creates various periodic body motions observed in different environments [68]. Because the CPG has been extensively studied and functions as a biological controller for rhythmic motions, it is one practical choice for the architecture of controllers to achieve coordinated oscillations [69].

Mathematical modeling and analyses of CPGs have concluded that both the stability of oscillation as well as the profile itself is intimately connected to the eigenvalue/eigenvectors of the neuronal interconnection matrix. More specifically, the frequency and phases of the CPG oscillation can be predicted by the maximal eigenvalue and corresponding eigenvector, respectively [28, 70]. In a similar manner, when the CPG is used as a controller in feedback with a plant, the control design for closed-loop oscillation can be posed as an eigenstructure assignment problem [29]. Within this framework, much research has been done with a focus on CPG-based controller design for entrainment to resonance modes [71–74]. However, these results only cover a subset of possible oscillation profiles, and the full potential of CPG control has yet to be explored to achieve closed-loop oscillations with an arbitrary profile.

In this chapter, we present a solution to the problem of designing a CPG-based controller to achieve closed-loop oscillations with prescribed amplitudes, phases, and frequency. We consider the linear time-invariant plant and the nonlinear feedback controller based on the CPG architecture. The controller is represented as the interconnection of multiple neurons, each with identical dynamics described by a first-order low-pass filter followed by a static nonlinearity. In our approach, the nonlinear problem is first reduced to a tractable quasi-linear form by approximating the nonlinearity by a describing function. The method of harmonic balance [28] then predicts that the original nonlinear closed-loop system has

a prescribed stable limit cycle if the quasi-linear system is marginally stable with only one pair of conjugate eigenvalues on the imaginary axis corresponding to the frequency, and the respective eigenvectors specifying the phases and amplitudes. The aforementioned problem can thus be formulated as an eigenstructure assignment problem for which the solution in Chapter 2 is applicable. We further consider the design of a single controller to achieve different eigenstructures for different plants. We demonstrate the efficacy of the proposed design method through an example of a three-link mechanical arm to achieve an arbitrarily specified oscillation and additionally, the design of a single controller to achieve two different oscillations for a leech in order to emulate a change in a gait due to a change in the environment.

4.1 Oscillation Control Problem

We consider a linear system described by

$$\dot{x} = Ax + Bu, \quad y = Cx \tag{4.1}$$

where $x(t) \in \mathbb{R}^n$ is the state, $u(t) \in \mathbb{R}^m$ is the control input, and $y(t) \in \mathbb{R}^p$ is the measured output. Denote by $P(s)$ the transfer function from u to y. A general oscillation control problem can be stated as follows:

Problem 2. Let a linear plant (4.1) and a desired oscillation profile for $x_i(t)$ be given, where the latter is specified in terms of the frequency ω, amplitude a_i, phase b_i, and shape σ_i (2π-periodic function with a normalized amplitude). Find a nonlinear dynamic output-feedback controller such that the closed-loop system has an orbitally stable limit cycle on which $x_i(t) = a_i\sigma_i(\omega t + b_i)$ holds for all $i \in \mathbb{I}_n$.

The orbital stability mentioned in Problem 2 is a property of a limit cycle which means that trajectories with initial conditions sufficiently close to the limit cycle orbit converges to the orbit. Since the plant is assumed linear, it would be necessary to have a nonlinear controller or else orbital stability could never be achieved due to the lack of structural stability for any periodic orbit of a linear system. To make the control design tractable,

we will fix the nonlinear architecture of the controller and search for the design parameters. In particular, we choose the CPG control structure because the CPG has been extensively studied in biology as a nonlinear oscillator that is known to generate stable limit cycles when used in a feedback loop.

A CPG is a neuronal circuit responsible for controlling rhythmic body movements during animal locomotion. By itself, it is a nonlinear oscillator and its oscillation profile is similar to (but not quite the same as) observed body motion. The CPG is placed in a feedback loop with the body so that the closed-loop system has a stable limit cycle whose projection onto the body variable space gives a gait. It is often represented mathematically as a set of interconnected neuron models, each of which is composed of a linear filter and static nonlinearity. More specifically, a CPG of n_c interconnected neurons can be represented by

$$v_i = \psi(q_i), \quad q_i = f(s)w_i, \quad w_i = \sum_{j=1}^{n_c} \mu_{ij} v_j$$

for $i \in \mathbb{I}_{n_c}$, where w_i is the input into the cell, μ_{ij} represents the strength and type (either inhibitory or excitatory) of connection from neuron j to neuron i, q_i is the internal variable, v_i is the output, $f(s)$ is a transfer function that captures time lag or adaptation properties observed in neuronal dynamics, and ψ is the static nonlinearity that captures the threshold property also observed in biology [75]. Although alternative choices for ψ and $f(s)$ exist, the work in this chapter will use

$$\psi(x) = \tanh(x), \quad f(s) = \frac{1}{1+\tau s}$$

where τ is the time constant for neuronal information processing and we assume that each neuron has identical dynamics, thereby sharing the same $f(s)$.

For compactness, the CPG can also be represented in vector form as

$$q = F(s)M\Psi(q), \quad v = \Psi(q), \quad w = Mv$$

where $q(t)$, $v(t)$, and $w(t)$ are n_c-dimensional vectors, M is the interconnectivity matrix which has μ_{ij} as its $(i,j)^{\text{th}}$ entry, $\Psi(q)$ is a vector that has $\psi(q_i)$ as its i^{th} entry, and $F(s) = f(s)I$.

In order to utilize the CPG as a feedback controller, it is necessary to insert an input-output interface to the CPG model. Let such a form be represented by

$$q = F(s)(M\Psi(q) + Hy), \quad u = G\Psi(q) + Ly, \tag{4.2}$$

where G, H, and L are constant matrices [68]. This can be visualized through the block diagram in Fig. 4.1.

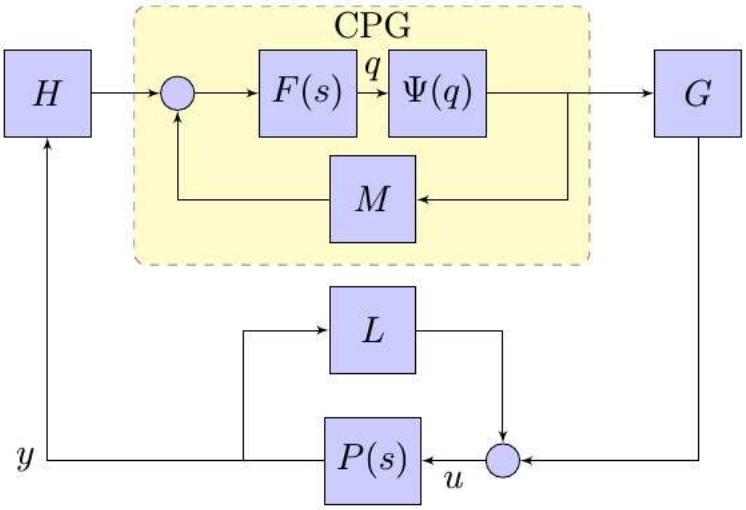

Figure 4.1: Closed-Loop System of CPG and Plant

The closed-loop system can be represented by

$$\begin{bmatrix} \dot{x} \\ \dot{\xi} \end{bmatrix} = \begin{bmatrix} A & 0 \\ 0 & A_f \end{bmatrix} \begin{bmatrix} x \\ \xi \end{bmatrix} + \begin{bmatrix} B & 0 \\ 0 & B_f \end{bmatrix} \begin{bmatrix} L & G \\ H & M \end{bmatrix} \begin{bmatrix} C & 0 \\ 0 & I \end{bmatrix} \begin{bmatrix} x \\ \Psi(q) \end{bmatrix} \tag{4.3}$$

where $q = C_f\xi$, and (A_f, B_f, C_f) is a minimal state space realization of $F(s)$ with state vector ξ. Within this framework, the control design parameters are L, G, H, M, and τ, and we search for these parameters to satisfy the design requirements described in Problem 2. Since τ is just a scalar and can be determined by a line search, we consider τ to be fixed in the theoretical development and discuss its effect later in a numerical example. In the rest of the chapter, we assume that the targeted oscillations for x_i are identical and sinusoidal, i.e., $\sigma_i(\theta) := \sin\theta$. Because Problem 2 is difficult to solve exactly, we will use the multivariable harmonic balance (MHB) method [28] to reduce it to an approximate but tractable problem.

4.2 The Multivariate Harmonic Balance

Consider the class of systems described as a feedback connection of a linear time-invariant system and static nonlinearities:

$$\dot{\mathsf{x}} = \mathsf{A}\mathsf{x} + \mathsf{B}\mathsf{w}, \quad \mathsf{z} = \mathsf{C}\mathsf{x}, \quad \mathsf{w} = \Psi(\mathsf{z}) \tag{4.4}$$

where w and z are vectors and the i^{th} entry of $\Psi(\mathsf{z})$ is assumed to depend only on the i^{th} entry of z. Note that the closed-loop system in Fig. 4.1 is just a special case of this type of system with $\mathsf{z} := q$.

In order to simplify the analysis or design of oscillations for the closed-loop system, it would be useful to eliminate the nonlinearity. To this end, we place the system in a quasi-linear form by approximating the static nonlinearity by its describing function,

$$\Psi(\mathsf{z}) \cong K(\alpha)\mathsf{z} \quad \text{for} \quad \mathsf{z}_i = \alpha_i \sin(\omega t),$$

where α is a vector with i^{th} entry α_i, and $K(\alpha)$ is a diagonal matrix such that $K(\alpha)\mathsf{z}$ coincides with the first harmonic of $\Psi(\mathsf{z})$. The resulting quasi-linearized system becomes

$$\dot{\mathsf{x}} = \mathsf{A}\mathsf{x} + \mathsf{B}\mathsf{w}, \quad \mathsf{z} = \mathsf{C}\mathsf{x}, \quad \mathsf{w} = K(\alpha)\mathsf{z}. \tag{4.5}$$

Previous MHB analysis [28] has concluded that the nonlinear system in (4.4) is expected to have a stable limit cycle when the quasi-linear system in (4.5) is marginally stable for some vector α, with a pair of eigenvalues of

$$\mathcal{A} := \mathsf{A} + \mathsf{B}K(\alpha)\mathsf{C}$$

on the imaginary axis and all the others in the open left half plane. Furthermore, the oscillation profile for the limit cycle is predicted as

$$\mathsf{x}_i(t) \cong \gamma_i \sin(\omega t + \delta_i), \tag{4.6}$$

where ω, γ_i, and δ_i satisfy the MHB equation

$$(j\omega I - \mathcal{A})\hat{\mathsf{x}} = 0, \quad \hat{\mathsf{x}}_i = \gamma_i e^{j\delta_i},$$

and $|\hat{\mathsf{z}}_i| = \alpha_i$ with $\hat{\mathsf{z}} := \mathsf{C}\hat{\mathsf{x}}$. Here, $\hat{\mathsf{x}}$ is a phasor representation of the sinusoid in (4.6), which can also be written as $\Im[\hat{\mathsf{x}}e^{j\omega t}]$. Note that the eigenvalue $j\omega$ on the imaginary axis specifies the oscillation frequency, and the eigenvector $\hat{\mathsf{x}}$ specifies the amplitudes and phases. Solving the MHB equation for (ω, x) is nontrivial due to the coupling of $\mathcal{A}$ and x through α.

4.3 Reduction to Eigenstructure Assignment

We now apply the MHB method to the closed-loop system in (4.3) and approximately reformulate Problem 2 in a more tractable form. Suppose $q(t)$ oscillates as

$$q_i(t) \cong \alpha_i \sin(\omega t + \beta_i)$$

when the desired limit cycle is achieved for the closed-loop system. Let $\hat{q}$ be the corresponding phasor, i.e., $\hat{q}_i = \alpha_i e^{j\beta_i}$. Approximating the nonlinearity $\Psi(q)$ by its describing function $K(\alpha)q$, the closed-loop system (4.3) can be simplified to

$$\begin{bmatrix} \dot{x} \\ \dot{\xi} \end{bmatrix} = \begin{bmatrix} A & 0 \\ 0 & A_f \end{bmatrix} \begin{bmatrix} x \\ \xi \end{bmatrix} + \begin{bmatrix} B & 0 \\ 0 & B_f \end{bmatrix} \begin{bmatrix} L & GK(\alpha) \\ H & MK(\alpha) \end{bmatrix} \begin{bmatrix} C & 0 \\ 0 & C_f \end{bmatrix} \begin{bmatrix} x \\ \xi \end{bmatrix}. \tag{4.7}$$

Let us introduce the change of variables $(L, G, H, M) \leftrightarrow (A_c, B_c, C_c, D_c)$ defined by

$$\begin{bmatrix} D_c & C_c \\ B_c & A_c \end{bmatrix} = \begin{bmatrix} 0 & 0 \\ 0 & A_f \end{bmatrix} + \begin{bmatrix} I & 0 \\ 0 & B_f \end{bmatrix} \begin{bmatrix} L & GK(\alpha) \\ H & MK(\alpha) \end{bmatrix} \begin{bmatrix} I & 0 \\ 0 & C_f \end{bmatrix}, \tag{4.8}$$

where the mapping is invertible because B_f and C_f are square invertible for the first order low pass filter $f(s)$. The system (4.7) can then be expressed as

$$\begin{bmatrix} \dot{x} \\ \dot{\xi} \end{bmatrix} = A_{cl} \begin{bmatrix} x \\ \xi \end{bmatrix}, \tag{4.9}$$

where

$$A_{cl} = \mathsf{A} + \mathsf{B}\mathcal{K}\mathsf{C}, \quad \mathsf{A} = \begin{bmatrix} A & 0 \\ 0 & 0 \end{bmatrix}, \quad \mathsf{B} = \begin{bmatrix} B & 0 \\ 0 & I \end{bmatrix}, \quad \mathsf{C} = \begin{bmatrix} C & 0 \\ 0 & I \end{bmatrix}, \quad \mathcal{K} = \begin{bmatrix} D_c & C_c \\ B_c & A_c \end{bmatrix}.$$

Note that the system (4.9) is of the form that arises from the standard output feedback problem with plant $C(sI - A)^{-1}B$ and controller $C_c(sI - A_c)^{-1}B_c + D_c$.

Based on the MHB analysis in the previous section, the nonlinear closed-loop system (4.3) is expected to have a stable limit cycle on which $x_i(t) \cong a_i \sin(\omega t + b_i)$ if

$$(j\omega I - A_{cl}) \begin{bmatrix} \hat{x} \\ \hat{\xi} \end{bmatrix} = 0 \tag{4.10}$$

holds for $\hat{x}_i = a_i e^{jb_i}$ and for some complex vector $\hat{\xi}$, and all the eigenvalues of A_{cl} other than $\pm j\omega$ are in the open left-half plane. Here, $\hat{\xi}$ is the phasor of $\xi(t)$, and is constrained by $|\hat{q}_i| = \alpha_i$ for $\hat{q} := C_f \hat{\xi}$. The design problem has now reduced to the search for real matrices (A_c, B_c, C_c, D_c), complex vector $\hat{\xi}$, and real scalar α_i, satisfying $|C_f \hat{\xi}| = \alpha$ and (4.10), the eigenvalue (marginal stability) condition. Note that α_i appears only in the latter constraint since the design freedom associated with α_i in (4.10) is absorbed into the new parameters (A_c, B_c, C_c, D_c) during the change of variables in (4.8). Consequently, the essential problem is to find $\mathcal{K} := (A_c, B_c, C_c, D_c)$ and $\hat{\xi}$ satisfying (4.10) and the marginal stability requirement since the parameter α_i can always be chosen as $\alpha_i := |\hat{q}_i|$ after the design. This is an eigenstructure assignment problem.

4.4 Further Reformulation

The eigenstructure assignment problem has two specifications: one is the MHB condition (4.10) on the eigenvalue/eigenvector pair specifying the desired oscillation, and the other is on the location of the rest of the eigenvalues aiming at orbital stability of the oscillation. It would be beneficial for the design to isolate the eigenspaces associated with those on the imaginary axis and the rest.

To this end, let

$$\mathcal{V} := \begin{bmatrix} X \\ \Xi \end{bmatrix}, \quad \Lambda := \begin{bmatrix} 0 & \omega \\ -\omega & 0 \end{bmatrix}, \quad X := \begin{bmatrix} \Re(\hat{x}) & \Im(\hat{x}) \end{bmatrix}, \quad \Xi := \begin{bmatrix} \Re(\hat{\xi}) & \Im(\hat{\xi}) \end{bmatrix}.$$

Then (4.10) becomes

$$A_{cl}\mathcal{V} = \mathcal{V}\Lambda. \tag{4.11}$$

Note that, for the oscillation control problem, $\mathcal{V}$ is necessarily full column-rank because if $\mathcal{V}$ were rank-deficient, then (4.11) would imply $\omega = 0$ or $\hat{x} = 0$, leading to a trivial solution to the MHB equation. Since $\mathcal{V}$ is full column-rank, there exists a matrix N such that $\begin{bmatrix} \mathcal{V} & N \end{bmatrix}$ is square nonsingular. Furthermore, matrices W and U can be uniquely defined by

$$\begin{bmatrix} U^\intercal \\ W^\intercal \end{bmatrix} \begin{bmatrix} \mathcal{V} & N \end{bmatrix} = I. \tag{4.12}$$

Below, (N, U, W) denotes any one of such matrix triples determined from $\mathcal{V}$ as described above. Then, when (4.11) is satisfied, the similarity transformation

$$\begin{bmatrix} U^\intercal \\ W^\intercal \end{bmatrix} A_{cl} \begin{bmatrix} \mathcal{V} & N \end{bmatrix} = \begin{bmatrix} \Lambda & U^\intercal A_{cl} N \\ 0 & W^\intercal A_{cl} N \end{bmatrix} \tag{4.13}$$

shows that the eigenvalues of A_{cl} are those of Λ and $W^\intercal A_{cl} N$. Hence, the eigenstructure assignment problem can be restated as follows:

Problem 3. Let a linear time-invariant plant of order n be given in terms of the state space realization (A, B, C) and let a desired oscillation profile be specified by $X \in \mathbb{R}^{n\times 2}$ and $\Lambda \in \mathbb{R}^{2\times 2}$. Find a controller $\mathcal{K}$ of order n_c and $\Xi \in \mathbb{R}^{n_c \times 2}$ such that a state-space realization of $\mathcal{K}$ exists to satisfy

(a) $A_{cl}\mathcal{V} = \mathcal{V}\Lambda$,

(b) $\text{eig}(W^\intercal A_{cl} N) \subset \mathbb{C}_-$,

where matrix A_{cl} is defined below (4.9) and matrices U, $\mathcal{V}$, and W are defined in the preceding paragraph.

With this reformulation, it becomes clear that the limit cycle design problem with a CPG-based controller reduces to the eigenstructure assignment problem defined in Chapter 2. In this case, we specify the oscillation as in (2.6) with $H_k = I$ and by Lemma 4, $\mathcal{V}$ can be assumed to have the structure $\mathcal{V} = \text{col}(X, \Xi_o)$ where $\Xi_o := \text{col}(I_r, 0)$. Since the value of Ξ is fixed, the choices of α and β in the oscillation profile of $q(t)$ have also been fixed.

The only remaining parameter is τ in $f(s)$, which is an important design parameter that affects both the convergence rate and accuracy of $x(t)$. Specifically, a smaller τ decreases the rate of convergence, but improves the accuracy in matching up to the desired profile.

Once $\mathcal{V}$ and the time constant in $f(s)$ have been set, then Problem 3 reduces to the search for an F to satisfy (2.13) and an output-feedback controller, $\mathring{Q}$, to stabilize $(A, \mathfrak{B}, C)$ where $\mathfrak{B} := \begin{bmatrix} B & -X \end{bmatrix}$. We can then map F and $\mathring{Q}$ back to $\mathcal{K}$ through

$$\begin{bmatrix} D_c & C_c \\ B_c & A_c \end{bmatrix} = \begin{bmatrix} \mathsf{F} & D_q & C_q \\ 0 & B_q & A_q \end{bmatrix} \begin{bmatrix} 0 & I & 0 \\ I & -CX & 0 \\ 0 & 0 & I \end{bmatrix},$$

$$\mathsf{F} = \begin{bmatrix} F \\ \Lambda \end{bmatrix}, \quad Q := \begin{bmatrix} D_q & C_q \\ B_q & A_q \end{bmatrix}.$$

Finally, we obtain the matrices (L, G, H, M) for the CPG-based controller in (4.7) by using the mapping in (4.8).

4.5 Design Example for a Single Limit Cycle

In order to illustrate the utility of the CPG control theory developed here, we apply the procedure described above to the design of a controller to achieve coordinated oscillations for a three link mechanical arm [72].

The plant is described by

$$J\ddot{\theta} + D\dot{\theta} + K\theta = \mathsf{B}u, \quad y = \mathsf{B}^{\mathsf{T}}\theta, \tag{4.14}$$

where $\theta(t) \in \mathbb{R}^3$ is the link angles with respect to the inertial frame, $y(t) \in \mathbb{R}^3$ is the angular displacements of the three joints connecting the links in series, and $u(t) \in \mathbb{R}^3$ is the joint torque inputs. Assuming identical links, the coefficient matrices are given by

$$J = (ml^2)(I/3 + L^{\mathsf{T}}L), \quad K = k\mathsf{B}\mathsf{B}^{\mathsf{T}}, \quad D = \rho K,$$

$$\mathsf{B} = \begin{bmatrix} 1 & -1 & 0 \\ 0 & 1 & -1 \\ 0 & 0 & 1 \end{bmatrix}, \quad L = \begin{bmatrix} 1 & 0 & 0 \\ 2 & 1 & 0 \\ 2 & 2 & 1 \end{bmatrix}$$

with parameter values

$$l = 0.5, \quad k = 1.0, \quad m = 1.0, \quad \rho = 0.1.$$

We set the target oscillation profile as follows:

$$\theta_i(t) \cong a_i \sin(\omega t + b_i),$$

where

$$a = \begin{bmatrix} 20 \\ 35 \\ 60 \end{bmatrix} \text{ deg}, \quad b = \begin{bmatrix} 0 \\ 120 \\ 240 \end{bmatrix} \text{ deg}, \quad \omega = 3 \ \text{ rad/s}.$$

We set the time constant in the neuronal dynamics, $f(s)$, to $\tau = 10$ because it gave us a fairly quick convergence rate without significantly affecting how well the resulting oscillation profile of the plant matched the desired specifications.

Recall that the problem centers around enforcing marginal stability of the quasi-linear system with one pair of conjugate eigenvalues on the imaginary axis at $\pm j\omega$, where ω is the oscillation frequency of the desired profile. Thus we would anticipate seeing this property satisfied for the closed-loop, quasi-linear system (4.9).

According to the eigenvalues of the closed-loop system displayed in Fig. 4.2, the marginal stability condition is satisfied and the eigenvalues on the imaginary axis have the correct values $\pm j3$. This marginal stability of the quasi-linear closed-loop system is also expected to result in the orbital stability of the nonlinear closed-loop system. As a test of this, we let the closed-loop system start with initial conditions away from the designed limit cycle and see that it converges to the desired profile. We see from Fig. 4.3 and similar simulation results for various initial conditions (not shown) that the marginal stability condition for the quasi-linear system resulted in orbital stability of the targeted limit cycle for the nonlinear

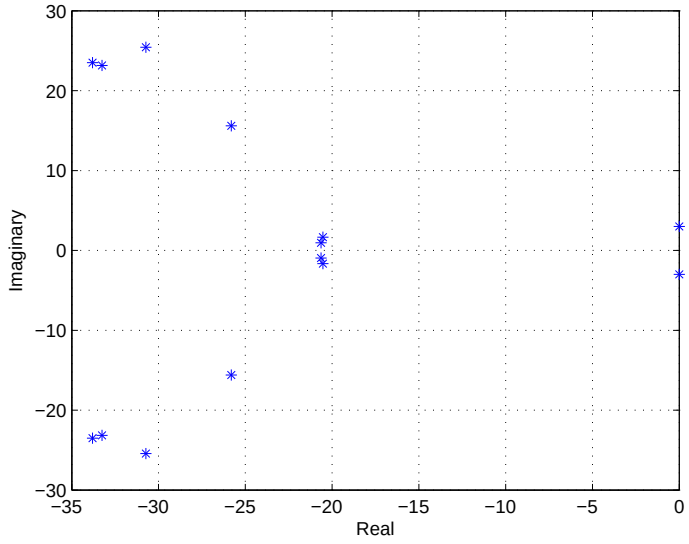

Figure 4.2: Eigenvalue Plot

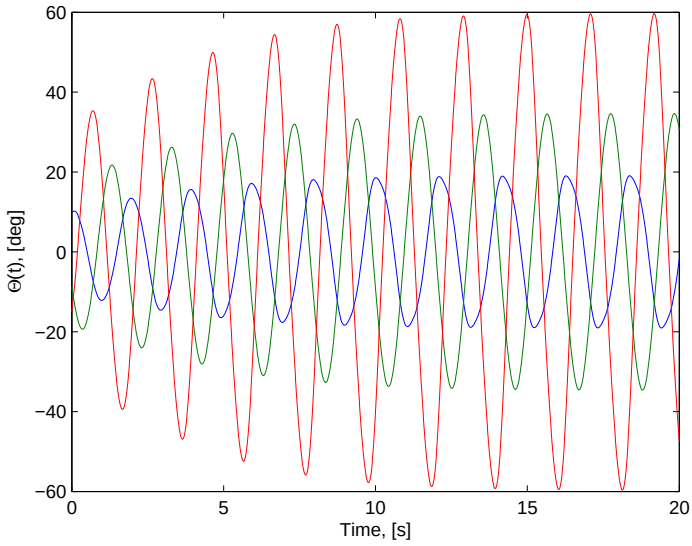

Figure 4.3: Oscillation Profile for Unstructured Single-Oscillation Design

system. Table 4.1 gives a quantitative summary of how closely the nonlinear control system satisfies the design specifications. Although the numerically simulated oscillations in Fig. 4.3 are not sinusoidal due to the nonlinearities in the CPG control, Fourier analysis on the results show that the amplitudes, phases, and frequency of the first harmonic component are very close to those of the target oscillations. Thus, the approximation through the use of the

Table 4.1: Single Oscillation Profile

	θ_1	θ_2	θ_3
Target Amplitude [deg]	20	35	60
Closed-Loop Amplitude [deg]	19.2	33.8	57.6
Target Phase [deg]	0	120	240
Closed-Loop Phase [deg]	0	120.2	240.4

Target Frequency=3 rad/s, Simulated Frequency= 2.99 rad/s

describing function did not significantly alter the resulting trajectory of the nonlinear closed-loop system with respect to the original specifications. Moreover, due to the invertibility of B, we could assign any limit cycle in the linear system and for almost every oscillation profile we designed, the eigenstructure condition was a highly reliable indicator that the nonlinear-closed loop system would have the specified oscillation profile as a limit cycle. Thus, it is fair to conclude that even without a rigorous mathematical proof that satisfaction of the MHB and stability equations will result in a limit cycle in the nonlinear closed-loop, the CPG architecture combined with the eigenstructure result is a very effective method for designing a limit cycle for an arbitrary LTI system.

4.6 Assignment of Multiple Limit Cycles

We now shift our focus to the design of a single set of controller parameters (L, G, H, M) to assign different limit cycles for different plants.[1] If we interpret each assigned limit cycle as a different gait for a mechanical system and different plants as variations in the environment, then the design of a single controller that can achieve different limit cycles for different plants would imply an autonomous adaptation property embedded in the controller.

[1]For the remainer of this chapter, we define the design of a single controller as the search for (L, G, H, M) from (4.2) to satisfy the specified eigenstructure conditions.

4.6.1 The Multi-Oscillation Problem

Consider equation (4.2) and simplify the nonlinear term using the describing function. Noting that because $f(s)$ is a first order low pass filter and thereby invertible, we can rewrite the MHB equation as

$$\underbrace{\begin{bmatrix} \hat{u}_i \\ \hat{q}_i/f(s) \end{bmatrix}}_{\hat{r}_i} = \begin{bmatrix} L & G \\ H & M \end{bmatrix} \underbrace{\begin{bmatrix} \hat{x}_i \\ K_i\hat{q}_i \end{bmatrix}}_{\hat{z}_i} \rightarrow R_i = \mathcal{K}Z_i,$$

$$R_i = \begin{bmatrix} \Re(\hat{r}_i) & \Im(\hat{r}_i) \end{bmatrix}, \quad Z_i = \begin{bmatrix} \Re(\hat{z}_i) & \Im(\hat{z}_i) \end{bmatrix}, \quad i = 1, 2,$$

where $\hat{u}_i$ and $\hat{q}_i$ are as specified in the previous sections.

With this formulation, the set of $\mathcal{K}$ that satisfy the MHB equation are given by

$$\mathcal{K} = RZ^\dagger + \mathsf{K}(I - ZZ^\dagger), \quad R = \begin{bmatrix} R_1 & R_2 \end{bmatrix}, \quad Z = \begin{bmatrix} Z_1 & Z_2 \end{bmatrix}. \tag{4.15}$$

To formulate the stability conditions, first define $U_i^\intercal$, $W_i^\intercal$, and N_i by

$$\begin{bmatrix} U_i^\intercal \\ W_i^\intercal \end{bmatrix} \begin{bmatrix} \mathcal{V}_i & N_i \end{bmatrix} = I, \quad i = 1, 2,$$

then the stability conditions are given by

$$W_i^\intercal(\mathsf{A}_i + \mathsf{B}_i\mathcal{K}T_i\mathsf{C}_i)N_i = Hurwitz.$$

Substituting in the definition of $\mathcal{K}$ from (4.15), we obtain

$$W_i^\intercal(\mathsf{A}_i + \mathsf{B}_i(RZ^\dagger + \mathsf{K}(I - ZZ^\dagger))T_i\mathsf{C}_i)N_i = Hurwitz.$$

or equivalently, a simultaneous static output feedback stabilization problem of the form

$$\underbrace{W_i^\intercal(\mathsf{A}_i + \mathsf{B}_iRZ^\dagger T_i\mathsf{C}_i)N_i}_{\mathcal{A}_i} + \underbrace{W_i^\intercal\mathsf{B}_i}_{\mathcal{B}_i}\,\mathsf{K}\,\underbrace{(I - ZZ^\dagger)T_i\mathsf{C}_iN_i}_{\mathcal{C}_i} = Hurwitz, i = 1, 2.$$

The simultaneous static output feedback stabilization problem is a very difficult one to solve in general and to the extent of our knowledge, there is no known solution to solve the simultaneous static output feedback stabilization problem. Thus, we will apply the

structured static output feedback stabilization approach described in Appendix E to reduce the problem to a set of LMIs given by

$$\min_{X_i,Y_i,\mathcal{K}} \operatorname{tr}(\mathsf{XY}) \quad s.t. \quad \begin{bmatrix} X_i & I + \varepsilon_i(\mathcal{A}_i + \mathcal{B}_i\mathcal{K}\mathcal{C}_i) \\ I + \varepsilon_i(\mathcal{A}_i + \mathcal{B}_i\mathcal{K}\mathcal{C}_i)^\intercal & Y_i \end{bmatrix} > 0, \quad \begin{bmatrix} X_i & I \\ I & Y_i \end{bmatrix} \geq 0,$$

where $i = 1, 2$ and $\mathsf{X} = \operatorname{diag}(X_1, X_2)$ and $\mathsf{Y} = \operatorname{diag}(Y_1, Y_2)$. If a solution exists, then this problem can be practically solved by the linearization algorithm by El Ghaoui [76].

4.6.2 An Alternative Formulation for Structured Controller Design

The multiple limit cycle controller design problem reduced to a simultaneous stabilization problem in the previous section after the controller was parameterized in terms of all possible controllers that satisfy the MHB equation and the stabilization was performed over the freedom in that parameterization. One disadvantage of this formulation is that the controller structure cannot be dictated because it never appears in the LMIs. An alternative to this would be to have both the stability conditions and MHB conditions inside the LMI itself. In this case, the equations that would need to be satisfied are

$$R_i = \mathcal{K}Z_i, \quad W_i^\intercal(\mathsf{A}_i + \mathsf{B}_i\mathcal{K}T_i\mathsf{C}_i)N_i = Hurwitz, \quad i = 1, 2.$$

This translates to the LMI conditions

$$\min_{X_i,Y_i,\mathcal{K}} \operatorname{tr}(\mathsf{XY}) \quad s.t. \quad \begin{bmatrix} \epsilon & R - \mathcal{K}Z \\ (R - \mathcal{K}Z)^\intercal & \epsilon \end{bmatrix} \geq 0, \quad \begin{bmatrix} X_i & I \\ I & Y_i \end{bmatrix} \geq 0,$$

$$\begin{bmatrix} X_i & I + \varepsilon_i(W_i^\intercal\mathsf{A}_iN_i + W_i^\intercal\mathsf{B}_i\mathcal{K}T_i\mathsf{C}_iN_i) \\ I + \varepsilon_i(W_i^\intercal\mathsf{A}_iN_i + W_i^\intercal\mathsf{B}_i\mathcal{K}T_i\mathsf{C}_iN_i)^\intercal & Y_i \end{bmatrix} > 0,$$

for $i = 1, 2$ where $\mathsf{X} = \operatorname{diag}(X_1, X_2)$, $\mathsf{Y} = \operatorname{diag}(Y_1, Y_2)$, $R = \begin{bmatrix} R_1 & R_2 \end{bmatrix}$, $Z = \begin{bmatrix} Z_1 & Z_2 \end{bmatrix}$ and ϵ is a number sufficiently close to zero. Notice that the MHB conditions have been enforced in the LMIs by bounding the maximum singular value of $R - \mathcal{K}Z$ by the scalar term ϵ.

4.6.3 Design Example for Multiple Limit Cycles

4.6.3.1 Link-chain Model and Fluid Parameters

We consider a link-chain model of a leech provided by [77] with $\mathfrak{n} = 6$ links that are actuated at each joint and the fluid model given by [78]. For the physical properties of the link-chain model, we use the typical properties of a leech defined as a ribbon of length $\ell = 10cm$, width $d = 1cm$, and weight $m = 1g$. Since each link is assumed to be identical, each individual link has half length $l_o = l/(2\mathfrak{n})$ and mass $m_o = m/\mathfrak{n}$. Let $\theta(t) \in \mathbb{R}^{\mathfrak{n}}$ be the link angles, $u(t) \in \mathbb{R}^{\mathfrak{n}-1}$ be the joint torque inputs, and $v(t) \in \mathbb{R}$ be the velocity of the CG of the whole body along the x-axis. With the assumption that link angles θ_i and the y component of the CG velocity are small, the equations of motion can be given by

$$J\ddot{\theta} + D\dot{\theta} + (v\Lambda + K)\theta = Bu, \tag{4.16}$$

$$m\dot{v} + (nc_t + c_o||\theta||^2)v + \dot{\theta}^{\intercal}\Lambda\theta = 0 \tag{4.17}$$

where with o being the $\mathfrak{n} - 1$ dimensional zero vector,

$$M = m_o I, \quad L = l_o I, \quad B^{\intercal} = \begin{bmatrix} I & o \end{bmatrix} - \begin{bmatrix} o & I \end{bmatrix}, A^{\intercal} = \begin{bmatrix} I & o \end{bmatrix} + \begin{bmatrix} o & I \end{bmatrix},$$

$$c_n = C_P \rho d l_o |V_N| + 4 l_o \sqrt{\rho \mu d V_N}, \quad c_t = 5.4 C_T l_o \sqrt{\rho \mu V_N d}, \quad c_o = c_n - c_t,$$

$$C_n = c_n I, \quad C_t = c_t I, \quad C_o = c_o I, \quad J_o = m_o l_o^2/3, \quad J = J_o + F^{\intercal} M F,$$

$$F = M^{-1} B (B^{\intercal} M^{-1} B)^{-1} A^{\intercal} L, \quad D = L C_n L/3 + F^{\intercal} C_n F, \quad \Lambda = F^{\intercal} C_o, \quad K = B k_o B^{\intercal},$$

and the spring constant for each joint $k_o = 4.2624$ (mN-cm)/rad. This spring stiffness was chosen such that the plant would have a natural frequency at 3 Hz.

We consider two different fluid enviroments with the same density: water and a high viscosity fluid (methyl cellulose). In the two different fluid environments, the fluid parameters are given by

$$\mu = 0.01 poise, \quad \rho = 1 g/cm^3, \quad C_P = 3, \quad C_T = 0.6.$$

and

$$\mu = 4 poise, \quad \rho = 1 g/cm^3, \quad C_P = 3, \quad C_T = 0.6.$$

for the water and methyl cellulose, respectively. Additionally, we specify the average normal velocity of the links to be $V_N = 3$ cm/s in water and $V_N = 0.047$ cm/s in the high viscosity fluid.

Let us consider a transformation from the absolute link angles θ to the joint angles $\phi \in \mathbb{R}^{\mathfrak{n}-1}$ and the orientation angle $\theta_o \in \mathbb{R}$,

$$\begin{bmatrix} \phi \\ \theta_o \end{bmatrix} := \begin{bmatrix} B^\intercal \\ e^\intercal/\mathfrak{n} \end{bmatrix} \theta = W^{-1}\theta.$$

Define

$$W^\intercal J W := \begin{bmatrix} J_{11} & J_{12} \\ J_{21} & J_{22} \end{bmatrix}, \quad W^\intercal D W := \begin{bmatrix} D_{11} & D_{12} \\ D_{21} & D_{22} \end{bmatrix}, \quad W^\intercal \Lambda W := \begin{bmatrix} \Lambda_{11} & \Lambda_{12} \\ \Lambda_{21} & \Lambda_{22} \end{bmatrix}.$$

Then (4.16) becomes

$$\begin{bmatrix} J_{11} & J_{12} \\ J_{21} & J_{22} \end{bmatrix} \begin{bmatrix} \ddot{\phi} \\ \ddot{\theta}_o \end{bmatrix} + \begin{bmatrix} D_{11} & D_{12} \\ D_{21} & D_{22} \end{bmatrix} \begin{bmatrix} \dot{\phi} \\ \dot{\theta}_o \end{bmatrix} + \left(v \begin{bmatrix} \Lambda_{11} & \Lambda_{12} \\ \Lambda_{21} & \Lambda_{22} \end{bmatrix} + \begin{bmatrix} k_o I & 0 \\ 0 & 0 \end{bmatrix} \right) \begin{bmatrix} \phi \\ \theta_o \end{bmatrix} = \begin{bmatrix} u \\ 0 \end{bmatrix}. \tag{4.18}$$

Defining another coordinate transformation by

$$\varphi := \theta_o + h^\intercal \phi, \quad h := J_{12} J_{22}^{-1},$$

we obtain

$$\begin{aligned} \tilde{J}_{11}\ddot{\phi} + \tilde{D}_{11}\dot{\phi} + (v\tilde{\Lambda}_{11} + k_o I)\phi &= u, \\ J_{22}\ddot{\varphi} + D_{22}\dot{\varphi} + v\tilde{\Lambda}_{21}\phi &= 0, \end{aligned} \tag{4.19}$$

where

$$\tilde{J}_{11} = J_{11} - J_{12}J_{22}^{-1}J_{21}, \quad \tilde{D}_{11} = (c_n/m_o)\tilde{J}_{11}, \quad \tilde{\Lambda}_{11} = \Lambda_{11} - h\Lambda_{21}, \quad \tilde{\Lambda}_{21} = \Lambda_{21} - \Lambda_{22}h^\intercal.$$

We will use (4.19) for our design. In particular, we can determine the necessary $\hat{u}$ for a given $\hat{\phi}$ with $\hat{u} = (-\omega^2\tilde{J}_{11} + j\omega\tilde{D}_{11} + (v_0\tilde{\Lambda}_{11} + k_o I))\hat{\phi}$. Note that v was replaced with v_0 in order to simplify the controller design. In general v will be an oscillatory state governed by equation (4.17). However, the controller will be designed with a constant velocity v_0 which stands for the nominal value of v.

4.6.4 Desired Oscillation Profiles for Gait and Controller

We base the design of the desired oscillation profile for the link-chain system on observational data from real leeches swimming in water and methyl cellulose [68]. Additionally, we consider two different gaits, $\phi_1(t) \cong a_1 \sin(\omega_1 t + b_1)$ for water and $\phi_2(t) \cong a_2 \sin(\omega_2 t + b_2)$ for the high viscosity fluid. In the water environment, we set the target oscillation profile as

$$a_1 = \begin{bmatrix} 34 \\ 32.75 \\ 31.5 \\ 30.25 \\ 29 \end{bmatrix} \text{deg}, \quad b_1 = \begin{bmatrix} 0 \\ 60 \\ 120 \\ 180 \\ 240 \end{bmatrix} \text{deg}, \quad \omega_1 = 3 \ \text{Hz}, \quad v_{0,1} = 15.6 cm/s.$$

In the high viscosity environment, the target oscillation profile is given by

$$a_2 = \begin{bmatrix} 34 \\ 32.75 \\ 31.5 \\ 30.25 \\ 29 \end{bmatrix} \text{deg}, \quad b_2 = \begin{bmatrix} 0 \\ 90 \\ 180 \\ 270 \\ 360 \end{bmatrix} \text{deg}, \quad \omega_1 = 2 \ \ Hz \ \ v_{0,2} = 0.244 cm/s.$$

Given these oscillation profiles and nominal velocities, we can calculate the desired oscillation for $\hat{u}$ in each of the environments using the phasor form of equation (4.19). In particular

$$\hat{u}_1 = \begin{bmatrix} -65.01 + 178.66j \\ -57.16 - 48.29j \\ 128.03 - 194.11j \\ 293.83 - 135.95j \\ 276.65 + 40.80j \end{bmatrix}, \quad \hat{u}_2 = \begin{bmatrix} 249.35 - 7.42i \\ 3.99 + 221.98i \\ -214.54 - 18.82i \\ 19.64 - 227.52i \\ 221.49 + 03.35i \end{bmatrix}.$$

Specifying the oscillation profiles for the joint angles only assigns the portion of the eigenvectors associated with the plant. Since we are using a dynamic controller with a CPG architecture, we must specify the oscillation profile of the controller states as well. For simplicity, we impose no structure on the neuronal connections and assume that all the

neurons have the same dynamics. We define the dynamics of each neuron by a low-pass filter with time constant $\tau = 0.2s$ in water and $\tau = 0.3s$ in methyl cellulose, which are typical time constants for neuronal processes.

We define $\hat{q}$ using the concept of segmental oscillators. In a segmental oscillator, each actuator is driven by a set of neurons that oscillate together with specified phase differences. For this example, we will consider the case in each actuator is driven by 4 neurons that oscillate with the same amplitude with evenly distributed phases. That is, given $\hat{u} \in \mathbb{C}^5$ and $\hat{u}^i$ being the i^{th} entry of $\hat{u}$, we define $\hat{q}$, by

$$\hat{q} = \text{col}(\hat{p}_1, \ldots, \hat{p}_m), \quad \hat{p}_i = \gamma r \angle \hat{u}^i, \quad r = \text{col}(e^0, e^{j\varphi}, e^{j2\varphi}, e^{j3\varphi}), \quad \varphi = \pi/2,$$

where we define $\gamma = 1.5$ in order to obtain a fair approximation of the desired oscillation while remaining in the nonlinear zone of the describing function. Defining $\hat{q}_1$ for $\hat{u}_1$ and $\hat{q}_2$ for $\hat{u}_2$ in the manner described above, we can further see that the oscillation of the controller is given as $\hat{\xi}_i = C_f^{-1}\hat{q}_i$ for $i = 1, 2$. Now that we have the desired oscillation profiles, we can proceed to search for a feasible controller using the formulation described in Subsection 4.6.1.

4.6.5 Unstructured Multi-gait Design Example

For this design example, we apply the formulation in subsection 4.6.1 to obtain a feasible controller to achieve the oscillation profiles for the link-chain model in water and the high viscosity fluid. Fig. 4.4 shows the ideal oscillation profile on the left and the simulated oscillation profile in the steady-state on the right.

While the oscillation profile does not match exactly with respect to amplitude, the frequency of oscillation and phases match almost exactly to the ideal situation. Even in the case of amplitude, all the amplitudes are within 15% of desired and share a similar pattern of decreasing amplitudes from head to tail. The amplitudes, phases, and frequency of the first harmonic component obtained through Fourier analysis are described below in Table 4.2.

Moreover, although the controller design was performed assuming a constant desired

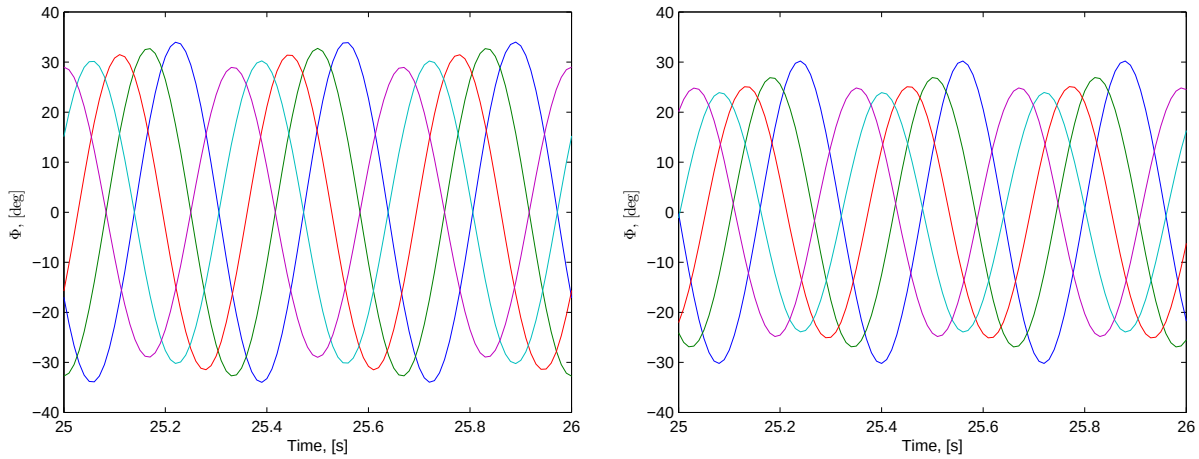

Figure 4.4: $\phi(t)$ for ideal oscillation (L) and simulated nonlinear limit cycle (R) in water environment.

Table 4.2: Oscillation Profile inside Water Environment

	ϕ_1	ϕ_2	ϕ_3	ϕ_4	ϕ_5
Target Amplitude [deg]	34	32.75	31.5	30.25	29
Closed-Loop Amplitude [deg]	30.02	27.07	25.3	23.92	24.91
Target Phase [deg]	0	60	120	180	240
Closed-Loop Phase [deg]	0	61.7	119.5	176.5	233.7

Target Frequency=3 Hz, Simulated Frequency= 3.13 Hz

velocity $v_{0,1}$, the simulation was performed with a nonconstant velocity governed by equation (4.17). The results of simulating the velocity are given in Fig. 4.5. The nominal velocity obtained through simulating (4.17) is lower than the desired nominal velocity of 15.6 cm/s by roughly 10% at 14 cm/s. It is reasonable to say that the controller designed roughly approximates the desired specifications for the link-chain system in water. The controller functions even better in the case where the link-chain system is placed in a higher viscosity fluid as evidenced in Fig.4.6.

Using the same controller and changing the plant to replicate a change in the environment, the oscillation profile changes to match the one prescribed for the higher viscosity fluid. The amplitudes, phases, and frequency of the first harmonic component obtained through Fourier

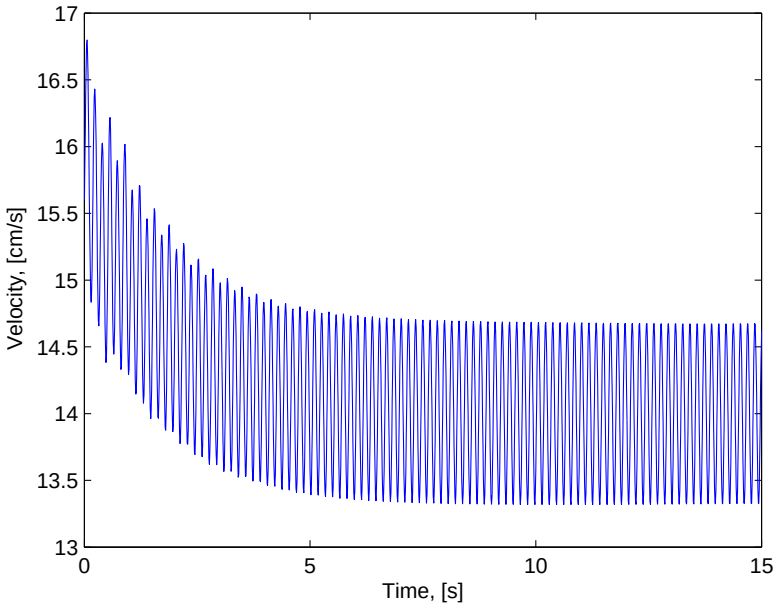

Figure 4.5: Simulated velocity in water environment.

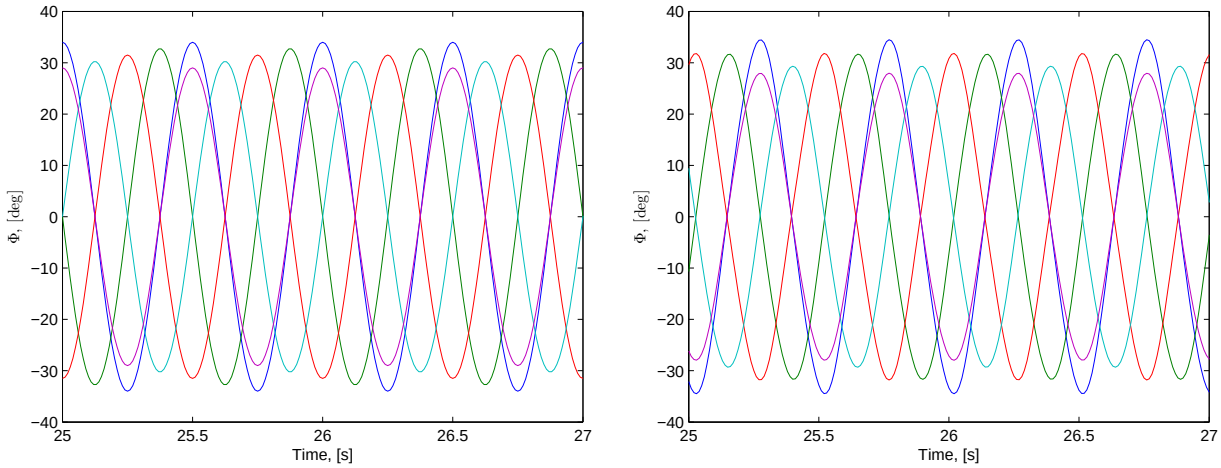

Figure 4.6: $\phi(t)$ for ideal oscillation (L) and simulated nonlinear oscillation (R) in the high viscosity environment.

analysis are described below in Table 4.3.

We can see that the controller achieves the prescribed oscillation better in the high viscosity fluid than in water. Every amplitude is within 5% of the desired value with the phases and frequency of oscillation following a similar trend. Because the oscillation profile

Table 4.3: Oscillation Profile inside the High Viscosity Environment

	ϕ_1	ϕ_2	ϕ_3	ϕ_4	ϕ_5
Target Amplitude [deg]	34	32.75	31.5	30.25	29
Closed-Loop Amplitude [deg]	33.83	31.32	30.83	29.1	27.69
Target Phase [deg]	0	90	180	270	360
Closed-Loop Phase [deg]	0	88.2	180.5	269.6	360.2

Target Frequency=2 Hz, Simulated Frequency= 2.01 Hz

of the nonlinear simulation so closely matches that of the designed profile, it is expected that the simulated velocity would also oscillate about a value close to $v_{0,2}$. Fig. 4.7 confirms that this is the case.

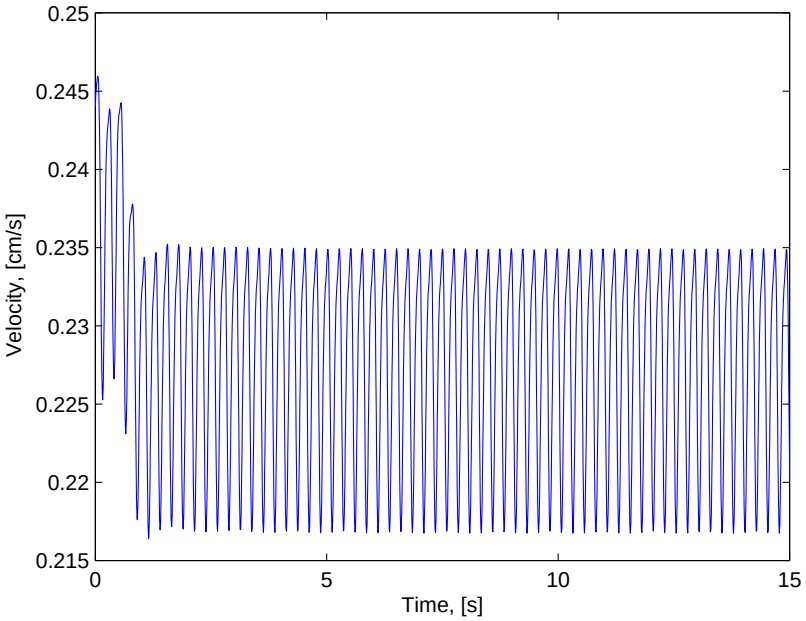

Figure 4.7: Simulated velocity in the high viscosity environment.

With a desired steady state nominal velocity of $v_{0,2} = 0.244$ cm/s, the simulated velocity is within 8% of the desired steady state nominal velocity at roughly 0.225 cm/s. Snapshots for the body shape of each of these gaits over one period is given in Fig. 4.8.

In the previous examples, we applied one controller to two different systems for which two different oscillation profiles were designed. In each simulation, we set the initial conditions

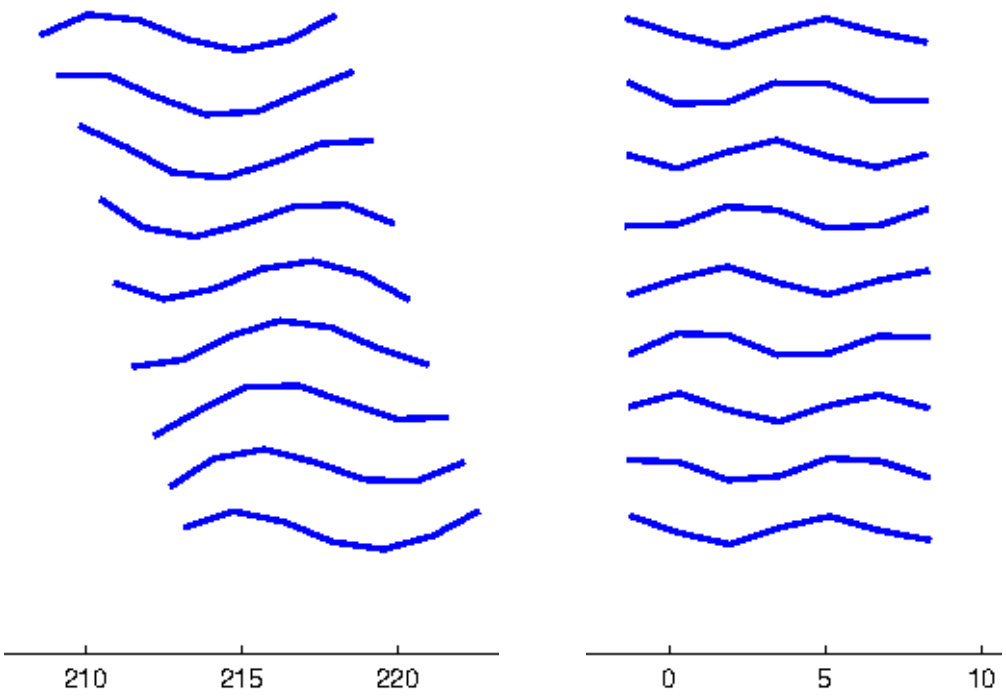

Figure 4.8: Snapshots of one cycle of the leech gait in water (L) and high viscosity fluid (R).

to be the desired oscillation profile for that given system; essentially, we started close to the desired limit cycle in the nonlinear simulation. However, in a real system, starting on a desired profile is impractical as conditions can change at any moment, thereby leading to an initial condition away from the desired. To test this, we first simulated the controller applied to the link-chain system in water and then, after the profile reached steady-state, we changed the plant to the one representing the high viscosity environment and applied the final steady state condition of the first simulation as the initial condition to the new simulation to emulate a change in environment. We then repeated the process in the other direction, changing the plant from the one used for the high viscosity environment to the one for water. The results of this simulation are given in Fig. 4.9.

In Fig. 4.9, the plant is changed from the one used in water to the high viscosity fluid at 15 seconds and from high viscosity fluid to water at 30 seconds. For each of these switches, the controller immediately changes the oscillation profile to the one designed for the respective plant. This situation is also observed in the simulated velocity given in Fig. 4.10.

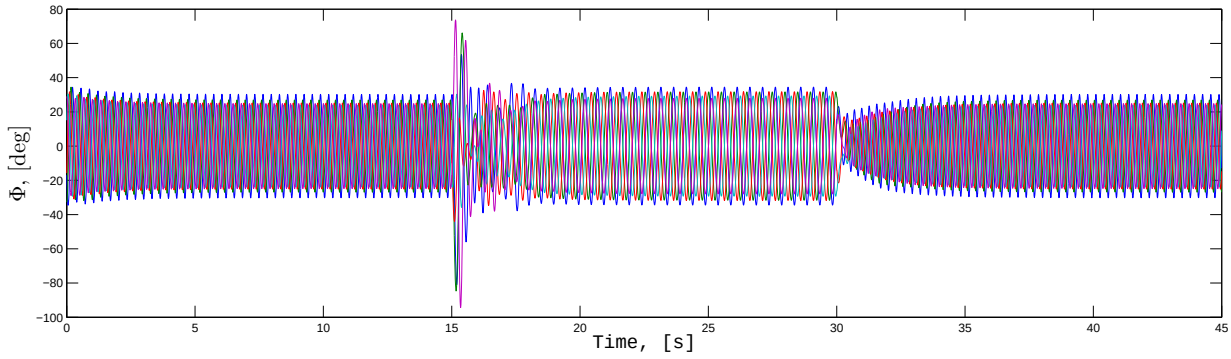

Figure 4.9: Simulated changes in gait in reponse to environment changes from water to the high viscosity fluid at 15s and the high viscosity fluid to water at 30s.

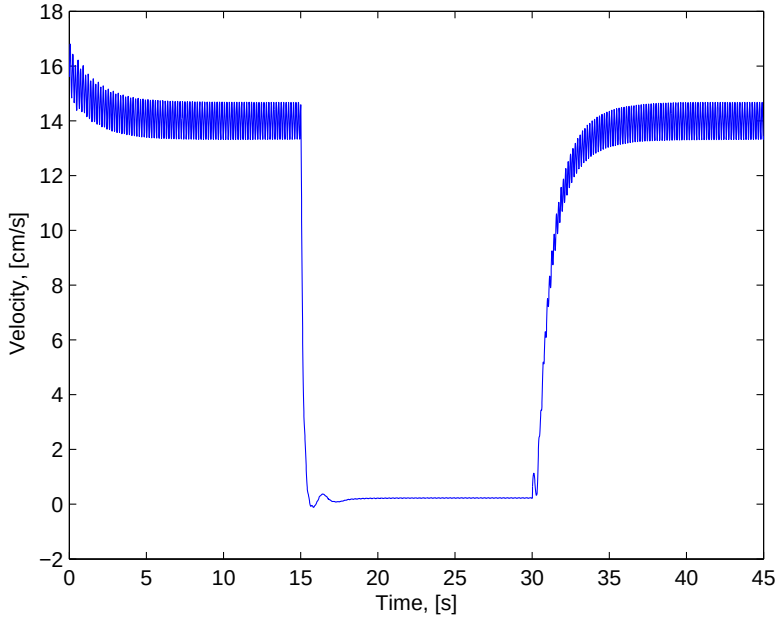

Figure 4.10: Simulated changes in velocity in reponse to environment changes from water to the high viscosity fluid at 15s and the high viscosity fluid to water at 30s.

From this example, it is clear that the proposed eigenstructure assignment method can be applied to the design of a single controller that can change gaits depending on the plant. Moreover, since a variation in the plant can represent a change in the environment, this switching ability signifies a method for the controller to autonomously change gaits depending on variations in environments. Although a comprehensive theory was not developed for the

case of multi-gait eigenstructure assignment, the example provided above shows that the problem is certainly feasible and it gives a potential direction for future research.

4.6.6 Structured Multi-gait Design Example

In this example, we design the controller to achieve the same limit cycles as in the previous section, but with the added condition that the interconnections of the neurons in the segmental oscillator, M, have a nearest neighbor structure of the form

$$M = \begin{bmatrix} M_o & M_1 & M_2 & 0 & 0 \\ M_3 & M_o & M_1 & M_2 & 0 \\ M_4 & M_3 & M_o & M_1 & M_2 \\ 0 & M_4 & M_3 & M_o & M_1 \\ 0 & 0 & M_4 & M_3 & M_o \end{bmatrix},$$

where M_o specifies the interconnections the neurons within one segmental oscillator and M_1, M_2, M_3, and M_4 specify the interconnection between the segmental oscillators. We utilize the formulation in subsection 4.6.2 to obtain a feasible controller.

Fig. 4.11 shows the steady state oscillations with a controller that solves the problem stated above with the structured M.

For Fig. 4.11, the simulations were performed by only simulating equation (4.16) where v was replaced by a constantly velocity ($v_{0,1}$ or $v_{0,2}$). Although the conditions were satisfied with the structured controller, simulating (4.16) with (4.17) resulting in convergence to a different limit cycle for the water environment. Tables 4.5 and 4.4 give the amplitudes, phases, and frequency of the first harmonic component found through a Fourier analysis of the ϕ oscillation in each environment.

Like the unstructured case, the limit cycles were very close in each aspect to the designed oscillation profiles. In the case of the water environment, the amplitudes were all within 3% of the designed and phases within 2%. Similarly, in the high viscosity environment, the nonlinear simulated amplitudes were all within 13% of the desired amplitudes and phases were within 3% of the desired. In both cases, the frequencies were almost exactly as designed.

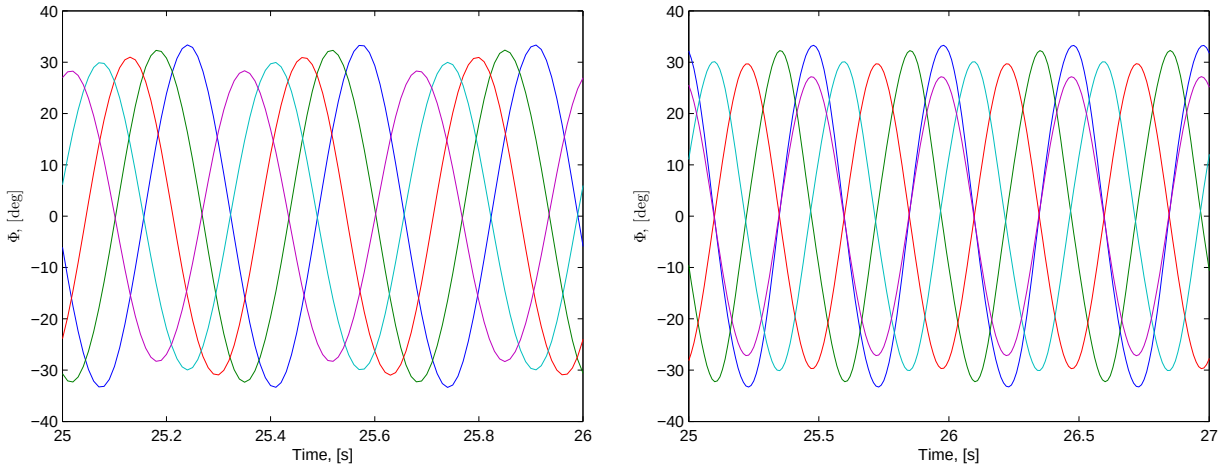

Figure 4.11: $\phi(t)$ from simulating (4.16) in water (L) and the high viscosity (R) environment using controller with structured M.

Table 4.4: Oscillation Profile inside Water Environment using Controller with Structured M

	ϕ_1	ϕ_2	ϕ_3	ϕ_4	ϕ_5
Target Amplitude [deg]	34	32.75	31.5	30.25	29
Closed-Loop Amplitude [deg]	33.16	32.25	31.13	29.96	28.4
Target Phase [deg]	0	60	120	180	240
Closed-Loop Phase [deg]	0	59.1	119.6	180.88	240.49

Target Frequency=3 Hz, Simulated Frequency= 2.99 Hz

Table 4.5: Oscillation Profile inside the High Viscosity Environment using Controller with Structured M

	ϕ_1	ϕ_2	ϕ_3	ϕ_4	ϕ_5
Target Amplitude [deg]	34	32.75	31.5	30.25	29
Closed-Loop Amplitude [deg]	33.34	31.19	29.38	29.35	26.95
Target Phase [deg]	0	90	180	270	360
Closed-Loop Phase [deg]	0	91.56	180.27	275.67	361.68

Target Frequency=2 Hz, Simulated Frequency= 2 Hz

Although we were able to design a controller with a specified structure for the neuronal interconnectivity matrix M that satisfied the eigenstructure conditions posed above, simu-

lating the nonlinear controller with the velocity equation (4.17) resulted in an entrainment to an unspecified limit cycle in the water environment as we show in Fig. 4.12.

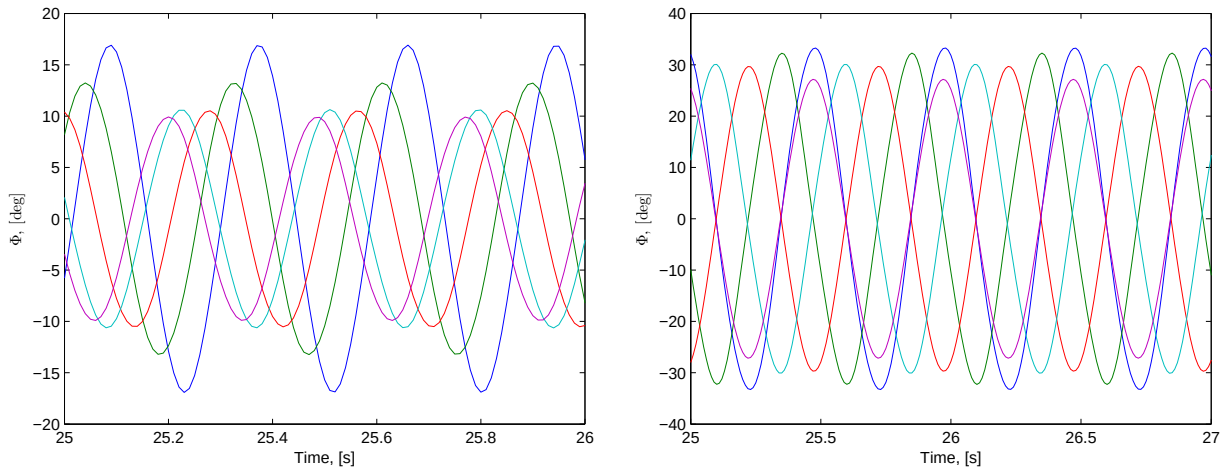

Figure 4.12: $\phi(t)$ from simulating (4.16) and (4.17) in water (L) and the high viscosity (R) environment using controller with structured M.

While simulating both equations (4.16) and (4.17) achieved the prescribed trajectory in the high viscosity environment, the prescribed profile was not achieved in water. Regardless, this is a step forward in designing structured controllers with a CPG architecture that can achieve and autonomously switch between multiple limit cycles. Ultimately, more research remains in fully developing a more robust and rigorous theory for designing limit cycles using the CPG-inspired controller.

CHAPTER 5

Conclusions

We considered the problem of designing a controller such that selected outputs of a linear plant exponentially converge to $Re^{\Lambda t}\eta_o$ for some vector η_o, with prescribed matrix, R, and matrix with non-negative eigenvalues, Λ. We demonstrated the equivalence of this problem to that of an eigenstructure assignment problem and provided necessary and sufficient conditions for solvability along with a parameterization of all feasible solutions. Using this parameterization, we showed that under a mild condition and linear independence of the eigenvectors associated with Λ, the problem could be solved with a static gain under state feedback and a dynamic controller of plant order, n, under output feedback. Moreover, when the condition for linear independence is not satisfied, the problem can be solved with a controller of order less than or equal to $n + r$, where r is the dimension of the desired dynamics Λ.

Recognizing that the multi-agent pattern formation problem is a special case of the eigenstructure assignment problem, we proceeded to apply the aforementioned result to design a structured controller for pattern formation of heterogeneous agents. In our method, we first performed a local controller design such that the desired eigenstructure was assigned to each agent, and the heterogeneous agent dynamics were homogenized. The inter-agent coupling is then designed by a Laplacian matrix representing a directed graph containing a spanning tree, to achieve coordination through exchange of relative information. The general result is shown to include an important existing result [1] as a special case, and have an additional capability of adaptive pattern formation through reference generator placed within the feedback loop.

To substantiate the utility of the proposed method for pattern formation control of mul-

tiple heterogeneous agents, we provided three numerical examples. In the first example, we designed a structured static state feedback gain to assign a trajectory described by a single eigenvalue for a multi-agent system to demonstrate how satisfaction of certain properties can greatly simplify the controller dynamics. In the second, our controller was compared to the one proposed by [1] in order to assert the importance of feedback in reaching a consensus. Finally, in the last example, we designed a linear distributed controller to achieve coordinated phase-locked oscillations for heterogeneous agents, and further added a local nonlinear feedback to lock the amplitudes of oscillation. The third example touched on the possibility of further research in expanding the linear eigenstructure framework to nonlinear pattern formation problems.

As a means of extending the linear eigenstructure framework to nonlinear pattern formation problems, we considered the design of a nonlinear controller for a linear time-invariant plant to achieve a specified oscillation in the closed-loop. To this end, we based our controller on the central pattern generator, a well-studied nonlinear oscillator in biology that can be represented by an interconnection of neurons, each of which contains dynamics described by a transfer function followed by a static nonlinearity. After simplifying the nonlinear problem via a describing function and the method of harmonic balance, we reduced the problem to an eigenstructure assignment problem characterized by a single controller satisfying an output-feedback problem and an eigenvalue/eigenvector equality relationship. We presented a numerical example demonstrating the utility of eigenstructure assignment for the design of CPG-based controller to achieve orbitally stable closed-loop oscillation.

We further considered the potential of designing a single CPG-based controller to achieve two specified limit cycles for two different plants; this situation parallels that of an organism changing gaits upon exposure to different environments. For this, we considered the swimming gait of a leech in water and a high viscosity fluid. A heuristic algorithm was applied to solve for a controller satisfying two pairs of eigenstructure assignments with a single controller. A numerical simulation was presented in which the controller achieved each of the limit cycles when applied to the respective plant. This example touches on the possiblity of designing controllers to achieve specified gaits for a given locomotor that can adapt to

different environments.

While a general theory and parameterization of all feasible controllers were presented to solve the linear pattern formation problem and expanded to the special cases of structured controller design for structured agents and nonlinear limit cycle design, there still remains work to be done in these topics. In particular, while the quasi-linearization of the central pattern generator inspired controller and satisfaction of the eigenstructure conditions were a realiable indicator of the existence of the desired limit cycle in the nonlinear closed-loop system, a proof to guarantee the existence of the limit cycle was not provided. Moreover,the design of a single controller to satisfy multiple eigenstructure assignment conditions was formulated and solutions found using heuristic algorithms, but necessary and sufficient conditions for existence of such a controller with a parameterization of all feasible controllers was outside of the scope of this dissertation; a complete solution to this problem would greatly improve the ease of finding a solution without having to resort to heuristic algorithms. Lastly, the proposed result for eigenstructure assignment is entirely a linear control theory. We touched on the possibility of expanding this linear result to nonlinear pattern formation problems with the design of limit cycles using a nonlinear damping term for multi-agent systems and a CPG-inspired controller for the general case, but more research must be done to extend the linear eigenstructure theory to encompass nonlinear pattern formation problems.

This research covered a vast spectrum of pattern formation problems for linear time-invariant systems. In showing that the general linear pattern formation problem is essentially an eigenstructure assignment problem, we have established a framework that can provide insight into the underlying principles governing problems such as multi-agent synchronization and limit cycle generation. Moreover, by combining our parameterization of all feasible controllers for eigenstructure assignment with a controller with CPG architecture, we have developed a systematic method for designing controllers to achieve a specified limit cycle for any arbitrary LTI system and further extended this by demonstrating the possibility of designing a single controller to achieve two different limit cycles for different systems. These developments not only brings us closer to the design of locomotors that can move in a

manner similar to biological organisms, but also the design of locomotors that can alter their behavior when placed in different environments. While there will always be more avenues of research that can improve on these developments, the work provided in this dissertation provides a solid foundation and framework for which future research can build.

APPENDIX A

Block-diagonalizing Transformation

Lemma 12 *Let matrices* (A, B, C, D) *and* (X, Λ) *be given. Suppose* A*,* D*, and* Λ *are square, and*

$$\begin{bmatrix} A & B \\ C & D \end{bmatrix} \begin{bmatrix} X \\ I \end{bmatrix} = \begin{bmatrix} X \\ I \end{bmatrix} \Lambda, \qquad \begin{array}{l} eig(\Lambda) \cap eig(\Omega) = \emptyset, \\ \Omega := A - XC. \end{array}$$

Then there exists a unique matrix M *satisfying*

$$\Lambda M - M\Omega = C,$$

and the matrix can be block-diagonalized by the following similarity transformation

$$\begin{bmatrix} M & I - MX \\ I & -X \end{bmatrix} \begin{bmatrix} A & B \\ C & D \end{bmatrix} \begin{bmatrix} X & I - XM \\ I & -M \end{bmatrix} = \begin{bmatrix} \Lambda & 0 \\ 0 & \Omega \end{bmatrix}.$$

Proof. The result can be verified by direct calculations. ∎

APPENDIX B

Proof for Lemma 1

We prove the equivalence for the case in which $\mathcal{A}$ has at least one eigenvalue in each of the open left-half plane (OLHP) and the closed right-half plane (CRHP). The proof is similar for the case where all the eigenvalues are in the CRHP. If all the eigenvalues are in the OLHP, the case is trivial since the specifications are violated. Since properties (a)–(c) and (i)–(ii) are preserved under state coordinate transformations, we may assume that system (2.3) is given in a Kalman canonical form,

$$\mathcal{A} = \begin{bmatrix} \mathcal{A}_{11} & \mathcal{A}_{12} \\ 0 & \mathcal{A} \end{bmatrix}, \quad \mathcal{H} = \begin{bmatrix} 0 & \mathcal{H} \end{bmatrix}, \quad \mathfrak{x} = \begin{bmatrix} \mathfrak{x}_1 \\ \chi \end{bmatrix}$$

where $(\mathcal{H}, \mathcal{A})$ is observable.

Suppose (a)–(c) hold. We will show that there exists a full column-rank matrix X such that

$$\mathcal{A}\mathsf{X} = \mathsf{X}\Lambda, \quad \mathcal{H}\mathsf{X} = R \tag{B.1}$$

and the eigenvalues of $\mathcal{A}$ except for those of Λ are in the OLHP. Given this, (i)–(ii) follow by setting $\mathcal{V} := \mathrm{col}(\mathsf{Y}, \mathsf{X})$ and recognizing that $\mathcal{A}_{11}$ is Hurwitz due to detectability of $(\mathcal{H}, \mathcal{A})$, where Y is the unique solution to the Sylvester equation

$$\mathcal{A}_{11}\mathsf{Y} + \mathcal{A}_{12}\mathsf{X} = \mathsf{Y}\Lambda.$$

To this end, let a spectral decomposition of $\mathcal{A}$ be given by

$$\mathcal{A} = \begin{bmatrix} L_u & L_s \end{bmatrix} \begin{bmatrix} \Lambda_u & 0 \\ 0 & \Lambda_s \end{bmatrix} \begin{bmatrix} R_u \\ R_s \end{bmatrix}, \quad \begin{bmatrix} R_u \\ R_s \end{bmatrix} \begin{bmatrix} L_u & L_s \end{bmatrix} = I,$$

where Λ_u and Λ_s have eigenvalues in the CRHP and OLHP, respectively. Then the output of (2.3) is given by

$$z(t) = \mathcal{H}e^{\mathcal{A}t}\chi(0) = \mathcal{H}L_u e^{\Lambda_u t}R_u\chi(0) + \mathcal{H}L_s e^{\Lambda_s t}R_s\chi(0).$$

We claim that $z(t) \to \eta(t)$ if and only if the persistent component of $z(t)$ is exactly equal to $\eta(t)$, that is,

$$e(t) := \mathcal{H}L_u e^{\Lambda_u t}R_u\chi(0) - Re^{\Lambda t}\eta(0) \equiv 0.$$

To see this, note that $z(t) \to \eta(t)$ holds if and only if $e(t) \to 0$ since the second term in $z(t)$ associated with Λ_s converges to zero. Regarding $e(t)$ as the output of a linear state-space system with all eigenvalues in the CRHP, it can be verified that $e(t) \to 0$ occurs if and only if the state trajectory is entirely in the unobservable subspace, i.e., $e(t) \equiv 0$. Taking the time derivatives of $e(t)$ for p times and stacking them, we have

$$\begin{aligned} &\mathsf{H}L_u e^{\Lambda_u t}R_u\chi(0) = \mathsf{R}e^{\Lambda t}\eta(0), \qquad (B.2)\\ &\mathsf{H} := \mathrm{col}(\mathcal{H}, \mathcal{H}\mathcal{A}, \ldots, \mathcal{H}\mathcal{A}^p), \qquad \mathsf{R} := \mathrm{col}(R, R\Lambda, \ldots, R\Lambda^p), \end{aligned}$$

where p is large enough so that H and R are full column-rank due to observability. Let $\chi(0)$ be the i^{th} column of the identity matrix and n_i be the corresponding $\eta(0)$ to satisfy (B.2). Define N as the matrix having n_i as the i^{th} column. Then

$$\mathsf{H}L_u e^{\Lambda_u t}R_u = \mathsf{R}e^{\Lambda t}N \qquad (B.3)$$

Similarly, let $\eta(0)$ be the i^{th} column of the $r \times r$ identity matrix and m_i be the corresponding $\chi(0)$ to satisfy (B.2). Define M as the matrix having m_i as the i^{th} column. Then

$$\mathsf{H}L_u e^{\Lambda_u t}R_u M = \mathsf{R}e^{\Lambda t}. \qquad (B.4)$$

From (B.3), using $\mathsf{H}^\dagger\mathsf{H} = I$, we have

$$\mathsf{H}(e^{\mathcal{A}t} - L_s e^{\Lambda_s t}R_s) = \mathsf{R}e^{\Lambda t}N, \quad \mathsf{X} := \mathsf{H}^\dagger\mathsf{R}, \quad \Rightarrow \quad e^{\mathcal{A}t} = \begin{bmatrix}\mathsf{X} & L_s\end{bmatrix}\begin{bmatrix}e^{\Lambda t} & 0\\ 0 & e^{\Lambda_s t}\end{bmatrix}\begin{bmatrix}N\\ R_s\end{bmatrix}. \qquad (B.5)$$

Setting $t = 0$ in (B.3), (B.4), and the above equation, we have

$$\begin{aligned} \mathsf{H}L_u R_u &= \mathsf{R}N, \\ \mathsf{H}L_u R_u M &= \mathsf{R}, \end{aligned} \qquad I = \begin{bmatrix} \mathsf{X} & L_s \end{bmatrix} \begin{bmatrix} N \\ R_s \end{bmatrix}.$$

Due to $\mathsf{R}^\dagger \mathsf{R} = I$, the first two equations yield $NM = I$ and $NL_s = 0$. Then, these conditions and the last equation imply that $\mathrm{col}(N, R_s)$ is square invertible. Hence, taking the time derivative of (B.5), setting $t = 0$, and multiplying $[\ \mathsf{X} \quad L_s\ ]$ from the right, the spectral decomposition of $\mathcal{A}$ is given by

$$\mathcal{A} \begin{bmatrix} \mathsf{X} & L_s \end{bmatrix} = \begin{bmatrix} \mathsf{X} & L_s \end{bmatrix} \begin{bmatrix} \Lambda & 0 \\ 0 & \Lambda_s \end{bmatrix}. \tag{B.6}$$

Therefore, $\mathcal{A}\mathsf{X} = \mathsf{X}\Lambda$ holds for a full column-rank X and the eigenvalues of $\mathcal{A}$ are given by those of Λ and Λ_s. Finally note from (B.4) at $t = 0$ that there exists a matrix Z such that $\mathsf{R} = \mathsf{H}Z$. Then $\mathsf{H}^\dagger \mathsf{R} = Z$ and

$$\mathsf{H}\mathsf{X} = \mathsf{H}\mathsf{H}^\dagger R = \mathsf{H}Z = \mathsf{R} \quad \Rightarrow \quad \mathcal{H}\mathsf{X} = R.$$

Thus, we have shown (B.1) and conclude that (a)-(c) $\Rightarrow$ (i)-(ii).

To show the converse, suppose (i) and (ii) hold. Note that

$$e^{\mathcal{A}t} \to \mathcal{V} e^{\Lambda t} \mathcal{U}, \quad z(t) = \mathcal{H} e^{\mathcal{A}t} \mathsf{x}(0) \to R e^{\Lambda t} \mathcal{U} \mathsf{x}(0),$$

where the rows of $\mathcal{U}$ span the left eigenspace corresponding to Λ, i.e., $\mathcal{U}\mathcal{A} = \Lambda\mathcal{U}$, and are normalized such that $\mathcal{U}\mathcal{V} = I$. Hence (a) holds for $\eta(0) := \mathcal{U}\mathsf{x}(0)$ and (b) holds for $\mathsf{x}(0) := \mathcal{V}\eta(0)$. To show (c), let (λ, v) be an arbitrary eigenvalue/eigenvector pair of Λ. Then (i) implies

$$(\mathcal{A} - \lambda I)(\mathcal{V}v) = 0, \quad \mathcal{H}(\mathcal{V}v) = Rv.$$

Since $\mathcal{V}$ has full column-rank and $v \neq 0$, we have $\mathcal{V}v \neq 0$. Moreover, since (R, Λ) is observable, $Rv \neq 0$. Hence λ is an observable mode of $(\mathcal{H}, \mathcal{A})$, i.e., all the eigenvalues of $\mathcal{A}$ shared with Λ are observable. Therefore, all the unobservable modes of $(\mathcal{H}, \mathcal{A})$ must be stable due to (ii), proving detectability of $(\mathcal{H}, \mathcal{A})$. Thus we can conclude that (i)–(ii) $\Rightarrow$ (a)-(c).

APPENDIX C

Proof for Theorem 3

A controller solves Problem 1 if and only if the closed-loop system satisfies conditions (i) and (ii) in Lemma 1. By Lemma 4 we can assume that V in condition (i) can be assumed to have the structure $\mathsf{V} = \mathrm{col}(X, \Xi_o)$ with $X \in \mathbb{R}^n$ and $\Xi_o := \mathrm{col}(I, 0, \ldots, 0)$ without loss of generality.

Suppose a dynamic controller in (2.2) solves Problem 1, where (i) and (ii) in Lemma 1 are satisfied with $\mathsf{V} = \mathrm{col}(X, \Xi)$ and $\Xi = \Xi_o$. Let Z be such that $\begin{bmatrix} \Xi & Z \end{bmatrix} = I$ and define S by

$$S = \begin{bmatrix} S_{11} & S_{12} & S_{13} \\ S_{21} & S_{22} & S_{23} \end{bmatrix} = \begin{bmatrix} D_c & C_c \\ B_c & A_c \end{bmatrix} \begin{bmatrix} CX & I & 0 \\ \Xi & 0 & Z \end{bmatrix}. \tag{C.1}$$

Then the first equation in (i) can be represented as

$$\mathcal{A}\mathsf{V} = \begin{bmatrix} A & 0 \\ 0 & 0 \end{bmatrix} \begin{bmatrix} X \\ \Xi \end{bmatrix} + \begin{bmatrix} B & 0 \\ 0 & I \end{bmatrix} \begin{bmatrix} S_{11} \\ S_{21} \end{bmatrix} = \begin{bmatrix} X \\ \Xi \end{bmatrix} \Lambda = \mathsf{V}\Lambda. \tag{C.2}$$

The first row block of (C.2) implies $AX + BF = X\Lambda$ with $F = S_{11}$, while the second equation in condition (i) gives $HX = R$ by noting that $\mathcal{H}\mathsf{V} = HX$. Thus we conclude that the existence of a controller solving Problem 1 implies the existence of X and F satisfying (2.13) in Theorem 3.

We now show that the given controller can be expressed as (2.17) for some $\mathring{Q}$ that stabilizes the augmented plant $(A, \begin{bmatrix} B & -X \end{bmatrix}, C)$. Let $\mathring{Q}$ be defined by

$$Q = \begin{bmatrix} D_q & C_q \\ B_q & A_q \end{bmatrix} = \begin{bmatrix} D_c & C_c \\ B_c & A_c \end{bmatrix} \begin{bmatrix} I & 0 \\ 0 & Z \end{bmatrix}, \tag{C.3}$$

where the dimensions of the square matrices A_c and A_q are n_c and $n_c - r$, respectively. Note that the closed-loop system of $\mathring{Q}$ and the augmented plant $(A, \begin{bmatrix} B & -X \end{bmatrix}, C)$ is given by $\dot{x}_q = \mathcal{A}_q x_q$ with

$$\mathcal{A}_q := \begin{bmatrix} A & 0 \\ 0 & 0 \end{bmatrix} + \begin{bmatrix} B & -X & 0 \\ 0 & 0 & I \end{bmatrix} Q \begin{bmatrix} C & 0 \\ 0 & I \end{bmatrix}. \tag{C.4}$$

To show that $\mathcal{A}_q$ is Hurwitz, let N be chosen such that $\begin{bmatrix} \mathsf{V} & N \end{bmatrix}$ is square invertible and define W and U such that $\mathrm{col}(U^\intercal, W^\intercal) \begin{bmatrix} \mathsf{V} & N \end{bmatrix} = \mathrm{I}$. One such combination would be

$$W^\intercal = \begin{bmatrix} I & -X\Xi^\intercal \\ 0 & Z^\intercal \end{bmatrix}, \quad N = \begin{bmatrix} I & 0 \\ 0 & Z \end{bmatrix}, \quad U^\intercal = \begin{bmatrix} 0 & \Xi^\intercal \end{bmatrix}. \tag{C.5}$$

It can then be verified using condition (i) of Lemma 1 that

$$\begin{bmatrix} U^\intercal \\ W^\intercal \end{bmatrix} \mathcal{A} \begin{bmatrix} \mathsf{V} & N \end{bmatrix} = \begin{bmatrix} \Lambda & * \\ 0 & \mathcal{A}_q \end{bmatrix} \tag{C.6}$$

holds where $*$ denotes irrelevant entries. Since the eigenvalues of $\mathcal{A}$ not associated with Λ have negative real part by condition (ii), we conclude that $\mathcal{A}_q$ is Hurwitz and Q as defined by (C.3) stabilizes $(A, \begin{bmatrix} B & -X \end{bmatrix}, C)$. Finally, substitution of the state equation for $\mathring{Q}$ into (2.17) yields

$$\begin{bmatrix} u \\ \dot{\xi} \\ \dot{q} \end{bmatrix} = \begin{bmatrix} D_{q1} & F - D_{q1}CX & C_{q1} \\ D_{q2} & \Lambda - D_{q2}CX & C_{q2} \\ B_q & -B_qCX & A_q \end{bmatrix} \begin{bmatrix} y \\ \xi \\ q \end{bmatrix} \tag{C.7}$$

where C_{qi} and D_{qi} for $i = 1, 2$ are partitioned blocks of C_q and D_q, respectively, and q is the state of $\mathring{Q}$. With Q in (C.3), conditions (C.1) and (C.2) imply that

(A_c, B_c, C_c, D_c) and (A_q, B_q, C_q, D_q) are related by

$$\begin{bmatrix} D_c & C_c \\ B_c & A_c \end{bmatrix} = \begin{bmatrix} \mathsf{F} & D_q & C_q \\ 0 & B_q & A_q \end{bmatrix} \begin{bmatrix} 0 & I & 0 \\ I & -CX & 0 \\ 0 & 0 & I \end{bmatrix}, \tag{C.8}$$

$$\mathsf{F} = \begin{bmatrix} F \\ \Lambda \end{bmatrix}, \quad Q := \begin{bmatrix} D_q & C_q \\ B_q & A_q \end{bmatrix}, \tag{C.9}$$

. We then see that (C.7) is identical to (2.2) with $x_c := \mathrm{col}(\xi, q)$.

To prove sufficiency, we now show that the controller (2.17) solves Problem 1 with $\mathsf{V} := \mathrm{col}(X, \Xi)$ where $\Xi := \Xi_o$. Let the state space matrices for $\mathring{Q}$ be given by (C.9). Then the controller (2.17) is described by the state space matrices given by (C.8). Define S by (C.1). Then

$$\begin{bmatrix} S_{11} & S_{12} & S_{13} \\ S_{21} & S_{22} & S_{23} \end{bmatrix} = \begin{bmatrix} \mathsf{F} & D_q & C_q \\ 0 & B_q & A_q \end{bmatrix}, \quad \mathsf{F} = \begin{bmatrix} F \\ \Lambda \end{bmatrix},$$

where $S_{11} \in \mathbb{R}^{n_u}$ and $\mathsf{F} \in \mathbb{R}^{n_u+r}$ with n_u being the dimension of $u(t)$. We then see that (C.2) holds. Thus condition (i) in Lemma 1 is satisfied. To show condition (ii), define N, W, and U by (C.5). The eigenvalues of $\mathcal{A}$ not associated with Λ are those of $\mathcal{A}_q := W^{\mathsf{T}}\mathcal{A}N$ due to (C.6), and $\mathcal{A}_q$ is given by (C.4). Since $\mathring{Q}$ is designed to stabilize $(A, \begin{bmatrix} B & -X \end{bmatrix}, C)$. we can conclude that $\mathcal{A}_q$ is Hurwitz. Thus, condition (ii) of Lemma 1 holds.

APPENDIX D

Proof for Corollary D

We first show that Theorem 5 holds when Φ_k that makes $\Lambda + \Gamma_k\Phi_k$ Hurwitz is replaced by Υ and Ψ that make $\mathsf{\Lambda} + \Gamma(\Upsilon + \Psi)$ Hurwitz and satisfy $\Psi\mathcal{I} = 0$, where $\mathcal{I} := \mathrm{col}(I, \ldots, I)$.

Suppose there exist F_k, and X_k satisfying (3.7). It suffices to prove the state feedback case due to the separation principle. Let the controller be denoted by $u = \mathring{\mathcal{K}}x$, where $C = I$ and (3.9) is replaced by $\hat{x}_k = x_k$. We see that the closed-loop system, $\mathcal{A} = \mathsf{A} + \mathsf{B}\mathcal{K}\mathsf{C}$, with state $\mathrm{col}(x,\, \xi,\, \hat{\eta})$ satisfies condition (i) of Lemma 1 with $\mathcal{V} = \mathrm{col}(X, \Xi, 0)$. That is,

$$\begin{bmatrix} A + B(K + \Psi_x M) & B(\mathsf{F} - K\mathsf{X} + \Psi_x(I - M\mathsf{X})) & B\Phi_x \\ J + \Psi_\xi M & \mathsf{\Lambda} - J\mathsf{X} + \Psi_\xi(I - M\mathsf{X}) & \Phi_\xi \\ LM + \Gamma\Psi M & L(I - M\mathsf{X}) + \Gamma\Psi(I - M\mathsf{X}) & \mathsf{\Lambda} + \Gamma\Phi - L \end{bmatrix} \begin{bmatrix} X \\ \Xi \\ 0 \end{bmatrix} = \begin{bmatrix} X \\ \Xi \\ 0 \end{bmatrix} \Lambda$$

where Φ_x and Φ_ξ are the matrices obtained by stacking $[\ I_{p_k} \quad 0\ ]\Phi_k$ and $[\ 0 \quad I_r\ ]\Phi_k$ in a column, respectively, with p_k being the number of columns of B_k and Φ_k being the k^{th} block row matrix of Φ associated with agent k, Ψ_x and Ψ_ξ are defined similarly, and

$$\Xi = \mathcal{I}, \quad \mathsf{X} = \mathrm{diag}(X_1, \ldots, X_N), \quad \mathsf{F} = \mathrm{diag}(F_1, \ldots, F_N),$$

and we noted that $L\mathcal{I} = 0$, $\mathsf{F}\mathcal{I} = F$, and $\mathsf{X}\mathcal{I} = X$. Thus, we see that condition (i) is satisfied.

Applying a similarity transformation defined by

$$T = \begin{bmatrix} \mathsf{X} & I - \mathsf{X}M & 0 \\ I & -M & 0 \\ I & 0 & I \end{bmatrix}, \quad T^{-1} = \begin{bmatrix} M & I - M\mathsf{X} & 0 \\ I & -\mathsf{X} & 0 \\ -M & -(I - M\mathsf{X}) & I \end{bmatrix},$$

we obtain

$$T^{-1}\mathcal{A}T = \begin{bmatrix} \Lambda + \Gamma(\Phi + \Psi) & 0 & * \\ * & A + BK - \mathsf{X}J & * \\ 0 & 0 & \Lambda - L \end{bmatrix}.$$

Since $\mathcal{L} \in \mathbb{L}_\Lambda$, $\Lambda - L$ will have eigenvalues in Λ with the rest in the open left-half plane. Furthermore, because $\mathrm{col}(K_k, J_k)$, Φ, and Ψ were chosen such that $A_k + \begin{bmatrix} B_k & -X_k \end{bmatrix} \mathrm{col}(K_k, J_k)$ and $\Lambda + \Gamma(\Phi + \Psi)$ are Hurwitz, we can conclude that condition (ii) of Lemma 1 is satisfied and the controller $u = \mathring{\mathcal{K}}x$ solves Problem 1.

We can thereby assume that w from (3.10) in Theorem 5 is defined by $w = \Phi\hat{\eta} + \Psi\eta$ without loss of generality. We will now show that if agent k has the property that Γ_k is full row-rank, then the agent's homogeneous dynamics, $\hat{\eta}_k$, can be removed. Suppose $k = 1$ for clarity, arbitrary k can be shown similarly.

Since Γ_1 is full column rank, define $\Psi_1 = -\Gamma_1^\dagger L_1$, where L_1 is defined as the rows of L associated with agent 1 and L_o as the rows of L associated with all other agents. Let $\Psi = \mathrm{col}(\Psi_1, 0)$ and let Φ be chosen such that $\Lambda + \Gamma(\Phi + \Psi)$ is Hurwitz. To ensure satisfaction of structural constraints, let $\Phi = -\Psi + \Phi_o$ where Φ_o is a block-diagonal matrix such that $\Lambda + \Gamma\Phi_o$ is Hurwitz.

Then

$$\begin{aligned}
\dot{\hat{\eta}} &= \Lambda + \Gamma w + v, \\
&= \Lambda\hat{\eta} + \Gamma(\Phi\hat{\eta} + \begin{bmatrix} \Gamma_1^\dagger L_1 \\ 0 \end{bmatrix} \eta) + v, \\
&= \Lambda\hat{\eta} + \Gamma(\Phi\hat{\eta} - \begin{bmatrix} \Gamma_1^\dagger L_1 \\ 0 \end{bmatrix} (\hat{\eta} - \varepsilon)) - L\varepsilon \\
&= (\Lambda + \Gamma\Phi)\hat{\eta} - \begin{bmatrix} L_1 \\ 0 \end{bmatrix} \hat{\eta} - \begin{bmatrix} 0 \\ L_o \end{bmatrix} \varepsilon \\
&= (\Lambda + \Gamma(\Phi + \Psi))\hat{\eta} - \begin{bmatrix} 0 \\ L_o \end{bmatrix} \varepsilon
\end{aligned}$$

By definition, $\Lambda + \Gamma(\Phi + \Psi)$ is Hurwitz. Thus $\hat{\eta}_1$ has stable, uncontrollable dynamics which can be removed. To see how to obtain (3.13), we once again show the case for $k = 1$ and note that

$$\begin{aligned} w_1 &= \Phi_1 \hat{\eta} + \Psi_1 \eta, \\ &= \Phi_1(\varepsilon + \eta) + \Psi_1 \eta, \\ &= \Phi_1 \varepsilon + (\Phi_1 + \Psi_1)\eta. \end{aligned}$$

Let $\Phi = -\Psi + \Phi_o$, where Φ_o is a block-diagonal matrix such that $\Lambda + \Gamma\Phi_o$ is Hurwitz. We can write w_1 by

$$w_1 = (-\Gamma_1^\dagger L_1 + \Phi_{o,1})\varepsilon + (\Phi_{o,1})\eta,$$

where $\Phi_{o,1}$ are the rows of Φ_o associated with agent 1. Since $\varepsilon = \hat{\eta} - \eta$, we have

$$w_1 = -\Gamma_1^\dagger L_1 \varepsilon,$$

where we noted that $\Phi_{o,1}\hat{\eta} = 0$ because $\hat{\eta}_1$ can be removed or set to zero and all other elements of $\hat{\eta}$ are multiplying zero due to the block diagonal structure of Φ_o. Thus, we verify the replacement in equation (3.13).

APPENDIX E

Derivation for Structured Static Output Feedback

Suppose $\dot{x} = Ax$ is stable. Then there exists $X = X^\intercal > 0$ such that

$$AX + XA^\intercal > 0.$$

In this case, there exists sufficiently small $\varepsilon > 0$ such that

$$\varepsilon AXA^\intercal + AX + XA^\intercal < 0,$$

which is equivalent to

$$(I + \varepsilon A)X(I + \varepsilon A)^\intercal < X. \tag{E.1}$$

By the Schur complement, this is further equivalent to

$$\begin{bmatrix} X & I + \varepsilon A \\ I + \varepsilon A^\intercal & Y \end{bmatrix} > 0, \quad X = Y^{-1} > 0.$$

Hence, a static output feedback control system

$$\dot{x} = Ax + Bu, \quad y = Cx, u = Ky$$

is stable if and only if there exists $X = X^\intercal > 0$ and sufficient small $\varepsilon > 0$ such that

$$\begin{bmatrix} X & I + \varepsilon(A + BKC) \\ I + \varepsilon(A + BKC)^\intercal & Y \end{bmatrix} > 0, \quad X = Y^{-1} > 0. \tag{E.2}$$

When $\varepsilon > 0$ is fixed, this condition holds if and only if the eigenvalues of $A + BKC$ are strictly inside the circle of radius $1/\varepsilon$ with center at $-1/\varepsilon$. This is easy to see once we notice that (E.1) is a discrete-time Lyapunov inequality and gives a condition for $|1+\varepsilon\lambda| < 1$ where λ is an arbitrary eigenvalue of $A + BKC$.

For a fixed value of $\varepsilon > 0$, the inequalities in (E.2) can be reformulated as

$$\min_{X,Y,K} \operatorname{tr}(XY) \quad s.t. \quad \begin{bmatrix} X & I + \varepsilon(A + BKC) \\ I + \varepsilon(A + BKC)^\intercal & Y \end{bmatrix} > 0, \quad \begin{bmatrix} X & I \\ I & Y \end{bmatrix} \geq 0.$$

Problem (E.2) is only feasible if and only if the minimum value is equal to n with minimizer $X = Y^{-1} > 0$. This problem can be practically solved by the linearization algorithm by El Ghaoui. It should be noted that a structural constraint on K can readily be imposed within this framework. Moreover, with such structural constraint on K, one can look for a control gain K such that each of the systems

$$\dot{x}_i = A_i x_i + B_i u_i, \quad y_i = C_i x_i, \quad u_i = K y_i$$

with $i = 1, \ldots, \ell$, has eigenvalues in the circle of radius $1/\varepsilon_i$ with center at $-1/\varepsilon_i$ by solving

$$\min_{X_i,Y_i,\mathcal{K}} \operatorname{tr}(\mathsf{XY}) \quad s.t. \quad \begin{bmatrix} X_i & I + \varepsilon_i(\mathcal{A}_i + \mathcal{B}_i \mathcal{K} \mathcal{C}_i) \\ I + \varepsilon_i(\mathcal{A}_i + \mathcal{B}_i \mathcal{K} \mathcal{C}_i)^\intercal & Y_i \end{bmatrix} > 0, \quad \begin{bmatrix} X_i & I \\ I & Y_i \end{bmatrix} \geq 0,$$

where $i = 1, \ldots, \ell$ and

$$\mathsf{X} := \operatorname{diag}(X_1, \ldots, X_\ell), \quad \mathsf{Y} := \operatorname{diag}(Y_1, \ldots, Y_\ell).$$

References

[1] P. Wieland, R. Sepulchre, and F. Allgöwer, "An internal model principle is necessary and sufficient for linear output synchronization," *Automatica*, vol. 47, no. 5, pp. 1068–1074, 2011.

[2] S. Srinathkumar and R. Rhoten, "Eigenvalue/eigenvector assignment for multivariable systems," *Electronic Letters*, vol. 11, no. 6, pp. 124–125, 1975.

[3] B. Porter and J. D'azzo, "Closed-loop eigenstructure assignment by state feedback in multivariable linear systems," *International Journal of Control*, vol. 27, no. 3, pp. 487–492, 1978.

[4] J. Kautsky, N. K. Nichols, and P. Van Dooren, "Robust pole assignment in linear state feedback," *International Journal of Control*, vol. 41, no. 5, pp. 1129–1155, 1985.

[5] M. Fahmy and H. Tantawy, "Eigenstructure assignment via linear state-feedback control," *International Journal of Control*, vol. 40, no. 1, pp. 161–178, 1984.

[6] K. Sobel and E. Shapiro, "Eigenstructure assignment for design of multimode flight control systems," *IEEE Control Systems Magazine*, vol. 5, no. 2, pp. 9–15, 1985.

[7] S. Mudge and R. Patton, "Analysis of the technique of robust eigenstructure assignment with application to aircraft control," in *IEE Proceedings D Control Theory and Applications*, vol. 135, no. 4. IET, 1988, pp. 275–281.

[8] J.-F. Magni, "Multimodel eigenstructure assignment in flight-control design," *Aerospace Science and Technology*, vol. 3, no. 3, pp. 141–151, 1999.

[9] B. Porter and S. Mohamed, "Genetic design of multivariable flight-control systems using eigenstructure assignment," in *Aerospace Control Systems, 1993. Proceedings. The First IEEE Regional Conference on.* IEEE, 1993, pp. 435–439.

[10] J. W. Choi and Y. B. Seo, "Lqr design with eigenstructure assignment capability [and application to aircraft flight control]," *IEEE Transactions on Aerospace Electronic Systems*, vol. 35, no. 2, pp. 700–708, 1999.

[11] J. Park and G. Rizzoni, "An eigenstructure assignment algorithm for the design of fault detection filters," *IEEE Transactions Automatic Control*, vol. 39, no. 7, pp. 1521–1524, 1994.

[12] R. J. Patton and J. Chen, "On eigenstructure assignment for robust fault diagnosis," *International Journal of Robust and Nonlinear Control*, vol. 10, no. 14, pp. 1193–1208, 2000.

[13] L.-C. Shen, S.-K. Chang, and P.-L. Hsu, "Robust fault detection and isolation with unstructured uncertainty using eigenstructure assignment," *Journal of guidance, control, and dynamics*, vol. 21, no. 1, pp. 50–57, 1998.

[14] B. Chen and S. Nagarajaiah, "Linear-matrix-inequality-based robust fault detection and isolation using the eigenstructure assignment method," *Journal of Guidance, Control, and Dynamics*, vol. 30, no. 6, pp. 1831–1835, 2007.

[15] R. J. Patton and J. Chen, "Robust fault detection of jet engine sensor systems using eigenstructure assignment," *Journal of Guidance, Control, and Dynamics*, vol. 15, no. 6, pp. 1491–1497, 1992.

[16] B. C. Moore, "On the flexibility offered by state feedback in multivariable systems beyond closed loop eigenvalue assignment," in *IEEE Conference on Decision and Control including the 14th Symposium on Adaptive Processes*. IEEE, 1975, pp. 207–214.

[17] M. Fahmy and J. O'Reilly, "On eigenstructure assignment in linear multivariable systems," *IEEE Transactions on Automatic Control*, vol. 27, no. 3, pp. 690–693, 1982.

[18] H. Kimura, "Pole assignment by gain output feedback," *IEEE Transactions on Automatic Control*, vol. 20, no. 4, pp. 509–516, 1975.

[19] S. Srinathkumar, "Eigenvalue/eigenvector assignment using output feedback," *IEEE Transactions on Automatic Control*, vol. 23, no. 1, pp. 79–81, 1978.

[20] B.-H. Kwon and M.-J. Youn, "Eigenvalue-generalized eigenvector assignment by output feedback," *Automatic Control, IEEE Transactions on*, vol. 32, no. 5, pp. 417–421, 1987.

[21] A. Andry, E. Shapiro, and J. Chung, "Eigenstructure assignment for linear systems," *IEEE Transactions on Aerospace Electronic Systems*, vol. 19, no. 5, pp. 711–729, 1983.

[22] D. W. Rew, J. L. Junkins, and J.-N. Juang, "Robust eigenstructure assignment by a projection method-applications using multiple optimization criteria," *Journal of Guidance, Control, and Dynamics*, vol. 12, no. 3, pp. 396–403, 1989.

[23] T. Clarke, S. Griffin, and J. Ensor, "Output feedback eigenstructure assignment using a new reduced orthogonality condition," *International Journal of Control*, vol. 76, no. 4, pp. 390–402, 2003.

[24] P. Apkarian *et al.*, "Continuous-time analysis, eigenstructure assignment, and h2 synthesis with enhanced linear matrix inequalities (lmi) characterizations," *IEEE Transactions on Automatic Control*, vol. 46, no. 12, pp. 1941–1946, 2001.

[25] J. A. Fax and R. M. Murray, "Information flow and cooperative control of vehicle formations," *IEEE Transactions on Automatic Control*, vol. 49, no. 9, pp. 1465–1476, 2004.

[26] G. Lafferriere, A. Williams, J. Caughman, and J. Veerman, "Decentralized control of vehicle formations," *Systems & control letters*, vol. 54, no. 9, pp. 899–910, 2005.

[27] L. Brinón-Arranz, A. Seuret, and C. Canudas-de Wit, "Cooperative control design for time-varying formations of multi-agent systems," *IEEE Transactions on Automatic Control*, vol. 59, no. 8, pp. 2283–2288, 2014.

[28] T. Iwasaki, "Multivariable harmonic balance for central pattern generators," *Automatica*, vol. 44, no. 12, pp. 3061–3069, 2008.

[29] T. Iwasaki and M. Wen, "Control design for coordinated oscillations with central pattern generator," in *American Control Conference (ACC)*. IEEE, 2013, pp. 2972–2977.

[30] R. Olfati-Saber, A. Fax, and R. M. Murray, "Consensus and cooperation in networked multi-agent systems," *Proceedings of the IEEE*, vol. 95, no. 1, pp. 215–233, 2007.

[31] W. Ren, R. W. Beard, and E. M. Atkins, "A survey of consensus problems in multi-agent coordination," in *American Control Conference, 2005. Proceedings of the 2005*. IEEE, 2005, pp. 1859–1864.

[32] ——, "Information consensus in multivehicle cooperative control," *IEEE Control systems magazine*, vol. 2, no. 27, pp. 71–82, 2007.

[33] A. Jadbabaie, J. Lin, and A. S. Morse, "Coordination of groups of mobile autonomous agents using nearest neighbor rules," *Automatic Control, IEEE Transactions on*, vol. 48, no. 6, pp. 988–1001, 2003.

[34] L. Scardovi and R. Sepulchre, "Synchronization in networks of identical linear systems," *Automatica*, vol. 45, no. 11, pp. 2557–2562, 2009.

[35] G.-R. Duan, "Solutions of the equation av+ bw= vf and their application to eigenstructure assignment in linear systems," *IEEE Transactions on Automatic Control*, vol. 38, no. 2, pp. 276–280, 1993.

[36] Y. Zheng *et al.*, "Consensus of heterogeneous multi-agent systems," *IET Control Theory & Applications*, vol. 5, no. 16, pp. 1881–1888, 2011.

[37] H. Kim, H. Shim, and J. H. Seo, "Output consensus of heterogeneous uncertain linear multi-agent systems," *IEEE Transactions on Automatic Control*, vol. 56, no. 1, pp. 200–206, 2011.

[38] T. Yang, A. Saberi, A. A. Stoorvogel, and H. F. Grip, "Output synchronization for heterogeneous networks of introspective right-invertible agents," *International Journal of Robust and Nonlinear Control*, vol. 24, no. 13, pp. 1821–1844, 2014.

[39] S. Chow and J. Mallet-Paret, "Pattern formation and spatial chaos in lattice dynamical systems — Part I," *EEE Transactions on Circuits and Systems I Fundamental Theory and Applications*, vol. 42, no. 10, pp. 746–751, 1995.

[40] S. Boccaletti and L. Pecora, "Introduction: Stability and pattern formation in networks of dynamical systems," *Chaos*, vol. 16, no. 015101, 2006.

[41] J. Lunze, "Synchronization of heterogeneous agents," *IEEE Transactions on Automatic Control*, vol. 57, no. 11, pp. 2885–2890, 2012.

[42] J. Huang, *Nonlinear Output Regulation: Theory and Applications*. SIAM, 2004.

[43] A. J. Laub, *Matrix Analysis for Scientists and Engineers*. SIAM, 2005.

[44] K. Hoffman and R. Kunze, "Linear algebra," *Englewood Cliffs, New Jersey*, 1971.

[45] S. Martínez, J. Cortés, and F. Bullo, "Analysis and design of oscillatory control systems," *IEEE Transactions on Automatic Control*, vol. 48, no. 7, pp. 1164–1177, 2003.

[46] P. Ge and M. Jouaneh, "Tracking control of a piezoceramic actuator," *IEEE Transactions on Control Systems Technology*, vol. 4, no. 3, pp. 209–216, 1996.

[47] M. Khalil, A. Sarkar, and S. Adhikari, "Tracking noisy limit cycle oscillation with nonlinear filters," *Journal of Sound and Vibration*, vol. 329, no. 2, pp. 150–170, 2010.

[48] J.-J. E. Slotine, W. Li *et al.*, *Applied Nonlinear Control*. Prentice-Hall Englewood Cliffs, NJ, 1991, vol. 199, no. 1.

[49] H. Giacomini, J. Llibre, and M. Viano, "On the nonexistence, existence and uniqueness of limit cycles," *Nonlinearity*, vol. 9, no. 2, p. 501, 1996.

[50] Y.-Q. Ye and C. Y. Lo, *Theory of limit cycles*. American Mathematical Soc., 1986, vol. 66.

[51] O. Fendrich, "Describing functions and limit cycles," *Automatic Control, IEEE Transactions on*, vol. 37, no. 4, pp. 486–487, 1992.

[52] C. Christopher and C. Li, *Limit cycles of differential equations*. Springer Science & Business Media, 2007.

[53] H. K. Khalil and J. Grizzle, *Nonlinear systems*. Prentice hall New Jersey, 1996, vol. 3.

[54] Q.-C. Pham and J.-J. Slotine, "Stable concurrent synchronization in dynamic system networks," *Neural Networks*, vol. 20, no. 1, pp. 62–77, 2007.

[55] X. Liu and T. Iwasaki, "Orbital stability analysis of coupled harmonic oscillators," in *Proceedings of the 51st Annual Conference on Decision and Control (CDC*. IEEE, 2012, pp. 5942–5947.

[56] Y. Fukuoka, H. Kimura, and A. H. Cohen, "Adaptive dynamic walking of a auadruped robot on irregular terrain based on biological concepts," *The International Journal of Robotics Research*, vol. 22, no. 3-4, pp. 187–202, 2003.

[57] A. Crespi, A. Badertscher, A. Guignard, and A. J. Ijspeert, "Amphibot i: an amphibious snake-like robot," *Robotics and Autonomous Systems*, vol. 50, no. 4, pp. 163–175, 2005.

[58] F. Delcomyn, "Neural basis of rhythmic behavior in animals," *Science*, vol. 210, no. 4469, pp. 492–498, 1980.

[59] S. Grillner, Ö. Ekeberg, A. El Manira, A. Lansner, D. Parker, J. Tegner, and P. Wallen, "Intrinsic function of a neuronal networka vertebrate central pattern generator," *Brain Research Reviews*, vol. 26, no. 2, pp. 184–197, 1998.

[60] A. Jean, "Brainstem control of swallowing: localization and organization of the central pattern generator for swallowing," in *Neurophysiology of the jaws and teeth*. Springer, 1990, pp. 294–321.

[61] E. Marder and D. Bucher, "Central pattern generators and the control of rhythmic movements," *Current biology*, vol. 11, no. 23, pp. R986–R996, 2001.

[62] P. A. Guertin, "The mammalian central pattern generator for locomotion," *Brain Research Reviews*, vol. 62, no. 1, pp. 45–56, 2009.

[63] J. Duysens and H. W. Van de Crommert, "Neural control of locomotion; part 1: The central pattern generator from cats to humans," *Gait & posture*, vol. 7, no. 2, pp. 131–141, 1998.

[64] A. H. Cohen and P. Wallén, "The neuronal correlate of locomotion in fish," *Experimental Brain Research*, vol. 41, no. 1, pp. 11–18, 1980.

[65] G. Zhong, N. A. Shevtsova, I. A. Rybak, and R. M. Harris-Warrick, "Neuronal activity in the isolated mouse spinal cord during spontaneous deletions in fictive locomotion: insights into locomotor central pattern generator organization," *The Journal of physiology*, vol. 590, no. 19, pp. 4735–4759, 2012.

[66] F. J. Eisenhart, T. W. Cacciatore, and W. B. Kristan Jr, "A central pattern generator underlies crawling in the medicinal leech," *Journal of Comparative Physiology A*, vol. 186, no. 7-8, pp. 631–643, 2000.

[67] D. Bucher, G. Haspel, J. Golowasch, and F. Nadim, "Central pattern generators," *eLS*, 2000.

[68] T. Iwasaki, J. Chen, and W. O. Friesen, "Biological clockwork underlying adaptive rhythmic movements," *Proceedings of the National Academy of Sciences*, vol. 111, no. 3, pp. 978–983, 2014.

[69] A. J. Ijspeert, "Central pattern generators for locomotion control in animals and robots: a review," *Neural Networks*, vol. 21, no. 4, pp. 642–653, 2008.

[70] Z. Chen, M. Zheng, W. O. Friesen, and T. Iwasaki, "Multivariable harmonic balance analysis of the neuronal oscillator for leech swimming," *Journal of computational neuroscience*, vol. 25, no. 3, pp. 583–606, 2008.

[71] Y. Futakata and T. Iwasaki, "Formal analysis of resonance entrainment by central pattern generator," *Journal of Mathematical Biology*, vol. 57, no. 2, pp. 183–207, 2008.

[72] ——, "Entrainment to natural oscillations via uncoupled central pattern generators," *IEEE Transactions on Automatic Control*, vol. 56, no. 5, pp. 1075–1089, 2011.

[73] T. K. Bliss, T. Iwasaki, and H. Bart-Smith, "Resonance entrainment of tensegrity structures via cpg control," *Automatica*, vol. 48, no. 11, pp. 2791–2800, 2012.

[74] M. M. Williamson, "Neural control of rhythmic arm movements," *Neural Networks*, vol. 11, no. 7, pp. 1379–1394, 1998.

[75] M. Zheng, W. O. Friesen, and T. Iwasaki, "Systems-level modeling of neuronal circuits for leech swimming," *Journal of Computational Neuroscience*, vol. 22, no. 1, pp. 21–38, 2007.

[76] L. El Ghaoui, F. Oustry, and M. AitRami, "A cone complementarity linearization algorithm for static output-feedback and related problems," *IEEE Transactions on Automatic Contro*, vol. 42, no. 8, pp. 1171–1176, 1997.

[77] J. Blair and T. Iwasaki, "Optimal gaits for mechanical rectifier systems," *IEEE Transactions on Automatic Control*, vol. 56, no. 1, pp. 59–71, 2011.

[78] J. Chen, W. Friesen, and T. Iwasaki, "Mechanisms underlying rhythmic locomotion: body–fluid interaction in undulatory swimming," *The Journal of experimental biology*, vol. 214, no. 4, pp. 561–574, 2011.